National Library of Canada
Canadian Theses Service
Ottawa, Canada
K1A 0N4

Bibliothèque nationale du Canada
Services des thèses canadiennes

CANADIAN THESES

THÈSES CANADIENNES

NOTICE

The quality of this microfiche is heavily dependent upon the quality of the original thesis submitted for microfilming. Every effort has been made to ensure the highest quality of reproduction possible.

If pages are missing, contact the university which granted the degree.

Some pages may have indistinct print especially if the original pages were typed with a poor typewriter ribbon or if the university sent us an inferior photocopy.

Previously copyrighted materials (journal articles, published tests, etc.) are not filmed.

Reproduction in full or in part of this film is governed by the Canadian Copyright Act, R.S.C. 1970, c. C-30.

AVIS

La qualité de cette microfiche dépend grandement de la qualité de la thèse soumise au microfilmage. Nous avons tout fait pour assurer une qualité supérieure de reproduction.

S'il manque des pages, veuillez communiquer avec l'université qui a conféré le grade.

La qualité d'impression de certaines pages peut laisser à désirer, surtout si les pages originales ont été dactylographiées à l'aide d'un ruban usé ou si l'université nous a fait parvenir une photocopie de qualité inférieure.

Les documents qui font déjà l'objet d'un droit d'auteur (articles de revue, examens publiés, etc.) ne sont pas microfilmés.

La reproduction, même partielle, de ce microfilm est soumise à la Loi canadienne sur le droit d'auteur, SRC 1970, c. C-30.

THIS DISSERTATION HAS BEEN MICROFILMED EXACTLY AS RECEIVED

LA THÈSE A ÉTÉ MICROFILMÉE TELLE QUE NOUS L'AVONS REÇUE

NL-339 (r.86/06)

Canada

THE UNIVERSITY OF ALBERTA

Kinetics of Oxidation of Reduced Nicotinamide Adenine Dinucleotide by Compounds I and II of Horseradish Peroxidase and of Ligand Binding to Dithionite Reduced Cytochrome P-450$_{scc}$

by

© MD. ABUL KASHEM

A THESIS

SUBMITTED TO THE FACULTY OF GRADUATE STUDIES AND RESEARCH IN PARTIAL FULFILMENT OF THE REQUIREMENTS FOR THE DEGREE OF DOCTOR OF PHILOSOPHY

DEPARTMENT OF CHEMISTRY

EDMONTON, ALBERTA

SPRING, 1987

Permission has been granted to the National Library of Canada to microfilm this thesis and to lend or sell copies of the film.

The author (copyright owner) has reserved other publication rights, and neither the thesis nor extensive extracts from it may be printed or otherwise reproduced without his/her written permission.

L'autorisation a été accordée à la Bibliothèque nationale du Canada de microfilmer cette thèse et de prêter ou de vendre des exemplaires du film.

L'auteur (titulaire du droit d'auteur) se réserve les autres droits de publication; ni la thèse ni de longs extraits de celle-ci ne doivent être imprimés ou autrement reproduits sans son autorisation écrite.

ISBN 0-315-37647-3

University of Alberta
Edmonton

Department of Chemistry
Faculty of Science

Canada T6G 2G2

E3-43 Chemistry Building East, Telephone (403) 432-3254

December 19, 1986.

To Whom It May Concern:

The undersigned gives permission to Md. Abdul Kashem to use the following studies in his thesis:

1. Kinetics of the Oxidation of Reduced Nicotinamide Adenine Dinucleotide by Horseradish Peroxidase Compounds I and II.

2. Rapid Spectral Scan and Stopped-Flow Studies of Carbon Monoxide Binding to Beef Adrenocortical Cytochrome P-450$_{scc}$.

3. The Formation and Decay of the Oxyferrous Complex of Beef Adrenocortical Cytochrome P-450$_{scc}$. Rapid-Scan and Stopped-Flow Studies.

H. Brian Dunford
Professor of Biophysical Chemistry

HBD/jj

THE UNIVERSITY OF ALBERTA

RELEASE FORM

NAME OF AUTHOR: MD. ABUL KASHEM

TITLE of THESIS: Kinetics of Oxidation of Reduced Nicotinamide Adenine Dinucleotide by Compounds I and II of Horseradish Peroxidase and of Ligand Binding to Dithionite Reduced Cytochrome $P\text{-}450_{scc}$

DEGREE FOR WHICH THESIS WAS PRESENTED: Doctor of Philosophy

YEAR THIS DEGREE GRANTED: 1987

Permission is hereby granted to THE UNIVERSITY OF ALBERTA LIBRARY to reproduce single copies of this thesis and to lend or sell such copies for private, scholarly or scientific research purposes only.

The author reserves other publication rights, and neither the thesis nor extensive extracts from it may be printed or otherwise reproduced without the author's written permission.

(Signed) M. A. Kashem

PERMANENT ADDRESS: Village: East Hinguli, Post: Karer Hat, Upa-Zila: Mirsarai, District: Chittagong, BANGLADESH

DATED Dec 19, 1986

THE UNIVERSITY OF ALBERTA

FACULTY OF GRADUATE STUDIES AND RESEARCH

The undersigned certify that they have read, and recommend to the Faculty of Graduate Studies and Research, for acceptance, a thesis entitled Kinetics of Oxidation of Reduced Nicotinamide Adenine Dinucleotide by Compounds I and II of Horseradish Peroxidase and of Ligand Binding to Dithionite Reduced Cytochrome P-450$_{scc}$ submitted by MD. ABUL KASHEM in partial fulfilment of the requirements for the degree of Doctor of Philosophy in Chemistry.

H.B. Dunford, Supervisor

External Examiner

Date Dec. 19, 1986

TO MY MOTHER

and

TO THE SACRED MEMORY OF MY FATHER

ABSTRACT

The transient state kinetics of the oxidation of reduced nicotinamide adenine dinucleotide (NADH) by horseradish peroxidase compounds I and II (HRP-I and HRP-II) were investigated as a function of pH at 25°C. The pH dependence of the second order rate constants indicates that the oxidation of NADH is influenced by a single ionization with pK_a of 4.7±0.5 and 4.2±1.4 at the active sites of HRP-I and HRP-II, respectively. An apparent reversibility of the HRP-II-NADH reaction was observed.

Carbon monoxide binding with both cholesterol-free (low-spin) and cholesterol-bound (high-spin) reduced forms of purified cytochrome $P\text{-}450_{scc}$ was investigated by rapid-scan and stopped-flow spectrometry at 25°C. Both "on" (k_1) and "off" (k_{-1}) rate constants are pH independent between pH 5 and 9. The values of k_1 for cholesterol-free and cholesterol-bound $P\text{-}450_{scc}$ are almost identical, while the value of k_{-1} for the former is about double that of the latter. Therefore the reduced-CO complex is somewhat more unstable in the absence of cholesterol.

The formation and spontaneous decay of the oxyferrous complex of cholesterol-bound cytochrome $P\text{-}450_{scc}$ were studied by means of rapid-scan and stopped-flow spectrometry at 4°C. The rate constants for oxygen binding are pH independent over the pH range 5 to 9, while the rate

constant for the decay appears to be influenced by an acid group with a pK_a of 7.1±0.1 on the oxyferrous complex.

Reduction of cholesterol-bound cytochrome $P\text{-}450_{scc}$ by sodium dithionite was studied by rapid-scan and stopped-flow spectrometry at 25°C. The reduction reaction has an initial lag phase and occurs by a mechanism involving $SO_2^{\cdot-}$ as the reducing species. The second order rate constant is pH independent over the pH range 5 to 8.

ACKNOWLEDGEMENTS

It is a great pleasure for me to express my deepest sense of gratitude and indebtedness to my research director, Professor H. Brian Dunford, for his generosity, invaluable guidance and constant encouragement without which this thesis would not have been in its present form.

Many thanks are due to Dr. A.-M. Lambeir and my fellow graduate students for their cooperation and helpful discussions, and to Jacki Jorgensen for her skillful typing of this thesis. I would also like to thank Dr. Michael A. Pickard, Professor of Microbiology, and the Department of Microbiology for allowing me to use their instruments.

I gratefully acknowledge the Alberta Heritage Foundation for Medical Research for a studentship, the Department of Chemistry for teaching and research assistantships, and the University of Chittagong (Bangladesh) for providing me with a study leave.

I am most grateful to my younger brother, Taher, who has cheerfully supported my mother and the rest of the family in my behalf. Finally, I must acknowledge my wife, Shahana, and also my little boy, Rana, for their understanding and for sharing with me both the times of frustration and elation.

TABLE OF CONTENTS

CHAPTER	PAGE
CHAPTER I	1
INTRODUCTION	1
Peroxidase and Oxygenase	2
Peroxidases	3
Horseradish Peroxidase	3
Cytochromes P-450	8
Cytochrome $P\text{-}450_{scc}$	11
References	17
CHAPTER II	25
KINETICS OF THE OXIDATION OF REDUCED NICOTINAMIDE ADENINE DINUCLEOTIDE BY HORSERADISH PEROXIDASE COMPOUNDS I AND II	25
Introduction	26
Materials and Methods	27
Results	32
Discussion	39
References	48
CHAPTER III	50
RAPID SPECTRAL SCAN AND STOPPED-FLOW STUDIES OF CARBON MONOXIDE BINDING TO BEEF ADRENOCORTICAL CYTOCHROME $P\text{-}450_{scc}$	50
Introduction	51
Materials and Methods	52

Results.....57
Discussion.....64
References.....67
CHAPTER IV.....70
THE FORMATION AND DECAY OF THE OXYFERROUS COMPLEX OF BEEF ADRENOCORTICAL CYTOCHROME $P\text{-}450_{scc}$.....70
Introduction.....71
Materials and Methods.....72
Results.....76
Discussion.....91
References.....95
CHAPTER V.....98
KINETICS OF REDUCTION OF BEEF ADRENOCORTICAL CYTOCHROME $P\text{-}450_{scc}$ BY DITHIONITE.....98
Introduction.....99
Materials and Methods.....100
Results.....102
Discussion.....108
References.....112
CHAPTER VI.....114
GENERAL DISCUSSION AND CONCLUSIONS.....114
References.....126
APPENDIX I.....130
PURIFICATION OF CYTOCHROMES $P\text{-}450_{scc}$ AND ADRENODOXIN.....130

Purification of Cholesterol-free Cytochrome $P\text{-}450_{scc}$.....131
Purification of Cholesterol-bound Cytochrome $P\text{-}450_{scc}$.....137
Purification of Adrenodoxin.....144
Other Procedures.....146
Materials.....155
Absorption Spectra of Purified Cytochromes $P\text{-}450_{scc}$ and Adrenodoxin.....155
References.....162
APPENDIX II.....164
BASIC EQUATION FOR PSEUDO-FIRST ORDER KINETIC MEASUREMENTS.....164

LIST OF TABLES

TABLE	Description	PAGE
II.1	Parameters Obtained from the pH Dependence of the Second-order Rate Constant for the Reduction of HRP-I by NADH	36
II.2	Parameters Obtained from the pH Dependence of the Second-order Rate Constant for the Reduction of HRP-II by NADH	40
II.3	Some Values of the Apparent Reverse Rate Constant, k_{-2}, for the HRP-II-NADH Reaction	41
II.4	Kinetic Parameters for the Reaction of NADH with HRP-I at 25°C	46
II.5	Kinetic Parameters for the Reaction of NADH with HRP-II at 25°C	47
III.1	Kinetic Parameters for Carbon Monoxide Binding to Reduced Cytochrome P-450_{scc} as a Function of pH at 25°C	63
IV.1	Kinetic Parameters for the Formation and Decay of Oxyferrous Complex of Beef Adrenocortical Cytochrome P-450_{scc} as a Function of pH at 4°C	85
IV.2	Parameters Obtained from the pH Dependence of the First-order Rate Constant for the Decay of Oxyferrous Complex of Beef Adrenocortical Cytochrome P-450_{scc} at 4°C	90

V.1 Rate Constants for the Reduction of Cholesterol-bound Cytochrome P-450$_{scc}$ by Sodium Dithionite as a Function of pH at 25°C.....109

LIST OF FIGURES

FIGURE	Description	PAGE
I.1	Structure of Ferriprotoporphyrin IX	5
I.2	Absorption Spectra in the Soret and Visible Regions of HRP and its Intermediate Compounds at pH 9.8 and 25°C	9
I.3	Catalytic Sequences for the Cholesterol Side-chain Cleavage Reaction	13
II.1	Absorbance Changes with Time of the Reaction of NADH with HRP-I at pH 6.13 and 25°C as Recorded on the Stopped-flow Apparatus at 411 nm	30
II.2	Absorbance Changes with Time of the Reaction of NADH with HRP-II at pH 6.14 and 25°C as Recorded on the Stopped-flow Apparatus at 420 nm	31
II.3	Pseudo-first Order Plot of the Reaction of NADH with HRP-I at pH 5.38 and 25°C	33
II.4	Plot of Logarithm of Second-order Rate Constant, $k_{1,app}$, for the Reaction of HRP-I with NADH vs. pH	34
II.5	Pseudo-first Order Plot of the Reaction of NADH with HRP-II at pH 5.62 and 25°C	37
II.6	Plot of Logarithm of Second-order Rate Constant, $k_{2,app}$, for the Reaction of HRP-II with NADH vs. pH	38

III.1 Absorbance Changes with Time of the Reaction of Carbon Monoxide with Cholesterol-free Cytochrome P-450_{scc} at 25°C as Recorded on the Stopped-flow Apparatus at 450 nm.....56

III.2 Spectral Changes Observed After Mixing Carbon Monoxide with Reduced Cholesterol-free and Cholesterol-bound Cytochromes P-450_{scc} at pH 7.40 and 7.32, Respectively.....58

III.3 Pseudo-first Order Plots of the Reaction of Carbon Monoxide with Reduced Cholesterol-free Cytochrome P-450_{scc} at pH 7.06 and Cholesterol-Cytochrome P-450_{scc} at pH 7.01.....61

III.4 Plots of (A) the Second-order Forward Rate Constant (k_1) and (B) First-order Reverse Rate Constant (k_{-1}) for CO Binding to Reduced Cytochrome P-450_{scc} as a Function of pH at 25°C.....62

IV.1 Spectral Changes Observed After Mixing Sodium Dithionite Reduced Cholesterol-bound Cytochrome P-450_{scc} with Oxygen at pH 7.30 and 4°C.....77

IV.2 Formation of Oxyferrous Complex of Cytochrome P-450_{scc} (Difference Spectra).....78

IV.3 Spectral Changes Observed After Mixing Sodium Dithionite Reduced Cholesterol-bound Cytochrome P-450_{scc} with Oxygen at pH 7.30 and 4°C (Decay of Oxyferrous Complex).....79

IV.4 Decay of Oxyferrous Complex of Cytochrome P-450$_{scc}$ (Difference Spectra).....80

IV.5 Absorbance Changes with Time for the Reaction of Ferrous Cytochrome P-450$_{scc}$ with Oxygen, Recorded on the Stopped-flow Apparatus at 430 nm, Leading to the Formation of the Oxyferrous Complex.....82

IV.6 The Observed Pseudo-first Order Rate Constants (k_{obs}) are Plotted as a Function of Oxygen Concentration at pH 7.30 and 4°C.....83

IV.7 Plot of the Second-order Forward Rate Constant (k_{on}) for the Formation of Oxyferrous Complex of Cytochrome P-450$_{scc}$ as a Function of pH at 4°C.....86

IV.8 Decay of Oxyferrous Complex of Cytochrome P-450$_{scc}$ (Time Dependence of the Absorbance Change).....87

IV.9 Plot of Logarithm of First-order Rate Constant for the Decay of Oxyferrous Complex of Cytochrome P-450$_{scc}$ (k_{decay}) vs. pH at 4°C.....89

V.1 Spectral Changes Associated with the Reduction of Cholesterol-bound Cytochrome P-450$_{scc}$ by Dithionite Anion at pH 7.34 and 25°C.....103

V.2 Reduction of Cholesterol-bound Cytochrome P-450$_{scc}$ (Difference Spectra).....104

V.3 Time Dependence of the Absorbance Changes After Mixing 3.3 mM Dithionite with 5.2 μM Cholesterol-bound Cytochrome P-450$_{scc}$ at pH 6.87 and 25°C.....105

V.4 The Observed Pseudo-first Order Rate Constants (k_{obs}) are Plotted as a Function of the Square Root of Dithionite Concentration at pH 7.34 and 25°C.....107

A.1 First Octylamine-Sepharose Column Elution Profile of Cholesterol-free Cytochrome P-450$_{scc}$.....134

A.2 Second Octylamine-Sepharose Column Elution Profile of Cholesterol-free Cytochrome P-450$_{scc}$.....136

A.3 First Aniline-Sepharose Column Elution Profile of Cholesterol-bound Cytochrome P-450$_{scc}$.....140

A.4 Second Aniline-Sepharose Column Elution Profile of Cholesterol-bound Cytochrome P-450$_{scc}$.....142

A.5 Adrenodoxin-Sepharose Column Elution Profile of Cholesterol-bound Cytochrome P-450$_{scc}$.....143

A.6 Chromatography of Adrenodoxin on Sephadex G-50.....147

A.7 Standard Curve (the Lowry Method).....153

A.8 Absorption Spectra of Various Forms of Purified Cholesterol-free Cytochrome P-450$_{scc}$.....156

A.9 Difference Spectrum of Carbon Monoxide-Complexed vs. Reduced Cholesterol-free Cytochrome P-450$_{scc}$.....158

A.10 Spectral Changes on Addition of Cholesterol to Low-spin Cytochrome P-450$_{scc}$.....159

A.11 Absorption Spectrum of Ferric Cholesterol-bound Cytochrome P-450$_{scc}$.....160

A.12 Absorption Spectrum of Purified Adrenodoxin....161

LIST OF ABBREVIATIONS

HRP, horseradish peroxidase (EC 1.11.1.7, donor-H_2O_2 oxidoreductase); HRP-I, HRP-II and HRP-III are compounds I, II and III of HRP (HRP-III is also known as oxyperoxidase); DHF, dihydorxyfumarate; NADH, reduced β-nicotinamide-adenine dinucleotide; AH_2, reducing substrate; NAD• and AH•, free radical oxidation products; SOD, superoxide dismutase; app, apparent; obs, observed; $P\text{-}450_{scc}$, cytochrome P-450 specific for cholesterol side-chain cleavage; $P\text{-}450_{cam}$, cytochrome P-450 specific for camphor hydroxylation; $P\text{-}450_{LM2}$ and $P\text{-}450_{LM4}$, rabbit liver microsomal P-450 species induced by phenobarbital and 5,6-benzoflavone, respectively; $P\text{-}450_{PB}$, phenobarbital induced P-450 from rat liver microsomes; NADPH, reduced β-nicotinamide-adenine dinucleotide phosphate; Emulgen 913, polyoxyethylene nonyl phenol ether.

CHAPTER ONE

INTRODUCTION

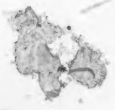

Peroxidase and Oxygenase

Oxygen, one of the most abundant elements on the earth and directly or indirectly essential for all forms of life, has been the subject of intensive studies by biochemists and physiologists ever since Lavoisier initiated the study of biological oxidation processes some 200 years ago. Since that time, the mechanism by which various nutrients are oxidized by living organisms has remained among the most important and interesting problems in biological science. At the turn of the twentieth century, Bach and his coworkers (1) proposed that oxygen reacted with an acceptor, A, in the primary reaction to produce an organic peroxide, which then reacted with a substrate, X, to form an oxide:

[1] $$A + O_2 \xrightarrow{\text{Oxygenase}} A\begin{matrix}O\\|\\O\end{matrix}$$

[2] $$A\begin{matrix}O\\|\\O\end{matrix} + X \xrightarrow{\text{Peroxidase}} AO + XO$$

The enzymes which catalyzed reactions [1] and [2] were named "oxygenase" and "peroxidase", respectively.

The names "oxygenase" and "peroxidase" are analogous because of their strong specificities for peroxide and oxygen, respectively. From the point of view of function, however, peroxidase is rather similar to oxidase, the name

which is now used in a narrow sense for electron transfer oxidases (2). The term "oxygenase" is restricted to a group of enzymes that catalyze the incorporation of either one or two atoms of oxygen per molecule of substrate. The terms "mono" and "di" oxygenases are generally assigned, respectively, to the enzyme catalyzing these types of reactions (3).

Peroxidases

Peroxidases are classified as the group of enzymes which catalyze the oxidation of numerous organic and inorganic compounds by hydrogen peroxide or other peroxides of the ROOH type. In the plant kingdom they exist in everything from apples to pineapples, from millet to wheat (4). Peroxidases are also widely distributed in animal tissues. Among the most studied are lactoperoxidase, myeloperoxidase and thyroid peroxidase. Several molds and yeasts also contain peroxidase. For example, chloroperoxidase from the mold Caldariomyces fumago is efficient in catalyzing the oxidation of chloride ions and most typical peroxidase reactions (5).

Horseradish Peroxidase

Horseradish peroxidase, HRP (EC.1.11.1.7, donor H_2O_2, oxidoreductase) is one of the better studied peroxidases since it is found in high concentration in horseradish root

and can therefore be readily isolated. There are seven major and thirteen minor isozymes of HRP (6).

The seven major isozymes have been isolated and characterized with respect to chromatographic behaviour, electrophoretic mobility, spectrophotometric properties, amino acid composition and carbohydrate composition (7,8). On the basis of these studies the seven major HRP isozymes are categorized into three groups: (a) acidic isozymes (isozymes A-1, A-2 and A-3); (b) neutral and slightly basic isozymes of little lower carbohydrate content (isozymes B, C, D and E); and (c) very basic (pI>11) isozymes of low carbohydrate content (HRP Vb) (6,7,9). The three groups of isozymes show marked differences in pH optima, specific activities and affinity toward inhibitors (7,8). The isozyme C of HRP dominates quantitatively (36%) among the isozymes of HRP and has an isoelectric point close to 9 (6). The purity number (reinheitzahl or RZ), the ratio of absorbance at 403 to 280 nm (corresponding to the ratio of hemin to protein absorbances), remains an excellent criterion of enzyme purity. The number should approach the value of 3.55 as an upper limit (6). Discussion will be limited to the isozyme C which is the dominant isozyme (10). The prosthetic group of HRP and most other peroxidases is ferriprotoporphyrin IX (Fig. I.1). HRP is a glycoprotein of molecular weight 44,000 (6), a carbohydrate

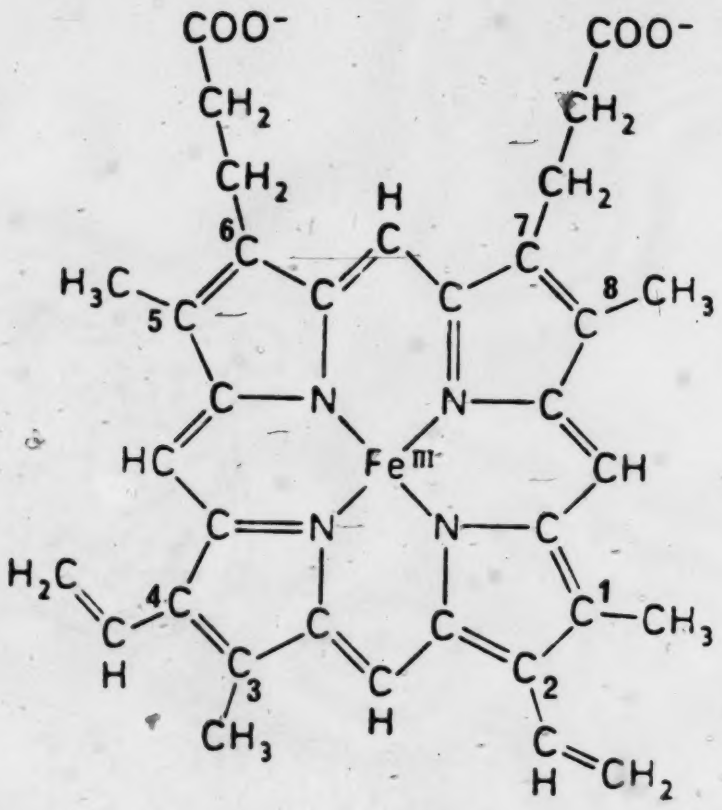

Heme
(Fe-protoporphyrin IX)

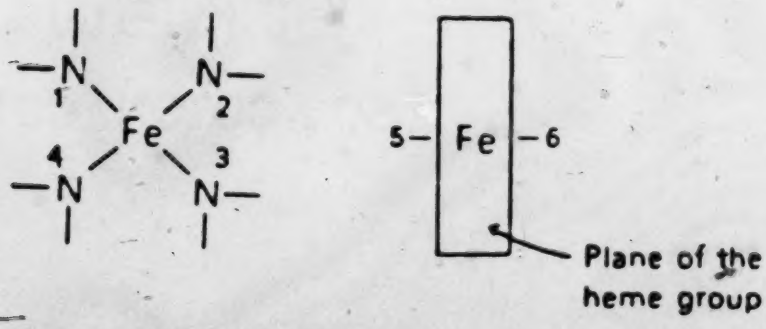

Figure I.1 Structure of ferriprotoporphyrin IX (ferric heme or hemin).

content of 18% by weight (11), and 43% α-helical structure (12). Two calcium ions are present in each enzyme (13,14); and a total of 308 amino acid residues were found in a single polypeptide chain, along with eight neutral carbohydrate side chains attached to asparagine residues (6). Four disulphide and three histidine residues are present. The imidazole group of one of the histidines occupies the fifth coordination position of the heme iron (15-18). There is a controversy over the presence or absence of water in the sixth coordination position. NMR results have yielded contradictory evidence (19,20). The physical changes accompanying the alkaline transition of HRP (pK ~11) were originally attributed to the conversion of water in the sixth position to hydroxide ion (21,22); however, an alternative explanation has been offered. It was suggested that a distal histidine coordinates to the ferric ion upon ionization at pH ~11 (23).

There are now five known oxidation states of HRP, ranging from ferrous to compound III, the latter of which is the equivalent of a ferrous-molecular oxygen complex (2,24,25). The range in oxidation states is therefore from +2 to +6 in unit steps. The intermediate oxidation states of +3, +5 and +4 are represented by HRP, compound I and compound II, with the conversions in that order representing the path of the normal enzymatic cycle (26,27):

$$HRP + H_2O_2 \rightarrow \text{compound I} + H_2O$$

$$\text{compound I} + AH_2 \rightarrow \text{compound II} + \cdot AH$$

$$\text{compound II} + AH_2 \rightarrow HRP + \cdot AH + H_2O$$

$$2 \cdot AH \rightarrow A_2H_2 \text{ (or AH-AH)}$$

in which AH_2 is a reducing substrate. During aerobic oxidations of DHF and NADH catalyzed by HRP the enzyme is converted to compound III (28-30):

$$NAD\cdot(DHF\cdot) + O_2 \rightarrow NAD^+(DHF^+) + O_2^{\cdot-}$$

$$HRP + O_2^{\cdot-} \rightarrow \text{compound III}$$

Compound I is believed to contain an iron(IV) porphyrin π-radical cation (31,32), compound II contains an iron(IV) heme (33,34), and compound III has been described as an oxyferrous heme (35-37). One of the two oxidizing equivalents in compound I was accounted for by the loss of an electron from the iron atom. The second oxidizing equivalent in compound I originates in the π-cation radical of the porphyrin (31). The four species of horseradish peroxidase

are easily distinguished by their Soret and visible absorption spectra, as shown in Fig. I.2.

Cytochromes P-450

Cytochrome P-450 is the term first assigned to proteins with an unusually red-shifted Soret band of the reduced carbon monoxide complex which occurs in the 450 nm region (38,39). The cytochromes P-450 were subsequently associated with a new class of heme proteins (40,41). These P-450 heme proteins contain ferriprotoporphyrin IX (Fig. I.1) as the prosthetic group. They catalyze monoxygenase or "mixed-function" oxidase reactions. A two-electron activation of dioxygen leads to formation of a molecule of water and the insertion of a single oxygen atom in a hydrocarbon substrate (42). Hence they are also characterized as monoxygenases or "mixed-function" oxidases (43). These unusual properties of the cytochromes P-450 are due to the ligation of the thiolate (S^-) of a cysteine residue in the fifth coordination position of the heme iron (44-48). Removal of the thiolate ligand, which can be achieved by protonation or use of detergent, will result in ordinary protoheme protein spectra ("P-420") (40,41,49). Concomitant with the transition to P-420, catalytic activity is lost. Two opposing concepts have been proposed concerning the sixth ligand *trans* to the thiolate ligand. Chevion and his

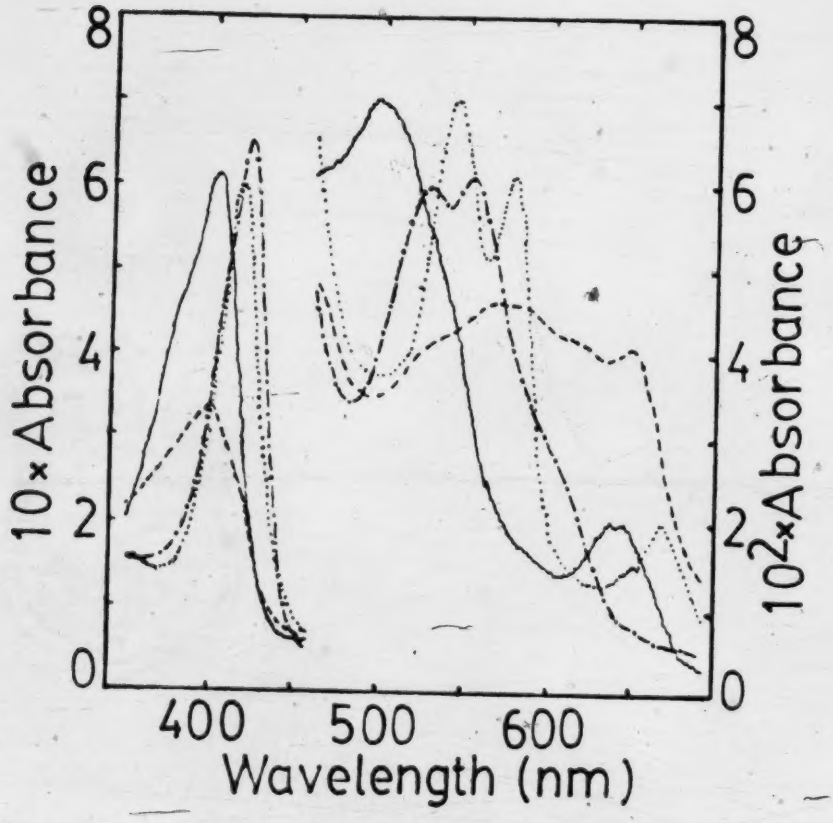

Figure I.2 Absorption spectra in the Soret and visible regions of horseradish peroxidase (HRP, 5.9 μM) and its intermediate compounds at pH 9.8 and 25°C. —— native HRP, --- compound I, -·-· compound II, and ···· compound III.

coworkers (50) deduced that the sixth ligand was the imidazole group of a histidine residue in the apoprotein by interpreting the EPR data of various cytochromes P-450 and their model complexes in terms of crystal-field theory. In contrast, Griffin and Peterson (51) suggested the presence of a water molecule at the sixth coordination position of the ferric low-spin form based on the measurement of spin relaxation rate of water protons by means of the pulse NMR technique. Most recent studies provide strong evidence that the native sixth ligand of the ferric low-spin cytochrome P-450 is oxygen rather than nitrogen (52-54).

The cytochromes P-450 are widely distributed in nature. They occur in various bacteria (55-57), insects (58), yeast (59), green plants (60) and several mammalian tissues (38,39,61). In addition to its biological role in oxygen activation for hydroxylation reactions, cytochromes P-450 possess a number of unique properties which have attracted the interest of biochemists studying its physical and chemical properties, pharmacologists concerned with drug metabolism, endocrinologists studying steroid biosynthesis, clinicians interested in bile pigment formation, and cell biologists examining the regulation and control of cellular metabolism (62).

Cytochrome P-450$_{scc}$

Since the first description of the existence of mitochondrial cytochrome P-450 in the adrenal cortex, reported in 1964 by Harding and his coworkers (61), much has been learned of its role on essential steroid hydroxylation in corticosteroid biosynthesis. The steroid production is initiated in the mitochondria through the action of cytochrome P-450$_{scc}$ which catalyzes the cholesterol side-chain cleavage reaction. Subsequently, the steroid produced, pregnenolone, is first converted to progesterone, and then hydroxylated at the C_{21} position by the microsomal cytochrome P-450$_{21}$ to form deoxycorticosterone. The mitochondrial cytochrome P-450$_{11\beta}$ catalyzing both the 11β-hydroxylase and 18-hydroxylase reactions complete the biosynthesis of corticosterone and aldosterone, respectively (63,64).

Cytochrome P-450$_{scc}$ is located in the inner mitochondrial membrane of the adrenal cortex (65,66). It catalyzes the rate-limiting step in steroidogenesis, the conversion of cholesterol to pregnenolone, which involves three consecutive hydroxylations (67-69). Each hydroxylation requires two electrons, which are furnished by NADPH via adrenodoxin reductase and adrenodoxin, and one oxygen molecule (70,71). The stoichiometry for the overall reaction is (71):

$$\text{cholesterol} + 3O_2 + 3\text{NADPH} + 3H^+ \rightarrow$$
$$\text{pregnenolone} + \text{isocaproic aldehyde} + 3H_2O + 3\text{NADP}^+$$

A catalytic sequence (Fig. I.3) for the cholesterol side-chain cleavage reaction is proposed in a recent study (72). Cholesterol first binds to the native low-spin ferric enzyme and induces a spin change to a high-spin state; the ferric-cholesterol complex accepts one electron to form a ferrous-cholesterol complex which in turn interacts with molecular oxygen to form a ternary complex termed oxygenated cytochrome P-450_{scc}-cholesterol. This ternary complex accepts a second electron to form an ill-defined irreversible intermediate whose decay results in the formation of 22R-hydroxycholesterol. However, instead of product release and regeneration of the low-spin cholesterol-free cytochrome P-450_{scc}, 22R-hydroxycholesterol is retained and a further catalytic cycle produces 20α,22R-dihydroxycholesterol. Similarly 20α,22R-dihydroxycholesterol is retained at the active site of cytochrome P-450_{scc} and a third cycle results in oxidative cleavage to pregnenolone and isocaproic aldehyde. One of the most important steps in this proposed enzymatic cycle is the binding of one molecule of oxygen to the one-electron reduced form of the enzyme (70,73). This

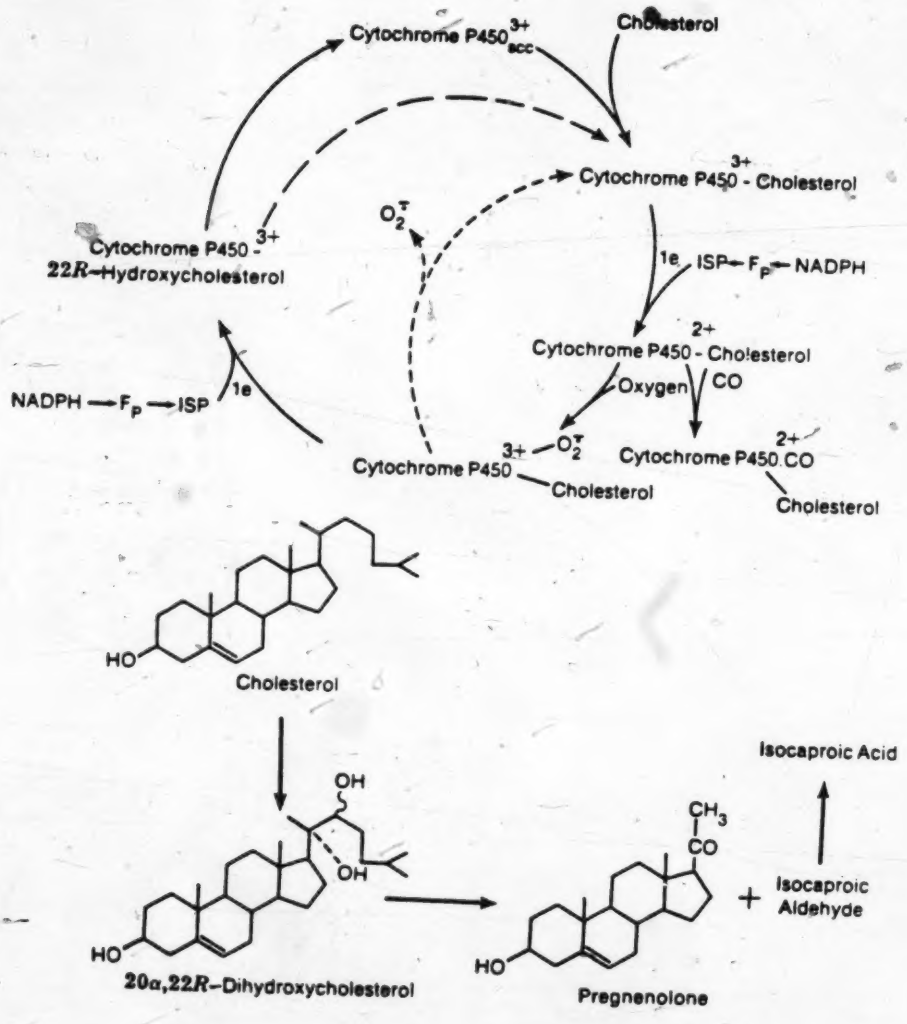

Figure I.3 Catalytic sequences for the cholesterol side-chain cleavage reaction. ISP, iron sulphur protein (adrenodoxin); F_p, flavoprotein (adrenodoxin reductase).

step is inhibited by carbon monoxide (74).

Cytochrome P-450$_{scc}$ has a molecular weight (M_r) of 49,000 and consists of two domains with M_r 27,000 and 22,000, respectively (75). It has been established that domain I containing a protoheme group is the N-terminal moiety, and domain II, the C-terminal moiety of the polypeptide chain of cytochrome P-450$_{scc}$ (76). The absorption spectra of various forms of beef adrenocortical cytochrome P-450$_{scc}$ are given in Appendix I.

The active site of cytochrome P-450$_{scc}$ has been probed by studies of cholesterol analogues that act as substrates and inhibitors. In the absence of cholesterol, P-450$_{scc}$ is essentially completely low-spin. Cholesterol combines with P-450$_{scc}$ to produce a predominantly high-spin state (80%) (72,77). Optical and EPR spectra primarily measure the proportions of high- and low-spin states. The EPR spectra of high- and low-spin heme proteins are distinct: low-spin ferric P-450$_{scc}$ has one unpaired electron and shows narrower EPR spectrum with g values of 2.424, 2.248 and 1.917 (78); high-spin P-450$_{scc}$ shows far wider separation between g values of 8.07, 3.60 and 1.70 (78,79). The interaction of hydroxylated derivatives with P-450$_{scc}$ depends on the position of the substitution. The effectiveness in inducing a high-spin state is particularly sensitive in enzymatically active positions: (20R,22R)-dihydroxy>(22R)>20α>pregnenolone

(80). Substitution at other positions around the cholesterol rings can either increase the extent of the high-spin state (7β OH) or favour the low-spin state (25 OH) relative to cholesterol (72). The steroid nucleus and hydrophobic side chain have different affinity and effect on spin state of cytochrome P-450$_{scc}$ (81). When the nucleus portion of steroid molecule binds to cytochrome P-450$_{scc}$ the low-spin state is formed. Conversely by binding of the side chain portion to the heme protein, the high-spin state is induced (81). A series of cholesterol analogues containing amino substituents in the side chain have also been tested for binding to cytochrome P-450$_{scc}$ (82-85). Substitution at 22-position produces a high-affinity for binding, potent competitive inhibition of cholesterol side-chain cleavage and a shift in the Soret absorption typical of amine complexes with P-450$_{scc}$ (λ_{max} 422 nm instead of 417 nm). When the amino substituent is shifted in either direction along the side chain, weaker inhibition and a shift of the Soret maximum back to 417 nm results. Thus the heme appears to be located sufficiently close to this position so that the 22R- and 22S-aminocholesterols competitively inhibit the side-chain cleavage by occupying the cholesterol binding pocket (84,85). The nature of cytochrome P-450$_{scc}$ cholesterol interaction has been studied using phospholipid-reconstituted heme proteins (86,87). Several lines of

evidence indicate that the substrate binding site is in the phospholipid membrane, since cholesterol is extremely hydrophobic and it is known to be integrated in biological membranes (86).

References

1. Bach, A. and Chodat, R. (1903) Ber. Deut. Chem. Ges. **36**, 600-605.
2. Yamazaki, I. (1974) in "Molecular Mechanisms of Oxygen Activation" (Hayaishi, O., ed.) Academic Press, New York, pp.535-538.
3. Hayaishi, O. (1964) Proc. Plenary Sessions, Int. Congr. Biochem. 6th, New York, 31-43.
4. Saunders, B.C., Holmes-Siedle, A.G. and Stark, B.P. (1964) in "Peroxidase", Butterworths, London, pp.40-52.
5. Hager, L.P., Morris, D.R., Brown, F.S. and Eberwein, H. (1966) J. Biol. Chem. **241**, 1769-1777.
6. Welinder, K.G. (1979) Eur. J. Biochem. **96**, 483-502.
7. Kay, E. Shannon, L.M. and Lew, J.Y. (1966) J. Biol. Chem. **242**, 2470-2473.
8. Delincee, H. and Radola, B.J. (1970) Biochim. Biophys. Acta **200**, 404-407.
9. Mazza, G., Job, C. and Bouchet, M. (1973) Biochim. Biophys. Acta **322**, 218-223.
10. Clarke, J. and Shannon, L.M. (1976) Biochim. Biophys. Acta **427**, 428-442.
11. Paul, K.-G. and Stigbrand, T. (1970) Acta Chem. Scand. **24**, 3607-3617.
12. Ellis, W.D. and Dunford, H.B. (1968) Can. J. Biochem. **46**, 1231-1235.

13. Haschke, R.H. and Friedhoff, J.M. (1978) Biochem. Biophys. Res. Commun. **80**, 1039-1042.

14. Ogawa, S., Shiro, Y. and Morishima, I. (1979) Biochem. Biophys. Res. Commun. **90**, 674-678.

15. Brill, A.S. and Sandberg, H.E. (1968) Biochemistry **7**, 4254-4260.

16. Yonetani, T., Yamamoto, H., Erman, J.E., Leigh, J.S. and Reed, G.H. (1972) J. Biol. Chem. **247**, 2447-2455.

17. Dunford, H.B. (1974) Physiol. Veg. **12**, 13-23.

18. Williams, R.J.P., Wright, P.E., Mazza, G. and Ricard, J.R. (1975) Biochim. Biophys. Acta **412**, 127-147.

19. Lanir, A. and Schejter, A. (1975) Biochem. Biophys. Res. Commun. **62**, 199-203.

20. Vuk-Pavlovic, S. and Benko, B. (1975) Biochem. Biophys. Res. Commun. **66**, 1154-1159.

21. Araiso, T. and Yamazaki, I. (1978) Biochemistry **17**, 942-946.

22. Job, D. and Dunford, H.B. (1978) Can. J. Chem. **56**, 1327-1334.

23. Morishima, I., Ogawa, S., Inubushi, T., Yonezawa, T. and Iizuka, T. (1977) Biochemistry **16**, 5109-5115.

24. Yamazaki, I., Yokota, K. and Tamura, M. (1966) in "Hemes and Hemoproteins" (Chance, B., Estabrook, R.H. and Yonetani, T., eds.) Academic Press, New York, pp.319-326.

25. Yamazaki, I. and Yokota, K. (1973) Mol. Cell. Biochem. **2**, 39-52.

26. Chance, B. (1952) Arch. Biochem. Biophys. **41**, 416-424.

27. George, P. (1952) Nature (London) **169**, 612-613.

28. Land, E.J. and Swallow, A.J. (1971) Biochim. Biophys. Acta **234**, 34-42.

29. Iyanagi, T., Nakamura, T., Ohnishi, T., Yamazaki, H. and Yamazaki, I. (1969) Biochim. Biophys. Acta **172**, 357-369.

30. Yokota, K. and Yamazaki, I. (1965) Biochim. Biophys. Acta **105**, 301-312.

31. Dolphin, D., Forman, A., Borg, D.C. and Fajer, J. (1971) Proc. Natl. Acad. Sci. U.S.A. **68**, 614-618.

32. Dolphin, D. and Felton, R.H. (1974) Accts. Chem. Res. **7**, 26-31.

33. George, P. (1953) Biochem. J. **54**, 267-276.

34. Hewson, W.D. and Hager, L.P. (1979) in "The Porphyrins" (Dolphin, D., ed.) Vol. VII, Academic Press, New York, pp.295-332.

35. Yamazaki, I. and Piette, L.H. (1963) Biochim. Biophys. Acta **77**, 47-64.

36. Tamura, M. and Yamazaki, I. (1972) J. Biochem. (Tokyo) **71**, 311-319.

37. Yamazaki, I. and Yokota, K. (1975) Biochem. Biophys. Res. Commun. **19**, 249-254.

38. Garfinkle, D. (1958) Arch. Biochem. Biophys. **77**, 493-509.

39. Klingenberg, M. (1958) Arch. Biochem. Biophys. **75**, 376-386.

40. Omura, T. and Sato, R. (1964) J. Biol. Chem. **239**, 2370-2378.

41. Omura, T. and Sato, R. (1964) J. Biol. Chem. **239**, 2379-2385.

42. Hayaishi, O. (ed.) (1974) in "Molecular Mechanisms of Oxygen Activation", Academic Press, New York, pp.1-28.

43. Ulrich, V. (1979) Topics in Current Chemistry **83**, 67-104.

44. Chang, C.K. and Dolphin, D. (1976) Proc. Natl. Acad. Sci. U.S.A. **73**, 3338-3342.

45. Cramer, S.P., Dawson, J.H., Hodgson, K.O. and Hager, L.P. (1978) J. Am. Chem. Soc. **100**, 7282-7290.

46. Jefcoate, C.R.E. and Gaylor, J.L. (1968) Biochemistry **8**, 3464-3472.

47. Koch, S., Tang, S.C., Holm, R.H., Frankel, R.B. and Ibers, J.A. (1975) J. Am. Chem. Soc. **97**, 916-918.

48. Ozaki, Y., Kitagawa, T., Kyogoku, Y., Imai, Y., Hashimoto-Yutsudo, C. and Sato, R. (1978) Biochemistry **17**, 5826-5831.

49. Jung, C. and Ristau, O. (1977) Chem. Phys. Lett. **49**, 103-108.

50. Chevion, M., Peisach, J. and Blumberg, W.E. (1977) J. Biol. Chem. **252**, 3637-3645.

51. Griffin, B.W. and Peterson, J.A. (1975) J. Biol. Chem. **250**, 6445-6451.

52. White, R.E. and Coon, M.J. (1982) J. Biol. Chem. **257**, 3073-3083.

53. Dawson, J.H., Anderson, L.A. and Sono, M. (1982) J. Biol. Chem. **257**, 3606-3617.

54. Yoshida, Y., Imai, Y. and Hashimoto-Yutsudo, C. (1982) J. Biochem. **91**, 1651-1659.

55. Peterson, J.A., Basu, D. and Coon, M.J. (1966) J. Biol. Chem. **241**, 5162-5164.

56. Katagiri, M., Ganguli, B.N. and Gunsalus, I.C. (1968) J. Biol. Chem. **243**, 3543-3546.

57. Appleby, C.A. (1969) Biochim. Biophys. Acta **172**, 71-87.

58. Fukami, J. Shishido, T., Fukunaga, K. and Casida, J. (1969) J. Agr. Food Chem. **17**, 1217-1226.

59. Lindenmayer, A. and Smith, L. (1964) Biochim. Biophys. Acta **93**, 445-461.

60. Hasson, E.P. and West, C.A. (1976) Plant Physiol. **58**, 479-486.

61. Harding, B.W., Wong, S.H. and Nelson, D.H. (1964) Biochim. Biophys. Acta **92**, 415-417.

62. Peterson, J.A., Ishimura, Y., Baron, J. and Estabrook, R.W. (1971) in "Oxidases and Related Redox Systems"

(King, T.W., Mason, H.S. and Morrison, M., eds.) Vol. II, University Park Press, Baltimore, pp.565-580.

63. Hall, P. (1984) Int. Rev. Cytol. **86**, 53-95.

64. Sato, H., Ashida, N., Suhara, K., Itagaki, E., Takemori, S. and Katagiri, M. (1978) Arch. Biochem. Biophys. **190**, 290-299.

65. Churchill, P.F., deAlvare, L.R. and Kimura, T. (1978) J. Biol. Chem. **253**, 4924-4929.

66. Churchill, P.F. and Kimura, T. (1979) J. Biol. Chem. **254**, 10443-10448.

67. Simpson, E.R. and Boyd, G.S. (1966) Biochem. Biophys. Res. Commun. **24**, 10-17.

68. Burstein, S. and Gut, M. (1976) Steroids **28**, 115-131.

69. Duque, C., Morisaki, M., Ikekawa, N. and Shikita, M. (1978) Biochem. Biophys. Res. Commun. **82**, 179-187.

70. Hume, R. and Boyd, G.S. (1978) Biochem. Soc. Trans. **6**, 893-898.

71. Shikita, M. and Hall, P.F. (1974) Proc. Natl. Acad. Sci. U.S.A. **71**, 1441-1445.

72. Hume, R., Kelly, R.W., Taylor, P.L. and Boyd, G.S. (1984) Eur. J. Biochem. **140**, 583-591.

73. Sato, R. and Omura, T. (eds.) (1978) in "Cytochrome P-450", Academic Press, New York, pp.214-220.

74. Simpson, E.R. and Boyd, G.S. (1967) Eur. J. Biochem. **2**, 275-285.

75. Chashchin, V.L., Vasilevsky, V.I., Shkumatov, V.M. and Akhrem, A.A. (1984) Biochim. Biophys. Acta **787**, 27-38.

76. Chashchin, V.L., Vasilevsky, V.I., Shkumatov, V.M., Lapko, V.N., Adamovich, T.B., Berikbaeva, T.M. and Akhrem, A.A. (1984) Biochim. Biophys. Acta **791**, 375-383.

77. Orme-Johnson, N.R., Light, D.R., White-Stevens, R.W. and Orme-Johnson, W.H. (1979) J. Biol. Chem. **254**, 2103-2111.

78. Simpson, E.R. and Williams-Smith, D.L. (1976) Biochim. Biophys. Acta **449**, 59-71.

79. Kominami, S., Ochi, H. and Takemori, S. (1979) Biochim. Biophys. Acta **577**, 170-176.

80. Jefcoate, C.R. (1986) in "Cytochrome P-450" (Ortiz de Montellano, P.R., ed) Plenum Press, New York, pp.387-428.

81. Kido, T., Yamakura, F. and Kimura, T. (1981) Biochim. Biophys. Acta **666**, 370-381.

82. Sheets, J.J. and Vickery, L.E. (1982) Proc. Natl. Acad. Sci., U.S.A. **79**, 5775-5777.

83. Sheets, J.J. and Vickery, L.E. (1983) J. Biol. Chem. **258**, 1720-1725.

84. Nagahisa, A., Foo, T., Gut, M. and Orme-Johnson, W.H. (1985) J. Biol. Chem. **260**, 846-851.

85. Sheets, J.J. and Vickery, L.E. (1983) J. Biol. Chem. **258**, 11446-11452.

86. Seybert, D.W., Lancaster, J.R., Lambeth, J.D. and Kamin, H. (1979) J. Biol. Chem. **254**, 12088-12098.

87. Yamakura, F., Kido, T. and Kimura, T. (1981) Biochim. Biophys. Acta **649**, 343-354.

CHAPTER TWO

KINETICS OF THE OXIDATION OF REDUCED NICOTINAMIDE ADENINE DINUCLEOTIDE BY HORSERADISH PEROXIDASE COMPOUNDS I AND II.[1]

[1]A version of this chapter has been published. Kashem, M.A. and Dunford, H.B. (1986) Biochem. Cell. Biol. 64, 323-327.

Introduction

HRP catalyzes the oxidation of a wide variety of reducing substrates, AH_2, by hydrogen peroxide. The generally accepted mechanism for the enzymatic cycle is (1,2):

[1] $$HRP + H_2O_2 \rightarrow HRP\text{-}I + H_2O$$

[2] $$HRP\text{-}I + AH_2 \rightarrow HRP\text{-}II + AH\cdot$$

[3] $$HRP\text{-}II + AH_2 \rightarrow HRP + AH\cdot$$

This is also the case when the reducing substrate is NADH. Under aerobic conditions, however, the one electron oxidized form of NADH (NAD·) reacts with molecular oxygen in the solution (3-5)

[4] $$NAD\cdot + O_2 \rightarrow NAD^+ + O_2^{\cdot-}$$

[5] $$HRP + O_2^{\cdot-} \rightarrow HRP\text{-}III$$

and a good yield of HRP-III is obtained. If the supply of molecular oxygen is depleted, then replenished in cycles, the concentrations of both HRP-III and O_2 oscillate in a very complicated reaction, which probably involves free radical chains (6-8).

The pH dependent kinetics of the reactions of HRP-I and HRP-II with several reducing substrates have been studied in our laboratory (for a review see Ref. 9). The results

indicate that an acid group with a pK_a around 5.0 is important in HRP-I catalyzed reactions. In HRP-II two groups, one with pK_a 8.6, the other with a very low pK_a, have varying influences upon reaction rates. The pK_a values of 5.0 in HRP-I reactions and 8.6 for HRP-II have been confirmed by spectrophotometric titration with acid or alkali and pH-stat titration of the oxidation-reduction reaction (10-11).

In this chapter we report for the first time the transient-state kinetics as a function of pH of HRP-I and HRP-II reactions using NADH as a reducing substrate. Rate constants at pH 5.6 were reported previously (8).

Materials and Methods

HRP was purchased from Boehringer Mannheim Corp. as an ammonium sulphate precipitate. The HRP stock solution was prepared by extensive dialysis of ammonium sulfate precipitate against distilled water purified by a Milli-Q water purification system (Millipore). The HRP solution was then filtered through a Millex-GV 0.22 μm filter (Millipore) to remove insoluble material. The enzyme concentration was determined from absorbance measurements at 403 nm using a molar absorptivity of 1.02×10^5 M^{-1} cm^{-1} (12). NADH was obtained from Sigma Chemical Company as a disodium salt. The NADH concentration was determined spectrophotometrically

at 340 nm using a molar absorptivity of 6.2×10^3 M^{-1} cm^{-1} (13). SOD from bovine blood containing 2-5% potassium phosphate buffer salts was also purchased from Sigma Chemical Company. All other chemicals were reagent grade and used without further purification.

Routine observations of the spectra of NADH and of HRP and its compounds, and all rate constants for the HRP-II - NADH reaction at pH 6.44 or greater were obtained at 25.0 ± 0.2°C on a Cary 219 spectrophotometer equipped with thermally jacketted cuvette holders. The stopped-flow kinetic experiments were performed on a Union Giken Rapid Reaction Analyzer model RA-601 equipped with a 1 cm cell thermostated to 25.0 ± 0.2°C. The total ionic strength of all solutions was adjusted to 0.11 using potassium sulphate as an inert salt if necessary.

HRP-I and HRP-II were prepared prior to each experiment: for HRP-I, by adding calculated amounts of HRP and hydrogen peroxide solutions; for HRP-II, HRP-I and potassium ferrocyanide solutions (9,14). To avoid denaturation of the enzyme in experiments below pH 5 a pH-jump method was used; buffer was placed only in the drive syringe containing the substrate. As NADH is unstable at acidic pH values, the sample solutions of NADH were prepared immediately before the experiment by diluting the stock solution (~1 mM in 10^{-4} M NaOH) in buffer of the desired pH

value. Blank experiments indicated negligible spontaneous decomposition of NADH under the conditions of our experiments. At the most acidic pH values a ~2.5-fold excess of SOD relative to HRP was added to the NADH solution in order to inhibit the formation of HRP-III (8). The reaction of HRP-I with NADH was followed at 411 nm, the isosbestic wavelength between HRP-II and native HRP. The HRP-II reaction with NADH was followed at 420 nm. Blank experiments on HRP-I and HRP-II indicated negligible spontaneous decomposition during the time required for the experiments.

The enzyme concentration for all kinetic measurements was 1.67 μM for HRP-II reactions and 2.25 μM for HRP-I reactions. NADH concentrations were chosen from 12.5 to 100.0 μM to yield conveniently measurable kinetics. For the above conditions, all kinetic curves were found to be pseudo-first-order (Fig. II.1, II.2) Rate constants were determined from a non-linear least-squares analysis (15) of experimental curves. Between five and six determinations of rate constants were performed for every NADH concentration and the mean value for the observed rate constant was used in the calculation.

The solutions were collected after the reactions and the pH values were determined with a Fisher digital pH meter model 420 equipped with a Fisher Microprobe combination

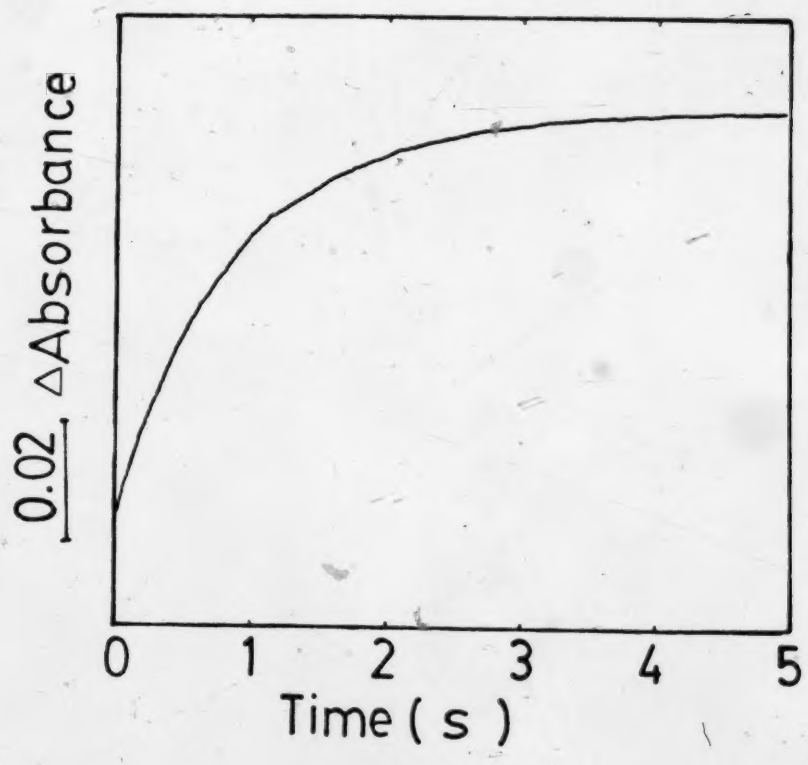

Figure II.1 **Absorbance changes with time of the reaction of NADH with HRP-I at pH 6.13 and 25°C as recorded on the stopped-flow apparatus at 411 nm. Final concentrations were 2.25 μM HRP-I and 100 μM NADH.**

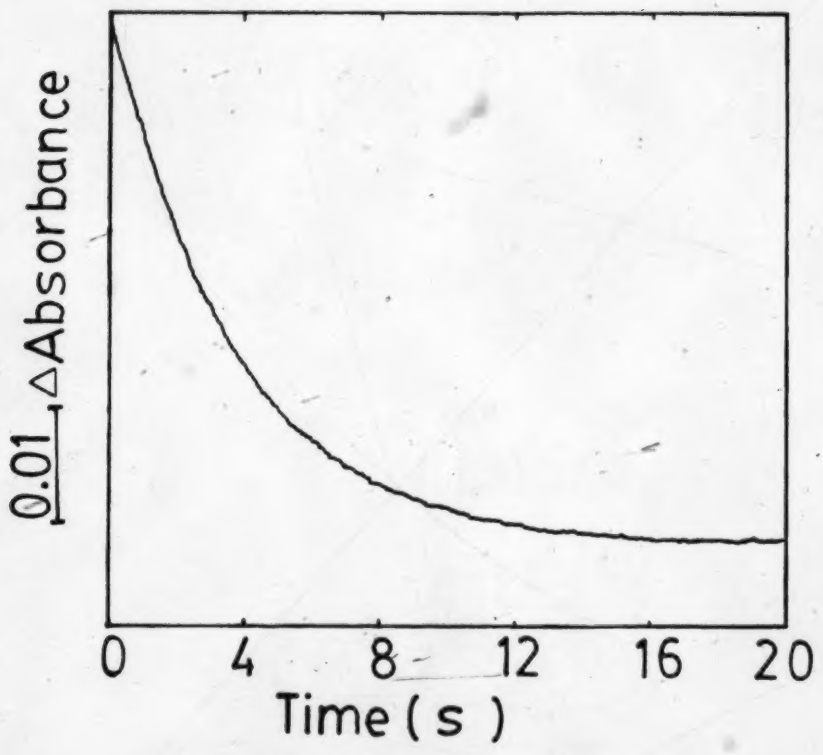

Figure II.2 Absorbance changes with time of the reaction of NADH with HRP-II at pH 6.14 and 25°C as recorded on the stopped-flow apparatus at 420 nm. Final concentrations were 1.67 μM HRP-II and 100 μM NADH.

glass electrode. The pH meter was calibrated to ±0.03 pH unit with standard buffers.

Results

Kinetics of the HRP-I-NADH reaction

It was found experimentally that with a sufficiently large excess of NADH, the reaction of HRP-I at a given pH is consistent with the differential rate expression

$$[6] \qquad \frac{-d[\text{HRP-I}]}{dt} = k_{1,obs}[\text{HRP-I}]$$

For all the pH values studied true second-order kinetics are demonstrated, within the limits of experimental error, by the linearity and zero intercept of the plots (Fig. II.3) obeying Eqn. [7]:

$$[7] \qquad k_{1,obs} = k_{1,app}[\text{NADH}]$$

The logarithm of $k_{1,app}$ is plotted versus pH in Fig. II.4. The results are in good agreement with the following mechanism:

$$[8] \qquad \begin{array}{ccccc} \text{E} & + & \text{S} & \xrightarrow{k_1} & \text{products} \\ \rightleftharpoons\ (H^+,\ K_1) & & & & \\ \text{EH} & + & \text{S} & \xrightarrow{k_2} & \text{products} \end{array}$$

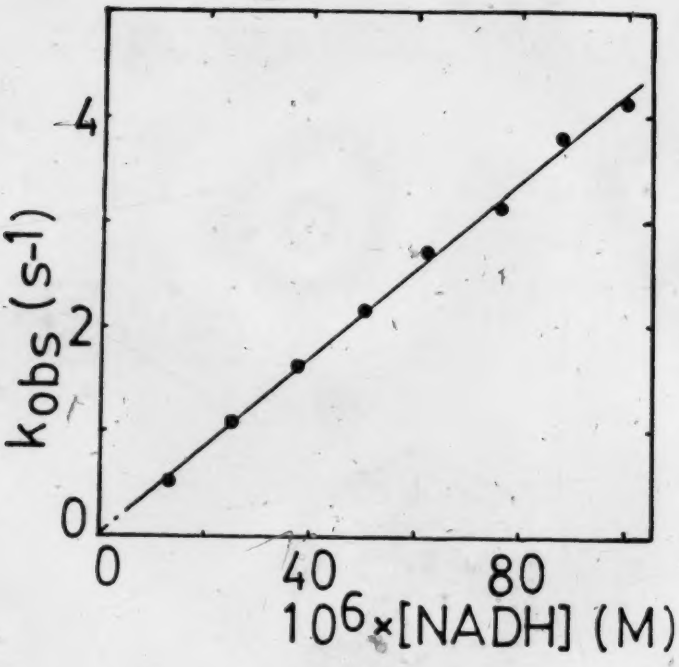

Figure II.3 Pseudo-first order plot of the reaction of NADH with HRP-I at pH 5.38 and 25°C. The straight line is the weighted least squares best-fit line. The HRP-I concentration was 2.25 μM.

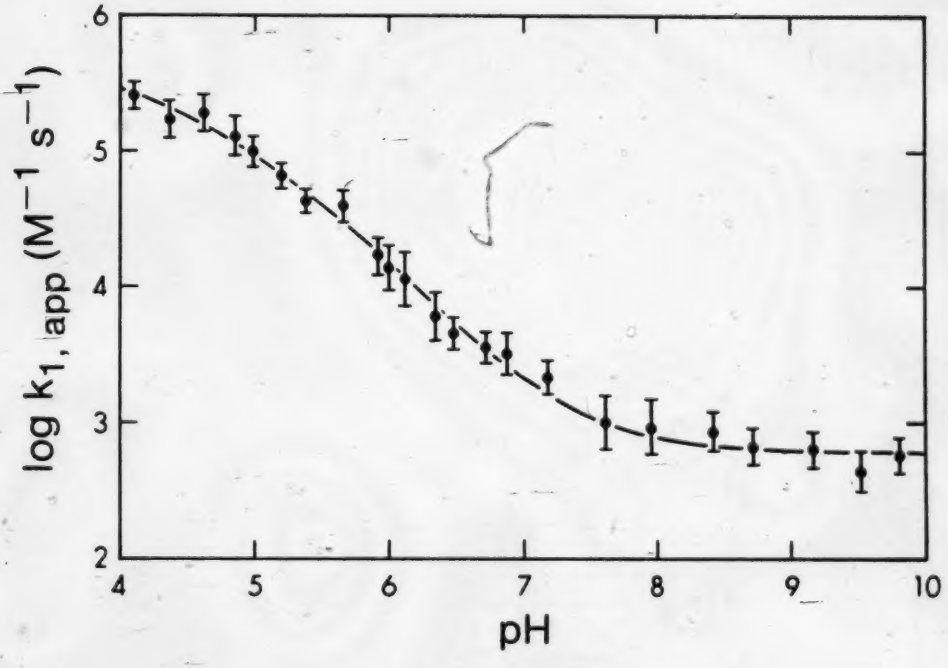

Figure II.4 Plot of logarithm of second-order rate constant, $k_{1,app}$, for the reaction of HRP-I with NADH vs. pH. The error limits drawn on the data points are based on the standard deviation calculated from the data. The curve was calculated from a least-squares fit of the data to Eqn. [9].

where EH and E represent HRP-I with a catalytically important group protonated and deprotonated, K_1 is the corresponding acid dissociation constant and k_1 and k_2 are second-order rate constants. The apparent second-order rate constant, $k_{1,app}$, is given by

$$[9] \qquad k_{1,app} = \frac{(k_1 + \frac{k_2[H^+]}{K_1})}{(1 + \frac{[H^+]}{K_1})}$$

which gave a best fit to the experimental data with parameter values given in Table II.1. The solid line in Fig. II.4 is calculated using the constants of Table II.I.

Kinetics of the HRP-II-NADH reaction

The kinetic behaviour of the HRP-II reaction with NADH is found to be rather different from that of HRP-I. At all pH values positive intercepts in the plots of $k_{2,obs}$ versus NADH concentration, Fig. II.5, were observed. These results can be fit by the equation

$$[10] \qquad k_{2,obs} = k_{2,app}[NADH] + k_{-2}$$

A plot of the logarithm of $k_{2,app}$ versus pH is shown in Fig. II.6. The simplest mechanism that leads to an approximation of the $k_{2,app}$ data is given by:

TABLE II.1. Parameters obtained from the pH dependence of the second-order rate constant for the reduction of HRP-I by NADH.

Parameters	Value[a]
k_1 (M^{-1} s^{-1})	$(6.2\pm0.5) \times 10^2$
k_2 (M^{-1} s^{-1})	$(3.3\pm0.7) \times 10^5$
pK_1	4.7 ± 0.5

[a]The errors are ± the relative standard deviation obtained from the non-linear least-squares fit to the experimental data.

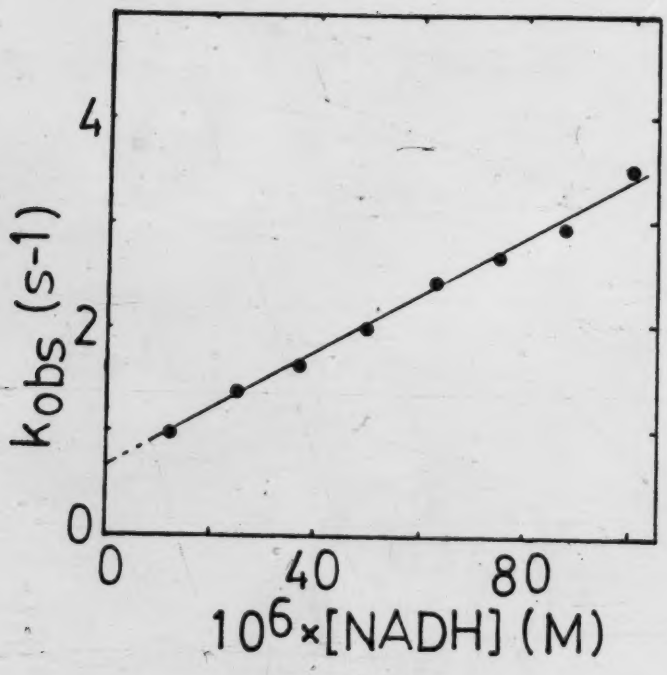

Figure II.5 Pseudo-first order plot of the reaction of NADH with HRP-II at pH 5.62 and 25°C. The straight line is the weighted least squares best-fit line. The HRP-II concentration was 1.67 μM.

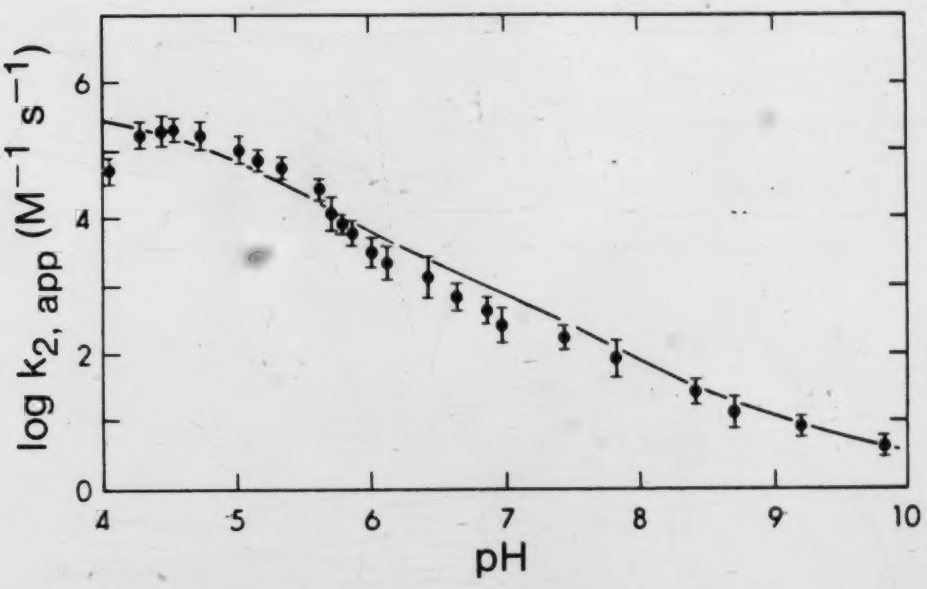

Figure II.6 Plot of the logarithm of the second-order rate constant, $k_{2,app}$, for the reaction of HRP-II with NADH vs. pH. The error limits drawn on the data points are based on the standard deviation calculated from the data. The curve was computed on the basis of best fit parameters obtained for Eqn. [12].

[11]

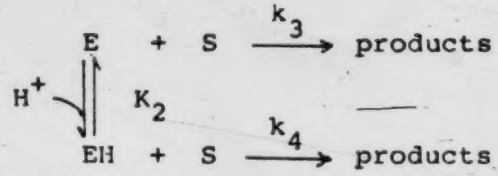

where EH, and E are two differently protonated forms of HRP-II, K_2 is the corresponding acid dissociation constant, and k_3, and k_4 are second-order rate constants. The apparent second-order rate constant, $k_{2,app}$, for this scheme is given by Eqn [12]:

[12]
$$k_{2,app} = \frac{(k_3 + \frac{k_4}{K_2}[H^+])}{(1 + \frac{[H^+]}{K_2})}$$

The best fit parameters, given in Table II.2, are used to calculate the solid line in Fig. II.6. A few representative values of k_{-2} are given in Table II.3.

Discussion

The previous determination at a single pH of rate constants for the reactions of HRP-I and HRP-II with NADH (8) are not in close agreement with ours. The comparison (with the results of Ref. 8, in brackets) is: for HRP-I - NADH $(4.0\pm0.1)\times10^4$ M^{-1} s^{-1}, pH 5.67 compared to (5.4×10^3 M^{-1} s^{-1}, pH 5.6) and for HRP-II - NADH $(2.6\pm0.1)\times10^4$ M^{-1} s^{-1}, pH 5.62 (8.0×10^2 M^{-1} s^{-1}, pH 5.6).

TABLE II.2. Parameters obtained from the pH dependence of the second-order rate constant for the reduction of HRP-II by NADH.

Parameters	Value[a]
k_3 (M^{-1} s^{-1})	3.0±1.9
k_4 (M^{-1} s^{-1})	(4.8±2.9) x 10^5
pK_2	4.2±1.4

[a]The errors are as in Table II.1.

TABLE II.3. Some values of the apparent reverse rate constant, k_{-2}, for the HRP-II - NADH reaction (Eq. 10).

pH	$k_{-2}(s^{-1})$
4.46	2.9 ± 0.3
5.62	$(6.7 \pm 0.3) \times 10^{-1}$
6.66	$(9.8 \pm 0.7) \times 10^{-3}$
8.71	$(1.4 \pm 0.1) \times 10^{-3}$

However, a reasonable support for our results might be found in the following consideration. Avigliano et al. (16) have reported that the initial oxidation rate of NADH in the presence of HRP and H_2O_2 are 160 nmol/min at pH 5.2 and 8 nmol/min at pH 7.2. Applying the steady state approximation to the peroxidase-oxidase enzymatic cycle (Eqs. 1-3) and using the values of our rate constants ($k_{1,app}$ and $k_{2,app}$) and also 1.8×10^7 M^{-1} s^{-1} as the rate constant for reaction 1 (9), the rate of NADH oxidation is calculated to be 790 nmol/min at pH 5.2 and 6.5 nmol/min at pH 7.2. Although the predicted value of the NADH oxidation rate at pH 7.2 is almost identical with the value of Avigliano et al., the value at pH 5.2 is about five times higher. An identical experiment done in our laboratory yielded the values of initial oxidation rate of NADH as 564 nmol/min at pH 5.2 and 5.4 nmol/min at pH 7.2 which are in agreement with the calculated values. It appears therefore that the transient state kinetic results obtained by this study for the HRP-I-NADH and HRP-II-NADH reactions are consistent with the simple enzymatic cycle (Eqs. 1-3).

The pK_1 value of 4.7 ± 0.5 for a catalytically active acid group in HRP-I and the lack of reversibility of the HRP-I - NADH reaction is in complete accord with results obtained in the reaction of HRP-I with other substrates such as ferrocyanide and p-aminobenzoic acid (9). The same reaction mechanisms would appear to apply.

The forward reaction of HRP-II with NADH does not fit the pattern observed for most other substrates. However, the pH-rate profile does resemble that obtained with bisulfite, a substrate which attacks the heme after a few reaction cycles (17,18). The vaguely defined value of 4.2 ± 1.4 for pK_2 can account for the decrease in rate with increasing pH. The decrease in rate constant for the HRP-II - NADH reaction with decreasing pH in the region of pH 4 may be accounted for by the acid ionization of the substrate NADH with a pK_s value of 3.9 (19,20) which has been assigned to the adenine-N-1 of the dinucleotide (21). However this minor correction does not improve the calculated fit to the data in Fig. II.6 at higher pH. There is a detectable break in the pH rate profile just below pH 6 (Fig. II.6). This is close to the region where we were forced to switch from stopped-flow to conventional spectrophotometric kinetic measurements. In this region where both types of measurements are being pushed to one of their limits some systematic errors may be involved. Therefore we did not attempt to fit the data with a more complicated equation. The more parameters the better the fit but we do not yet feel that additional parameters are justified.

The apparent reversibility of the HRP-II reaction with NADH would indicate that NAD• can oxidize native HRP to HRP-II. The reduction potential of NAD•/NADH couple has

been estimated to be about 0.30 V at pH 7.0 (22,23). The reduction potentials of HRP-I/HRP-II and HRP-II/HRP couples have been intensively investigated as a function of pH using both equilibrium and kinetic measurements (24). At acidic pH (near pH 6.3) the reduction potentials for both the couples are almost idential (~0.96 V). Above pH 8.6 (isozyme C), the HRP-I/HRP-II potential is constant (~0.82 V), the HRP-II/HRP potential continues to decrease and at pH 12.0 it becomes ~0.5 V. Thus, it becomes easier to oxidize HRP to HRP-II at higher pH. In accord with this, the rate constant for the oxidation of HRP to HRP-II by K_2IrCl_6 increases with increasing pH (24). In contrast, the values of k_{-2} decreases with increasing pH (Table II.3). Moreover, the redox potential values indicate that the oxidation of HRP to HRP-II by NAD• is not a thermodynamically advantageous process. A possible explanation may be found in the complexities of the oxidase reaction of HRP with NADH.

When HRP is mixed with an oxygenated solution of NADH in a closed system an extremely complicated reaction cycle occurs which has been explained using eleven elementary reactions and nine rate equations (6,8). The cycle, initiated by introducing trace amounts of H_2O_2 either deliberately or by the autoxidation of the NADH, passes through burst, induction, steady state and termination

phases. The NAD• is known to react with O_2 with a rate constant of 2.0×10^9 M^{-1} s^{-1} (3). Other competing reactions for NAD• have been proposed (8). It would appear therefore that our values of k_{-2} reflect only that fraction of NAD• which is oxidizing HRP to HRP-II with a large amount of the NAD• being consumed elsewhere. In the absence of molecular oxygen as a scavenger, the NAD• radicals dimerize (3) forming a product which is also reactive with HRP (16). However these conditions do not apply to our experiments.

The new transient state kinetic data presented in this chapter define accurately the rate constants for two of the elementary reactions involved in the oxidase reaction of HRP with NADH as a function of pH. The apparent reversibility of the HRP-II - NADH reaction has been noted for the first time. These kinetic constants, of value in their own right, contribute to a better understanding of details of the normal peroxidatic cycle. They are also relevant to the action of peroxidase as an oxidase and to oscillatory reactions of HRP.

Supplementary material available

All rate constants with standard deviations for the reaction of HRP-I (Table II.4) and HRP-II (Table II.5) with NADH as a function of pH with the buffers used are listed on two supplementary pages.

TABLE II.4. Kinetic parameters for the reaction of NADH with HRP-I at 25.0°C and μ = 0.11

pH	$k_{1,app}$[a] (M^{-1} s^{-1})	Buffer[b]
4.08	$(2.6\pm0.1) \times 10^5$	A
4.37	$(1.7\pm0.1) \times 10^5$	A
4.63	$(1.9\pm0.1) \times 10^5$	A
4.84	$(1.3\pm0.1) \times 10^5$	A
4.98	$(8.3\pm0.3) \times 10^4$	A
5.21	$(6.7\pm0.1) \times 10^4$	A
5.38	$(4.2\pm0.1) \times 10^4$	A
5.67	$(4.0\pm0.1) \times 10^4$	A
5.92	$(1.6\pm0.1) \times 10^4$	B
5.98	$(1.3\pm0.1) \times 10^4$	B
6.13	$(1.2\pm0.1) \times 10^4$	B
6.33	$(5.6\pm0.4) \times 10^3$	B
6.48	$(4.2\pm0.1) \times 10^3$	B
6.72	$(3.6\pm0.1) \times 10^3$	B
6.89	$(3.1\pm0.1) \times 10^3$	B
7.20	$(2.0\pm0.1) \times 10^3$	B
7.62	$(9.3\pm0.8) \times 10^2$	B
7.96	$(9.1\pm0.9) \times 10^2$	C
8.42	$(8.7\pm0.4) \times 10^2$	C
8.71	$(5.9\pm0.3) \times 10^2$	C
9.15	$(6.0\pm0.2) \times 10^2$	C
9.51	$(4.1\pm0.2) \times 10^2$	D
9.81	$(5.6\pm0.2) \times 10^2$	D

[a]Errors of rate constants represents the standard deviation calculated from data at a given pH.
[b]Buffer abbreviations are: A, citric acid-sodium citrate; B, potassium dihydrogen phosphate-disodium hydrogen phosphate; C, tris-nitric acid; D, sodium bicarbonate-sodium hydroxide.

TABLE II.5. Kinetic parameters for the reaction of NADH with HRP-II at 25.0°C and μ = 0.11

pH	$k_{2,app}$[a] (M^{-1} s^{-1})	k_{-2}[a] (s^{-1})	Buffer[b]
4.06	$(4.4\pm0.5) \times 10^{4}$	(1.1 ± 0.1)	A
4.29	$(1.7\pm0.1) \times 10^{5}$	(1.4 ± 0.2)	A
4.46	$(2.2\pm0.1) \times 10^{5}$	(2.9 ± 0.3)	A
4.54	$(2.1\pm0.2) \times 10^{5}$	(2.3 ± 0.4)	A
4.74	$(1.6\pm0.1) \times 10^{5}$	(2.6 ± 0.2)	A
5.03	$(9.4\pm0.4) \times 10^{4}$	$(8.9\pm1.0) \times 10^{-1}$	A
5.18	$(8.2\pm0.3) \times 10^{4}$	$(5.0\pm0.5) \times 10^{-1}$	A
5.36	$(6.3\pm0.4) \times 10^{4}$	$(9.7\pm1.5) \times 10^{-1}$	A
5.62	$(2.6\pm0.1) \times 10^{4}$	$(6.7\pm0.3) \times 10^{-1}$	A
5.74	$(1.2\pm0.1) \times 10^{4}$	$(2.8\pm0.3) \times 10^{-1}$	A
5.80	$(9.7\pm0.4) \times 10^{3}$	$(4.1\pm0.4) \times 10^{-1}$	A
5.87	$(7.5\pm0.5) \times 10^{3}$	$(4.6\pm0.3) \times 10^{-1}$	B
6.02	$(3.4\pm0.2) \times 10^{3}$	$(1.0\pm0.1) \times 10^{-2}$	B
6.14	$(2.1\pm0.2) \times 10^{3}$	$(1.4\pm0.2) \times 10^{-2}$	B
6.44	$(1.4\pm0.2) \times 10^{3}$	$(1.7\pm0.1) \times 10^{-2}$	B
6.66	$(7.3\pm0.3) \times 10^{2}$	$(9.8\pm0.7) \times 10^{-3}$	B
6.88	$(4.6\pm0.4) \times 10^{2}$	$(4.9\pm0.5) \times 10^{-3}$	B
6.98	$(2.3\pm0.2) \times 10^{2}$	$(3.8\pm0.2) \times 10^{-3}$	B
7.46	$(1.8\pm0.2) \times 10^{2}$	$(7.1\pm1.0) \times 10^{-3}$	B
7.85	$(8.0\pm0.7) \times 10^{1}$	$(1.7\pm0.1) \times 10^{-3}$	C
8.42	$(2.6\pm0.2) \times 10^{1}$	$(5.3\pm0.4) \times 10^{-3}$	C
8.71	$(1.4\pm0.1) \times 10^{1}$	$(1.4\pm0.1) \times 10^{-3}$	C
9.21	(8.3 ± 0.5)	$(8.0\pm0.4) \times 10^{-4}$	D
9.82	(4.1 ± 0.3)	$(1.3\pm0.1) \times 10^{-4}$	D

[a]Errors of rate constants represents the standard deviation calculation from data at a given pH.
[b]Buffer abbreviations are: A, citric acid-sodium citrate; B, potassium dihydrogen phosphate-disodium hydrogen phosphate; C, tris-nitric acid; D, sodium bicarbonate-sodium hydroxide.

References

1. Chance, B. (1952) Arch. Biochem. Biophys. **41**, 416-424.
2. George, P. (1952) Nature **169**, 612-613.
3. Land, E.J. & Swallow, A.J. (1971) Biochim. Biophys. Acta **234**, 34-42.
4. Iyanagi, T., Nakamura, T., Ohnishi, T., Yamazaki, H. & Yamazaki, I. (1969) Biochim. Biophys. Acta **172**, 357-369.
5. Yokota, K. & Yamazaki, I. (1965) Biochim. Biophys. Acta **105**, 301-312.
6. Olsen, L.F. (1984) in Stochastic Phenomena and Chaotic Behaviour in Complex Systems (Schuster, P., Ed.) pp.116-123, Springer-Verlag, Berlin.
7. Degn, H. & Olsen, L.F. (1978) Biochim. Biophys. Acta **523**, 321-334.
8. Yokota, K. & Yamazaki, I. (1977) Biochemistry **16**, 1913-1920.
9. Dunford, H.B. & Stillman, J.S. (1976) Coord. Chem. Rev. **19**, 187-251.
10. Hayashi, Y. & Yamazaki, I. (1978) Arch. Biochem. Biophys. **190**, 446-453.
11. Yamada, H. & Yamazaki, I. (1974) Arch. Biochem. Biophys. **165**, 728-738.
12. Schonbaum, G.R. & Lo, S. (1972) J. Biol. Chem. **247**, 3353-3360.

13. Bock, R.M., Montgomery, B.A. & Siegel, J.M. (1959) Arch. Biochem. Biophys. **82**, 288-299.

14. Dunford, H.B., Hewson, W.D. & Steiner, H. (1978) Can. J. Chem. **56**, 2844-2852.

15. Dunford, H.B., Evett, M. & Roman, R. (1971) Can. J. Chem. **49**, 3059-3063.

16. Avigliano, L., Carelli, V., Casini, A., Finazzi-Agro, A. and Liberatore, F. (1985) Biochem. J. **226**, 391-395.

17. Roman, R. and Dunford, H.B. (1973) Am. J. Chem. **51**, 588-596.

18. Araiso, T., Miyoshi, K. and Yamazaki, I. (1976) Biochemistry **15**, 3059-3063.

19. Kaplan, N.O., Lamborg, M. & Stolzenback, F.E. (1958) J. Biol. Chem. **231**, 685-694.

20. Moore, C.E. & Underwood, A.L. (1969) Anal. Biochem. **29**, 149-153.

21. Blumenstein, M. & Raftery, M.A. (1972) Biochemistry **9**, 1643-1646.

22. Farrington, J.A., Land, E.J. and Swallow, A.J. (1980) Biochim. Biophys. Acta **590**, 273-276.

23. Anderson, R.F. (1980) Biochim. Biophys. Acta **590**, 277-281.

24. Hayashi, Y. & Yamazaki, I. (1979) J. Biol. Chem. **254**, 9101-9106.

CHAPTER THREE

RAPID SPECTRAL SCAN AND STOPPED-FLOW STUDIES OF CARBON MONOXIDE BINDING TO BEEF ADRENOCORTICAL CYTOCHROME $P\text{-}450_{scc}$[1]

[1] A version of this chapter by Kashem, M.A., Lambeir, A.-M. and Dunford, H.B. has been accepted for publication in Biochim. Biophys. Acta.

Introduction

The cytochromes P-450 are a unique class of hemoproteins that catalyze the hydroxylation of a wide variety of organic compounds through the activation of molecular oxygen (1). In the adrenal cortex cytochrome $P\text{-}450_{scc}$ catalyzes the rate limiting step in steroidogenesis, cleavage of the side chain of cholesterol to produce pregnenolone (2-3). The reaction requires three oxidative steps, utilizing 3 mol of NADPH and 3 mol of O_2/mol of pregnenolone formed. Each hydroxylation requires 2 electrons which are furnished by NADPH via adrenodoxin reductase and adrenodoxin (4-7). One of the most important steps in the proposed catalytic cycle (6) for the cholesterol side-chain cleavage reaction is the binding of one molecule of oxygen to the one-electron-reduced form of the enzyme (4,7). This step is inhibited by carbon monoxide (8). Thus, understanding the mechanism of ligand binding to reduced cytochrome $P\text{-}450_{scc}$, of importance in its own right, is essential to an understanding of the enzymatic reaction cycle.

Cytochrome $P\text{-}450_{scc}$ is in many respects similar to the Pseudomonas putida cytochrome $P\text{-}450_{cam}$ which functions in the camphor hydroxylation (9,10). Previous studies on carbon monoxide binding with Pseudomonas putida cytochrome $P\text{-}450_{cam}$ indicate that camphor is bound to ferrous

cytochrome P-450$_{cam}$ at a site which markedly modifies the carbon monoxide (oxygen) binding site on the heme iron (11).

In this chapter we report upon the rapid spectral scan and transient-state kinetics as a function of pH of carbon monoxide binding with the cholesterol-free and cholesterol-bound forms of reduced cytochrome P-450$_{scc}$. Both cholesterol-free and cholesterol-bound forms of the enzyme were purified independently from beef adrenocortical mitochondria by using two different procedures (10,12). Rate constants at a single pH have been reported previously (13).

Materials and Methods

Purification of cytochromes P-450$_{scc}$

Cholesterol-free cytochrome P-450$_{scc}$ was purified from beef adrenocortical mitochondria by cholate extraction, octylamine-Sepharose 4B affinity chromatography, and DEAE-cellulose column chromatography as described previously (12). The purified sample had a specific concentration of 5 nmol of P-450-heme per mg of protein. Octylamine-Sepharose 4B gel was prepared by a slight modification of the reported methodology (12). CNBr-activated Sepharose 4B was used instead of Sepharose 4B and the coupling reaction was carried out at room temperature for 2 h.

Cholesterol-bound cytochrome P-450$_{scc}$ was purified from beef adrenocortical mitochondria using described methodology

(10) by cholate extraction, ammonium sulfate fractionation, aniline-Sepharose 4B affinity chromatography, and adrenodoxin-Sepharose 4B affinity chromatography. Purified P-450$_{scc}$ had an A_{280}/A_{393} ratio of 1.2, which corresponds to 13 nmol P-450$_{scc}$/mg protein as determined by the Lowry assay (14) and the reduced-CO difference spectrum (15). Aniline-Sepharose 4B was prepared according to the published procedure (10) using CNBr-activated Sepharose 4B rather than Sepharose 4B.

Adrenodoxin was purified from beef adrenal cortex as described previously (10,16) by DEAE-cellulose (DE 52) chromatography, ammonium sulfate fractionation and Sephadex G-100 and G-50 chromatography. The purified protein had an A_{280}/A_{414} ratio of 1.2. Adrenodoxin-Sepharose 4B was prepared by the described procedure (10,17).

Protein concentrations were measured by the Lowry method (14) with bovine serum albumin as a standard. The concentrations of cytochrome P-450$_{scc}$ were determined from the reduced CO minus the reduced difference spectrum, using a difference extinction coefficient of 91 mM^{-1} cm^{-1} for $A_{450}-A_{490}$ (15). The concentration of adrenodoxin was calculated using an extinction coefficient of 11 mM^{-1} cm^{-1} at 414 nm (18). All optical spectra were recorded on a Cary 219 spectrophotometer.

Carbon monoxide binding studies

All experiments were performed at 25°C and ionic strength 0.11 M with the contribution of the buffer being 0.06. The ionic strength was adjusted with NaCl or KCl, and all buffers contained 0.1 mM EDTA. The following buffers were used: phosphate for pH's 5-8, Tris for pH's 8-9. The pH was measured after each experiment using a Fisher Microprobe electrode and Fisher digital pH meter.

Rapid scan and stopped-flow experiments were performed anaerobically in a Union Giken RA601 Rapid Reaction Analyzer using the procedures reported elsewhere (19). The dead time of the flow apparatus was 4 ms. The absorption spectra were scanned from 390 to 486 nm for cholesterol-free cytochrome P-450$_{scc}$, and from 378 to 474 nm for cholesterol-bound cytochrome P-450$_{scc}$. All kinetic measurements were performed at 450 nm, the wavelength of the reduced CO absorbance maximum. Sodium dithionite stock solutions were made by adding a weighed amount to 5 mL of anaerobic 1 mM NaOH. Ferrous protein samples were obtained by adding microliter amounts of the freshly prepared dithionite stock solution to a final concentration of 0.2 or 0.1 mM. To avoid denaturation of cytochrome P-450$_{scc}$ below pH 6.0 and above pH 8.0 (6,20) a pH jump method was used; buffer was placed only in the drive syringe containing CO. Carbon monoxide-saturated buffer was obtained by bubbling argon-

flushed buffer with high purity carbon monoxide (Liquid Carbonic Canada Ltd.) for about 30 minutes. Sample solutions of carbon monoxide were obtained by diluting the carbon monoxide-saturated buffer with argon-flushed buffer contained in the same syringe. The concentration of carbon monoxide-saturated buffer at 25°C, taken from the reference table (21), was 4.64 mM. The final cytochrome P-450$_{scc}$ concentrations for the rapid-scan experiments were 4 μM for cholesterol-free enzyme and 3.2 μM for cholesterol-bound enzyme, and for the stopped-flow experiments were 1.0-1.5 μM. All kinetic curves were found to be pseudo-first order. A typical trace is given in Fig. III.1. Rate constants were determined from a non-linear least-squares analysis (22) of experimental curves. Between four to six determinations of the rate constants were performed for every carbon monoxide concentration and the mean value for the observed rate constant was used in the calculations.

Chemicals

CNBr-activated Sepharose 4B, Sephadex G-50 and Sephadex G-100 were purchased from Pharmacia Fine Chemicals. DEAE - cellulose was from Whatman. Sodium cholate, sodium pyrophosphate, dithiothreitol, n-octylamine, aniline were from Sigma. Emulgen 913 was from Kao-Atlas (Tokyo, Japan) and bovine serum albumin from Pentex (Kankakee, Illinois). All

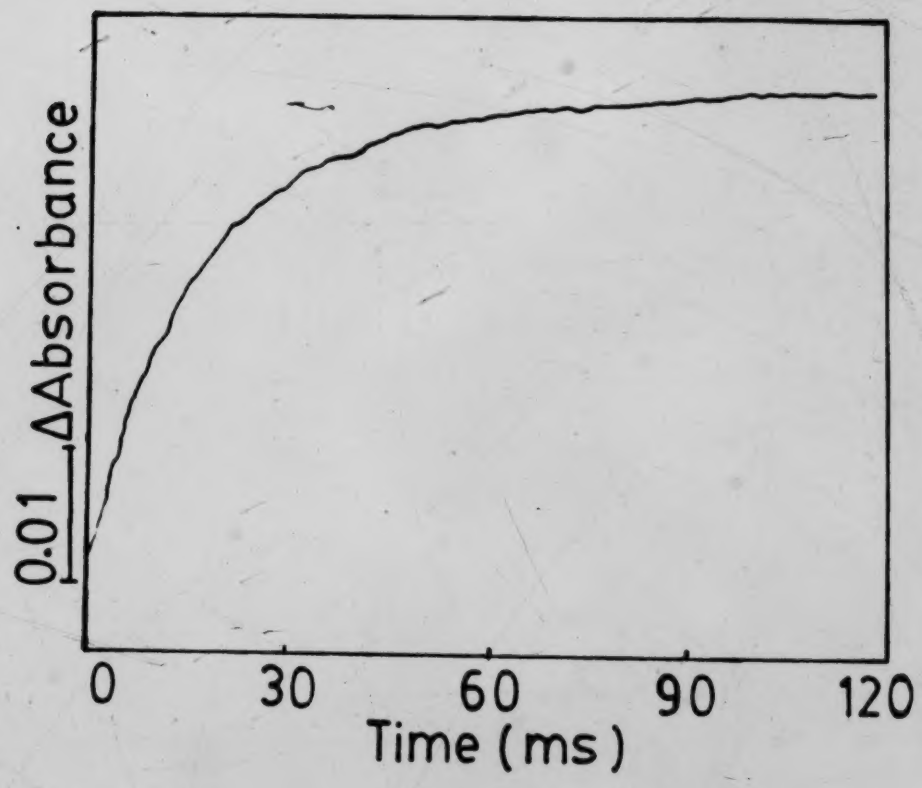

Figure III.1 Absorbance changes with time of the reaction of carbon monoxide with cholesterol-free reduced cytochrome P-450_{scc} at 25°C as recorded on the stopped-flow apparatus at 450 nm. Final concentrations were 2.34 μM cytochrome P-450_{scc}, 116 μM carbon monoxide in 10 mM Na phosphate buffer, pH 7.40, 0.1 mM EDTA, and 0.1 M NaCl.

other reagents were of the best grade available from commercial sources.

Results

Rapid-Scan Absorption Spectra of the Reduced-CO Complex of Beef Adrenocortical Cytochromes P-450$_{scc}$

When carbon monoxide-saturated buffer is mixed with dithionite-reduced cholesterol-free and cholesterol-bound cytochrome P-450$_{scc}$ at 25°C the formation of the reduced-CO complex is observed (Fig. III.2). The spectral features of this binding process, which occurred within ~150 ms after mixing, are almost identical for the two cytochromes P-450$_{scc}$: the reduced peak at approximately 414 nm decreases and the reduced-CO peak appears at 450 nm (Figs. III.2A and III.2C). Difference spectra are recorded versus the reduced enzyme (Figs. III.2B, III.2D). The isosbestic points between reduced-CO and reduced cholesterol-free enzyme are at 434 and 471 nm (Fig. III.2B), and between reduced-CO and reduced cholesterol-bound enzyme are at 433 and 469 nm (III.2D).

Fig. III.2. Spectral changes observed after mixing carbon monoxide with reduced cholesterol-free (A,B) and cholesterol-bound (C,D) cytochromes P-450$_{scc}$ at pH 7.40 and 7.32, respectively. The spectra were recorded at 25°C. Final concentrations were 4.0 μM cholesterol-free P-450$_{scc}$, 3.2 μM cholesterol-bound P-450$_{scc}$, 200 μM Na dithionite and 464 μM carbon monoxide. The arrows indicate the direction of absorbance change with increasing time. The right-hand scale corresponds to A and B, while the left-hand side scale to C and D. The following spectra are shown: (A) Reduced cholesterol-free cytochrome P-450$_{scc}$, traces recorded 1, 3, 14, 24, 146 ms after mixing and the final spectrum. (B) Difference spectra taken 1, 3, 14, 24, 146 ms after mixing and final spectrum versus initial reduced cholesterol-free spectrum. (C) Reduced cholesterol-bound cytochrome P-450$_{scc}$, traces recorded 1, 3, 6, 11, 24, 72, 143 ms after mixing and the final spectrum. (D) Difference spectra taken 1, 3, 6, 11, 24, 72, 143 ms after mixing and the final spectrum versus initial reduced cholesterol-bound spectrum.

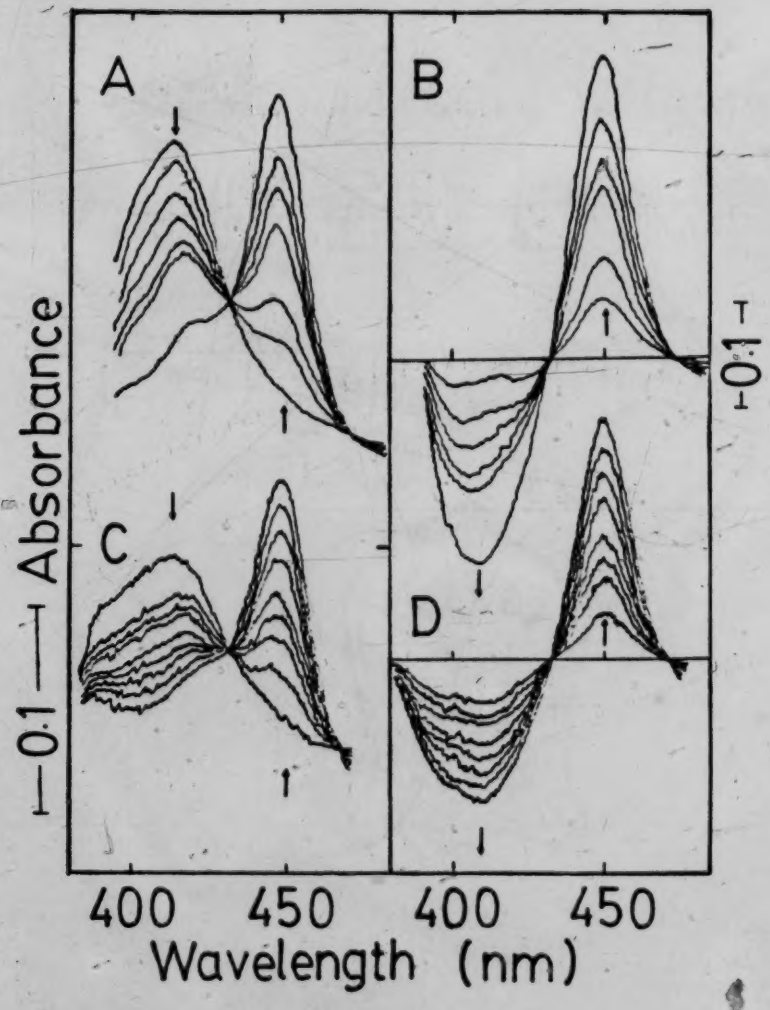
A
B
C
D
0·1
Absorbance
0·1
400
450
400
450
Wavelength (nm)

Kinetics of Formation and Decay of the Reduced-CO Complex of Beef Adrenocortical Cytochromes P-450$_{scc}$

The kinetics of carbon monoxide binding to both cholesterol-free and cholesterol-bound reduced cytochrome P-450$_{scc}$ were studied between pH 5 and 9. At all pH values the observed rate constants for the reactions of reduced cytochromes with a sufficiently large excess of CO are found to be in good agreement with the equation:

$$k_{obs} = k_1[CO] + k_{-1}$$

where k_{obs}, k_1 and k_{-1} are the observed pseudo-first order, "on" rate and "off" rate constants, respectively. Typical plots of k_{obs} versus CO concentration are given in Fig. III.3. The values of k_1 and k_{-1}, calculated from the slopes and intercepts of such plots by weighted linear least-squares analysis, are summarized in Table III.1.

The mean values of k_1 for both cholesterol-free ($(1.8\pm0.2)\times10^5$ M^{-1} s^{-1}) and cholesterol-bound ($(1.9\pm0.1)\times10^5$ M^{-1} s^{-1}) forms of the enzyme are identical within the experimental error limits, while the mean value of k_{-1} for cholesterol-free ($(2.3\pm0.3)\times10$ s^{-1}) is almost double that for the cholesterol-bound enzyme ($(1.2\pm0.1)\times10$ s^{-1}). The pH profiles of the CO binding rate constants k_1 and k_{-1} for both cholesterol-free and cholesterol-bound reduced cytochromes P-450$_{scc}$ are shown in Fig. III.4.

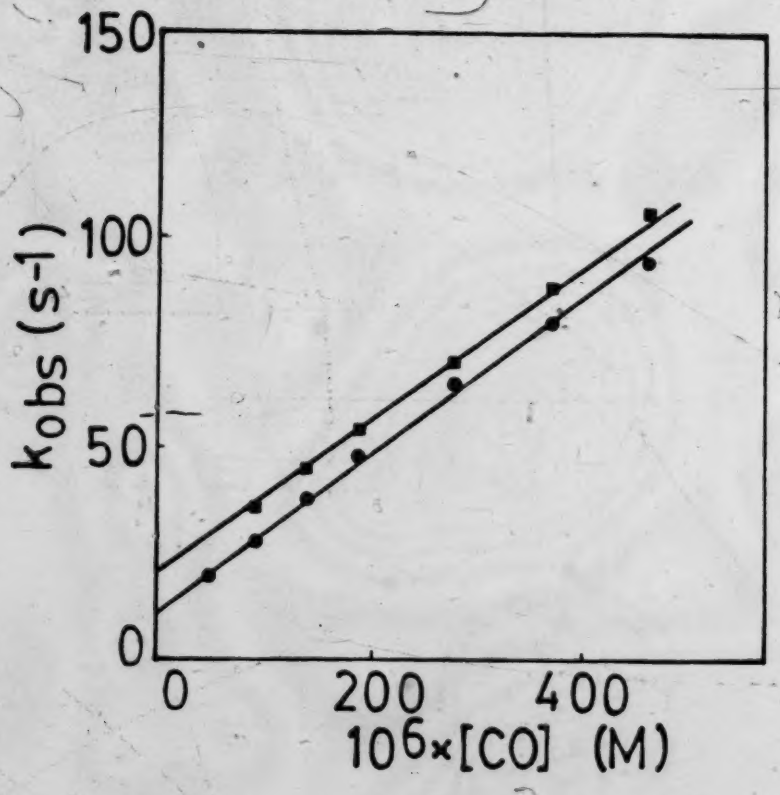

Fig. III.3. Pseudo-first order plots of the reaction of carbon monoxide with reduced (■) cholesterol-free cytochrome P-450_{scc} at pH 7.06 and (●) cholesterol-bound cytochrome P-450_{scc} at pH 7.01. The temperature of the reaction was 25°C. The straight lines are the weighted least squares best-fit lines.

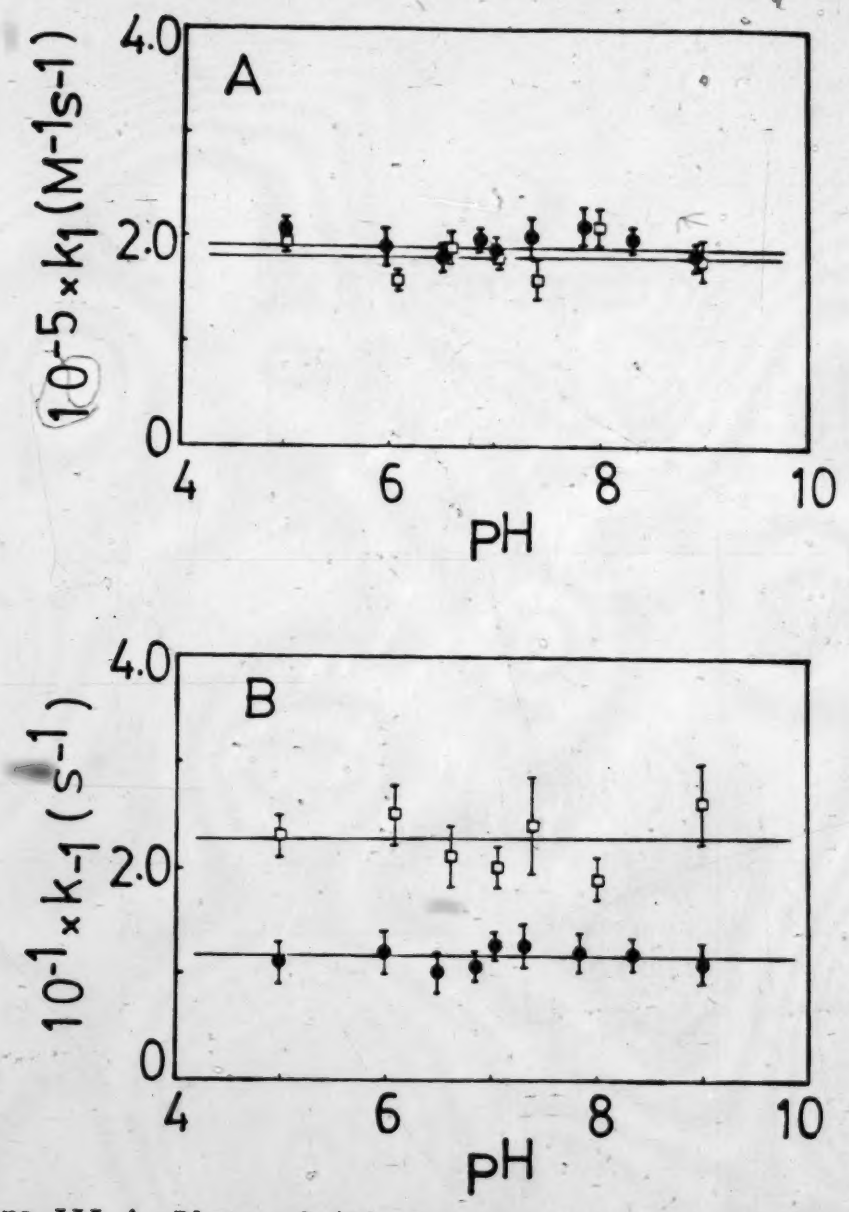

Figure III.4. Plots of (A) the second-order forward rate constant (k_1) and (B) first-order reverse rate constant (k_{-1}) for CO binding to reduced cytochrome P-450$_{scc}$ as a function of pH at 25°C. (●) cholesterol-free and (◐) cholesterol-bound cytochrome P-450$_{scc}$.

Table III.1 Kinetic parameters for carbon monoxide binding to reduced cytochrome P-450$_{scc}$ as a function of pH at 25°C.

	$10^{-5}xk_1$ (M^{-1} s^{-1})[a]	$10^{-1}xk_{-1}$ (s^{-1})[a]
A. Low Spin P-450$_{scc}$		
5.00	2.0±0.1	2.3±0.2
6.08	1.6±0.1	2.5±0.3
6.58	1.9±0.2	2.1±0.3
7.06	1.8±0.1	2.0±0.2
7.40	1.6±0.2	2.4±0.5
8.00	2.1±0.2	1.9±0.2
9.00	1.8±0.2	2.6±0.4
B. High Spin P-450$_{scc}$		
5.01	2.1±0.1	1.1±0.2
5.98	1.9±0.2	1.2±0.2
6.51	1.8±0.1	1.0±0.2
6.85	2.0±0.1	1.1±0.1
7.01	1.9±0.1	1.3±0.1
7.32	2.0±0.2	1.3±0.2
7.85	2.1±0.2	1.2±0.2
8.27	2.0±0.1	1.2±0.1
8.97	1.8±0.1	1.1±0.2

[a]Errors of rate constants represent the standard deviation calculated from data at a given pH.

Discussion

The rapid-scan and stopped-flow experiments for carbon monoxide binding with dithionite-reduced cytochrome $P\text{-}450_{scc}$ suggest the fast and reversible formation of the carbon monoxide complex in a simple bimolecular process. This is in contrast to the two-step CO binding process consisting of bimolecular association followed by a unimolecular rearrangement step found for cytochromes $P\text{-}450_{LM2}$, $P\text{-}450_{LM4}$ and $P\text{-}450_{PB}$ (23,24); but is in complete accord with the monophasic CO binding process observed for cytochrome $P\text{-}450_{cam}$ (11), cytochrome $P\text{-}450_{scc}$ (13) and cytochrome $P\text{-}450_{PB}$ (25). It has been suggested that the observed biphasicity of CO binding to reduced cytochrome $P\text{-}450_{PB}$ is due to heterogeneity of the proteins (25). The similarity of the absolute spectra (Figs. III.2A, III.2C) and the difference spectra (III.2B, III.2D) for the two forms of $P\text{-}450_{scc}$ is in accord with the previous findings for cytochrome $P\text{-}450_{cam}$ that the absorption spectrum of the reduced enzyme is unchanged by the addition of camphor (26). The small difference observed between the isosbestic points of cholesterol-free (434 and 471 nm) and cholesterol-bound (433 and 469 nm) appears within experimental error. However, the nonionic detergent Emulgen 913, which was used for the purification of cholesterol-free $P\text{-}450_{scc}$, increases the extinction coefficient of the spectral peak (at ~450 nm)

of the reduced carbon monoxide complex (27). Thus, the small shift of isosbestic points might be due to the presence of Emulgen 913 (~0.02%) in the purified cholesterol-free P-450$_{scc}$.

The second-order "on" rate constants in Table III.1 correspond well with the rate constants (2.0×10^5 M^{-1} s^{-1} for cholesterol-free and 2.2×10^5 M^{-1} s^{-1} for cholesterol-bound P-450$_{scc}$) reported previously at the single pH value of 7.2 (13). However the values of "off" rate constants are not in close agreement. The comparison (with the results of Ref. 13, in brackets) is: for cholesterol-free $(2.3 \pm 0.3) \times 10$ s^{-1}, compared to (0.06 s^{-1}, pH 7.2) and for cholesterol-bound P-450$_{scc}$ $(1.2 \pm 0.2) \times 10$ s^{-1}, compared to (0.15 s^{-1}, pH 7.2). Also the reported results show a two-fold increase of "off" rate constant with cholesterol-binding to the heme iron, whereas we have observed the opposite trend.

However, a three-fold decrease in the "off" rate constant for carbon monoxide binding when camphor is bound with cytochrome P-450$_{cam}$ at 4°C has been reported (11). In another study it was suggested that the reduced carbon monoxide complex in the absence of cholesterol (28) is unstable. This is consistent with our results, and is comparable to the (i) fifteen-fold increase in the stability of the oxyferrous complex at -17°C when cholesterol is bound to cytochrome P-450$_{scc}$ (29) and (ii) twelve-fold increase in

the half-time for the autoxidation of the oxyferrous complex of cytochrome P-450$_{cam}$ at -20°C in 50% glycol, when camphor is bound (30).

Although the presence of an acid group with a pK_a of 6.8 on the cholesterol-free cytochrome P-450$_{scc}$ has previously been suggested for binding of both cholesterol and 20α,22R-dihydroxy cholesterols (31), Fig. III.4 and the data in Table III.1 shows that both "on" (k_1) and "off" rate constants (k_{-1}) are independent of pH between the pH range studied for both cholesterol-free and cholesterol-bound forms of P-450$_{scc}$. Other studies suggest that the rate of autoxidation of the oxygenated cytochrome P-450$_{scc}$-cholesterol complex is influenced by pH (6), and the heme midpoint potential of cytochrome P-450$_{scc}$-cholesterol complex is independent of pH from 6 to 8 (32).

References

1. Gunsalus, I.C., Meeks, J.R., Lipscomb, J.D., Debrunner, P. and Munck, E. (1974) in Molecular Mechanisms of Oxygen Activation, ed. Hayaishi, O. (Academic Press, New York), pp.559-613.
2. Stone, D. and Hechter, O. (1954) Arch. Biochem. Biophys. **51**, 457-469.
3. Simpson, E.R. and Boyd, G.S. (1966) Biochem. Biophys. Res. Commun. **24**, 10-17.
4. Hume, R. and Boyd, G.S. (1978) Biochem. Soc. Trans. **6**, 893-898.
5. Shikita, M. and Hall, P.F. (1974) Proc. Natl. Acad. Sci. U.S.A. **71**, 1441-1445.
6. Hume, R., Kelly, R.W., Taylor, P.L. and Boyd, G.S. (1984) Eur. J. Biochem. **140**, 583-591.
7. Sato, R. and Omura, T. (eds.) (1978) in Cytochrome P-450, pp.214-220, Academic Press, New York.
8. Simpson, E.R. and Boyd, G.S. (1967) Eur. J. Biochem. **2**, 275-285.
9. Mitani, F. (1979) Mol. Cell. Biochem. **24**, 21-43.
10. Hanukoglu, I., Spitsberg, V., Bumpus, J.A., Dus, K.M. and Jefcoate, C.R. (1981) J. Biol. Chem. **256**, 4321-4328
11. Peterson, J.A. and Griffin, B.W. (1972) Arch. Biochem. Biophys. **151**, 427-433.

12. Wang, H.-P. and Kimura, T. (1976) J. Biol. Chem. **251**, 6068-6074.

13. Tuckey, R.C. and Kamin, H. (1983) J. Biol. Chem. **258**, 4232-4237.

14. Lowry, O.H., Rosebrough, N.J., Farr, A.L. and Randall, R.J. (1951) J. Biol. Chem. **193**, 265-275.

15. Omura, T. and Sato, R. (1964) J. Biol. Chem. **239**, 2379-2385.

16. Orme-Johnson, W.H. and Beinert, H. (1969) J. Biol. Chem. **244**, 6143-6148.

17. March, S.C., Parikh, I. and Cuatrecasas, P. (1974) Anal. Biochem. **60**, 149-152.

18. Huang, J.J. and Kimura, T. (1973) Biochemistry **12**, 406-409.

19. Lambeir, A.-M., Appleby, C.A. and Dunford, H.B. (1985) Biochim. Biophys. Acta **828**, 144-150.

20. Kido, T., Arakawa, M. and Kimura, T. (1979) J. Biol. Chem. **254**, 8377-8385.

21. Lange, N.A. and Forker, G.M. (eds.) (1967) Handbook of Chemistry, 10th edn. p.1101, McGraw-Hill, New York.

22. Dunford, H.B., Evett, M. and Roman, R. (1971) Can. J. Chem. **49**, 3059-3063.

23. Gray, R.D. (1982) J. Biol. Chem. **257**, 1086-1094.

24. Gray, R.D. (1983) J. Biol. Chem. **258**, 3764-3768.

25. Oertle, M., Richter, C., Winterhalter, K.H. and

DiIorio, E.E. (1985) Proc. Natl. Acad. Sci. U.S.A. **82**, 4900-4904.

26. Peterson, J.A. (1971) Arch. Biochem. Biophys. **144**, 678-693.

27. Takikawa, O., Gomi, T., Suhara, K., Itagaki, E., Takemori, S. and Katagiri, M. (1978) Arch. Biochem. Biophys. **190**, 300-306.

28. Kido, T., Yamakura, F. and Kimura, T. (1981) Biochim. Biophys. Acta **666**, 370-381.

29. Tuckey, R.C. and Kamin, H. (1982) J. Biol. Chem. **257**, 9309-9314.

30. Eisenstein, L., Debey, P. and Douzou, P. (1977) Biochem. Biophys. Res. Commun. **77**, 1377-1383.

31. Lambeth, J.D., Kitchen, S.E., Farooqui, A.A., Tuckey, R.C. and Kamin, H. (1982) J. Biol. Chem. **257**, 1876-1884.

32. Lambeth, J.D. and Pember, S.O. (1983) J. Biol. Chem. **258**, 5596-5602.

CHAPTER FOUR

THE FORMATION AND DECAY OF THE OXYFERROUS COMPLEX OF BEEF ADRENOCORTICAL CYTOCHROME P-450$_{scc}$. RAPID-SCAN AND STOPPED-FLOW STUDIES.[1]

[1]A version of this chapter has been submitted for publication by Kashem, M.A. and Dunford, H.B. in Biochem. Cell Biol.

Introduction

Adrenocortical cytochrome P-450$_{scc}$ catalyzes the side-chain cleavage of cholesterol through three consecutive oxidation cycles on the C20-22 bond to yield pregnenolone as the final product (1). P-450$_{scc}$ belongs to the diverse class of P-450 heme protein systems, which catalyze the addition of oxygen to a substrate via molecular oxygen activation (2). The binding of molecular oxygen to the ferrous form of the enzyme is an essential step in the enzymatic cycle of cytochrome P-450 (3).

The first step in the activation of molecular oxygen by cytochrome P-450 involves the formation of an oxyferrous complex (4). The occurrence of a stable oxyferrous complex of cytochrome P-450$_{cam}$ from Pseudomonas putida has been reported earlier (5-7) and oxygen binding to the reduced form of this enzyme has been studied thoroughly (8,9). Oxyferrous complexes of P-450 from mammalian sources have been more difficult to characterize because of the rapid rate at which they autoxidize. However, optical absorption spectra obtained for oxyferrous complexes of cytochrome P-450$_{LM_2}$ (10,11) and cytochrome P-450$_{scc}$ (12,13) at sub-zero temperatures were shown to be very similar to the spectrum of oxyferrous complex of cytochrome P-450$_{cam}$. In the most recent rapid reaction studies the formation of oxygenated intermediates of cytochromes P-450$_{LM_4}$ and P-450$_{LM_{3b}}$ (14) and Rhizobium cytochromes P-450 (15) has been detected.

Although autoxidation of the oxygenated complex of cytochrome P-450$_{scc}$ had previously been observed at 4°C (16), little is known about the formation and stability of this complex above 0°C. In the present study we have investigated the formation and spontaneous decay of the oxyferrous complex of purified beef adrenocortical cholesterol-bound cytochrome P-450$_{scc}$ in the Soret region by means of rapid-scan spectrometry at 4°C. We have also studied the transient state kinetics as a function of pH of the formation and decay of the oxyferrous complex of this enzyme using the stopped-flow technique.

Materials and Methods

Purification of Enzyme

Cholesterol-bound cytochrome P-450$_{scc}$ was purified from beef adrenocortical mitochondria using reported methodology (17) by cholate extraction, ammonium sulfate fractionation, aniline-Sepharose 4B and adrenodoxin-Sepharose 4B affinity chromatography. Purified P-450$_{scc}$ had an A_{280}/A_{393} ratio of 1.2, which corresponds to 13 nmol P-450$_{scc}$/mg protein as determined by the Lowry assay (18) and the reduced-CO difference spectrum (19). Adrenodoxin was also purified from beef adrenal cortex as described previously (17,20) by DEAE-cellulose (DE 52) chromatography, ammonium sulfate

fractionation, Sephadex G-100 and G-50 chromatography. The purified protein had an A_{280}/A_{414} ratio of 1.2. Aniline-Sepharose 4B was prepared by a modification of the reported procedure (17). About 30 g of freeze-dried CNBr-activated Sepharose 4B was swelled and washed with 1 mM HCl (200 mL/g of dried gel) followed with 150 mL of coupling buffer ($NaHCO_3$, 0.1 M, pH 8.3, containing 0.5 M NaCl). The gel was then transferred to a beaker containing 190 mL of ligand solution (10 mL of freshly distilled aniline in 180 mL of coupling buffer) and gently stirred for 16 h in the cold room. This gel was washed successively with 500 mL each of coupling buffer; water; 50 mM NaOH and water. The aniline-Sepharose was stirred gently for 1 h at room temperature with an equal volume of blocking solution (1 M glycine, pH 9.0) and then washed alternately with three cycles of 0.1 M acetate (pH 4.0) and 0.1 M $NaHCO_3$ (pH 8.3) each containing 0.5 M NaCl. Finally, the aniline-Sepharose gel was washed with water and stored in the cold room in 50 mM K phosphate, pH 7.3, 0.02% sodium azide. Adrenodoxin-Sepharose 4B was prepared by the described procedure (17,21).

Protein concentrations were measured by the Lowry method (18) with bovine serum albumin as a standard. The concentration of cytochrome $P\text{-}450_{scc}$ was determined from the reduced CO minus the reduced spectrum, using an extinction coefficient of 91 mM^{-1} cm^{-1} for $A_{450-490}$ (19). The concen-

tration of adrenodoxin was calculated using an extinction coefficient of 11 mM^{-1} cm^{-1} at 414 nm (22). All optical spectra were recorded on a Cary 219 spectrophotometer.

Oxygen Binding Studies

All experiments were performed at 4°C and ionic strength 0.11 M, the contribution of the buffer being 0.06. The ionic stength was adjusted with KCl and all buffers contained 0.1 mM EDTA. The following buffers were used: phosphate for pH's 5-8, Tris for pH's 8-9. The pH was measured after each experiment using a Fisher digital pH meter.

Rapid-scan and stopped-flow experiments were performed anaerobically using a Union Giken Rapid Reaction Analyzer Model RA601, the properties of which were reported previously (23). The dead time of the flow apparatus was 4 ms. The absorption spectra were scanned from 378 to 474 nm; and all kinetic measurements were performed at 430 nm, the wavelength of maximum absorbance change for both the formation and decay of the oxyferrous complex. Enzyme solutions were prepared in the cold under anaerobic conditions obtained by evacuating and flushing of the solutions with high purity argon (Zero gas, Canadian Liquid Air) purified by passage through an oxygen trap (Oxypurge N, Altech Associates). Argon was flushed over the surface of

the enzyme solutions and bubbled through all other solutions. Solutions were handled and transferred by means of gas-tight Hamilton syringes. Sodium dithionite stock solutions were made by adding a weighed amount to 5 mL of anaerobic 1 mM NaOH. Ferrous enzyme samples were obtained by adding microliter amounts of the freshly prepared dithionite stock solution to a final concentration of 0.1 mM. To avoid denaturation of cytochrome $P\text{-}450_{scc}$ below pH 6.0 and above pH 8.0 (16,24) a pH jump method was used; buffer was placed only in the drive syringe containing oxygen. Oxygen solutions were obtained by adding air-saturated buffer to argon-flushed buffer contained in the same syringe. The concentration of oxygen in air-saturated buffer at 4°C was taken from a standard reference table (25). To obtain anaerobic conditions in the instrument, the driving gas (which is in contact with the solution) was replaced by high purity argon, which was also used to flush the internal flow system before every experiment. The reservoir caps of the instrument were modified so that solutions could be transferred from the gas-tight syringe to the reservoir under a gentle stream of argon. The final cytochrome $P\text{-}450_{scc}$ concentrations for the rapid-scan experiments were 7.5 μM and 3.9 μM for the formation and decay of the oxyferrous complex, respectively; and for the stopped-flow experiments were 1.5-2.5 μM. All kinetic

curves were found to be pseudo-first order. Rate constants were determined from a nonlinear least-squares analysis. Between four to six determinations of the rate constants were performed for every oxygen concentration and the mean values for the observed rate constant was used in the calculations.

Chemicals

CNBr-activated Sepharose 4B, Sephadex G-50 and G-100 were purchased from Pharmacia Fine Chemicals. DEAE-cellulose (DE-52) was from Whatman. Sodium cholate, dithiothreitol and aniline were from Sigma. Bovine serum albumin from Pentex (Kankakee, Illinois). All other reagents were of the best grade available from commercial sources.

Results

When dithionite reduced cholesterol-bound cytochrome P-450$_{scc}$ is mixed with oxygen at 4°C two different processes are observed (Fig. IV.1-IV.4). The first process is the formation of the oxyferrous complex of cytochrome P-450$_{scc}$. Between 1 ms and 40 ms after mixing the ferrous peak at about 414 nm disappears and a new peak appears at 422 nm, approximately equal in height (Fig. IV.1). The largest changes in absorbance occur in the vicinity of 390

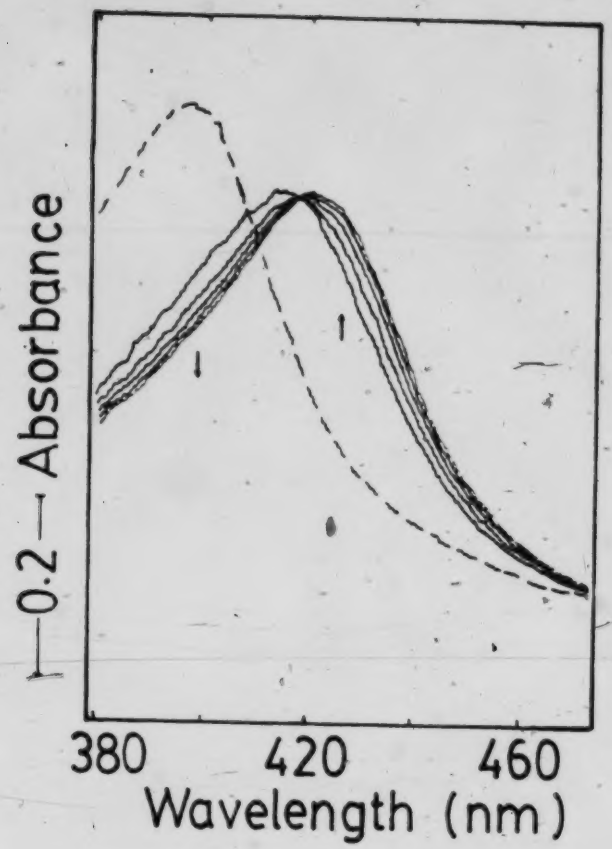

Figure IV.1 Spectral changes observed after mixing sodium dithionite-reduced cholesterol-bound cytochrome P-450$_{scc}$ with oxygen at pH 7.30 and 4°C. The arrows indicate the direction of the absorbance change with increasing time. Final concentrations were 7.5 μM cytochrome P-450$_{scc}$, 100 μM sodium dithionite and 487 μM oxygen. The following spectra are shown: (——) reduced cytochrome P-450$_{scc}$, traces recorded 1, 6, 11 and 40 ms after mixing; and (- -) final spectrum recorded 2 min after mixing.

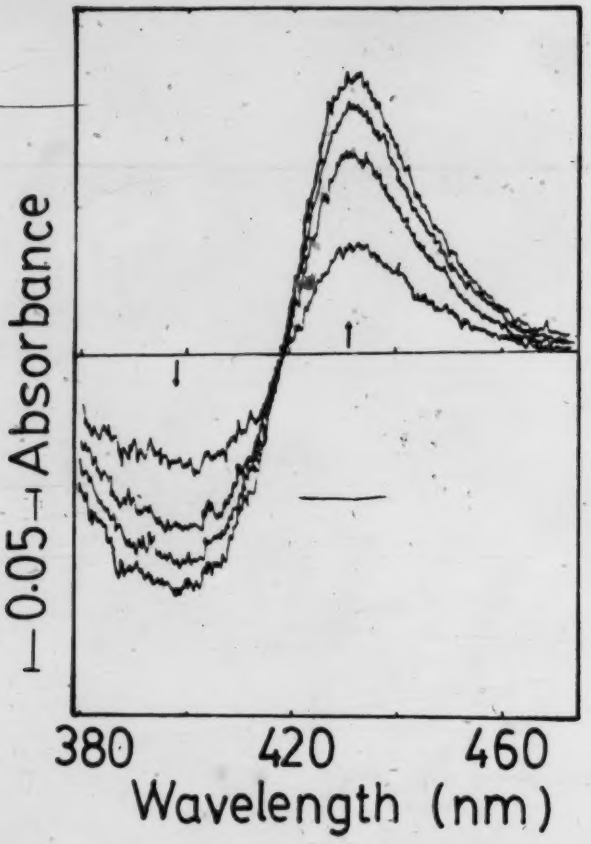

Figure IV.2 Formation of oxyferrous complex of cytochrome P-450$_{scc}$. Difference spectra taken 1, 6, 11 and 40 ms after mixing versus initial reduced spectrum. The arrows indicate the direction of the absorbance change with increasing time. Experimental conditions were identical with those described in Fig. 1.

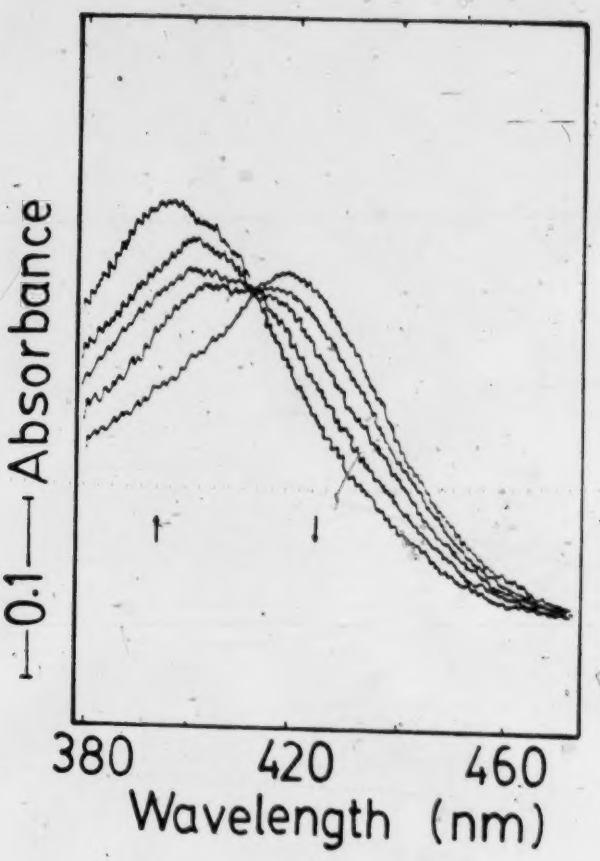

Figure IV.3 Spectral changes observed after mixing sodium dithionite-reduced cholesterol-bound cytochrome P-450$_{scc}$ with oxygen at pH 7.30 and 4°C. The arrows indicate the direction of the absorbance change with increasing time. Final concentrations were 3.9 μM cytochrome P-450$_{scc}$, 100 μM sodium dithionite and 487 μM oxygen. Rapid-scan spectra recorded 50, 110, 170, 360 and 940 ms after mixing, leading to decay of the oxyferrous complex, are shown.

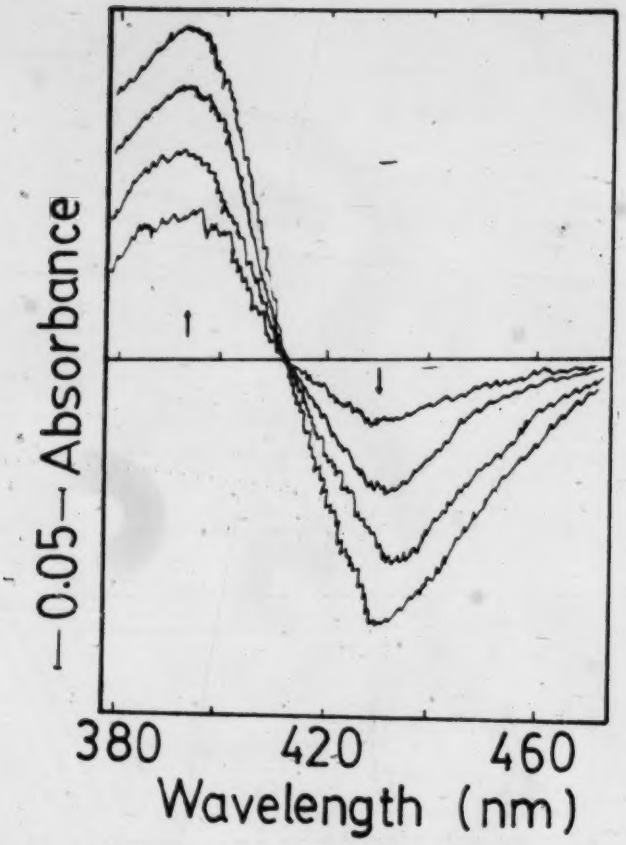

Figure IV.4 Decay of oxyferrous complex of cytochrome P-450$_{scc}$. Conditions as described in Fig. 3 caption. Difference spectra taken 110, 170, 360 and 940 ms after mixing versus the oxyferrous complex spectrum (spectrum recorded 50 ms after mixing).

nm and 430 nm (Fig. IV.1 and IV.2). The difference spectra for this process are recorded versus the ferrous enzyme (Fig. IV.2). The isosbestic point between ferrous P-450$_{scc}$ and the oxyferrous complex is at 418 nm.

The second process is the spontaneous decay of the oxyferrous complex. The final spectrum, recorded in Fig. IV.1 after 2 min of mixing, is the ferric form of P-450$_{scc}$ (cholesterol-bound) with the familiar peak at ~393 nm. The family of spectra observed between 50 ms and 940 ms after mixing show the conversion of the oxyferrous complex to ferric cytochrome P-450$_{scc}$ (Fig. IV.3). Difference spectra taken versus the spectrum of the oxyferrous complex (spectrum recorded at 50 ms) over the 110 ms and 940 ms range have an isosbestic point at 411 nm (Fig. IV.4).

A series of stopped-flow experiments were performed at 4°C over the pH range 5.1-8.8 with ferrous cholesterol-bound cytochrome P-450$_{scc}$ in order to obtain accurate values for the rate constants of the different steps (formation and decay of the oxyferrous complex) observed in the rapid-scan experiments. At all pH values single exponential traces were obtained for the formation of the oxyferrous complex of cytochrome P-450$_{scc}$ with a sufficiently large excess of oxygen. A typical trace is shown in Fig. IV.5. Also the plots of the observed pseudo-first order rate constants versus oxygen concentration (Fig. IV.6) have a finite

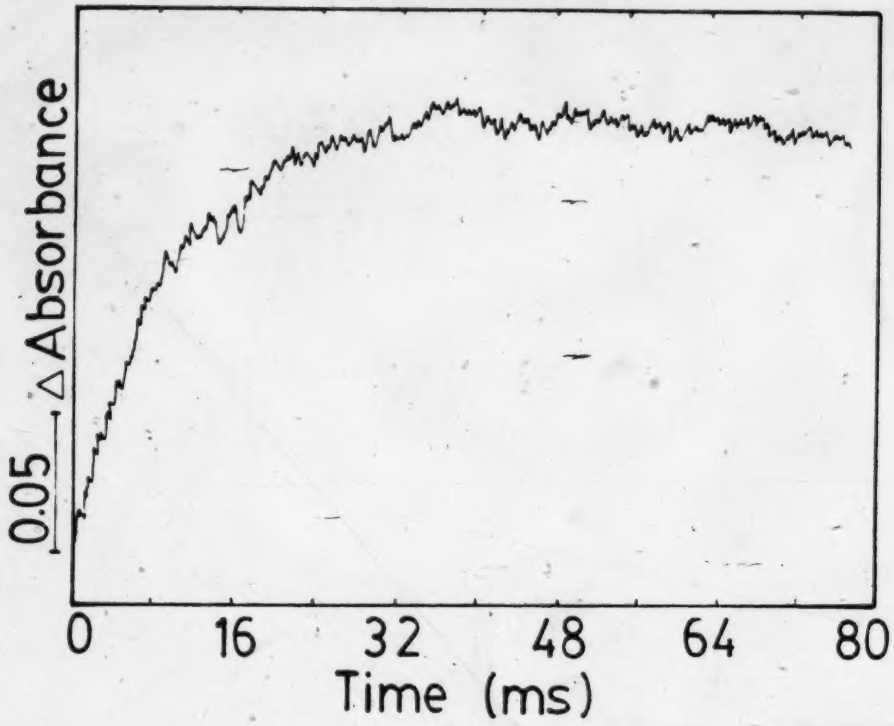

Figure IV.5 Absorbance changes with time for the reaction of ferrous cytochrome P-450$_{scc}$ with oxygen, recorded on the stopped-flow appratus at 430 nm, leading to the formation of the oxyferrous complex. The trace was recorded at pH 7.52 and 4°C. Final concentrations were 2.5 μM cytochrome P-450$_{scc}$, 100 μM sodium dithionite, 195 μM oxygen. The delay time of the instrument was 63 ms.

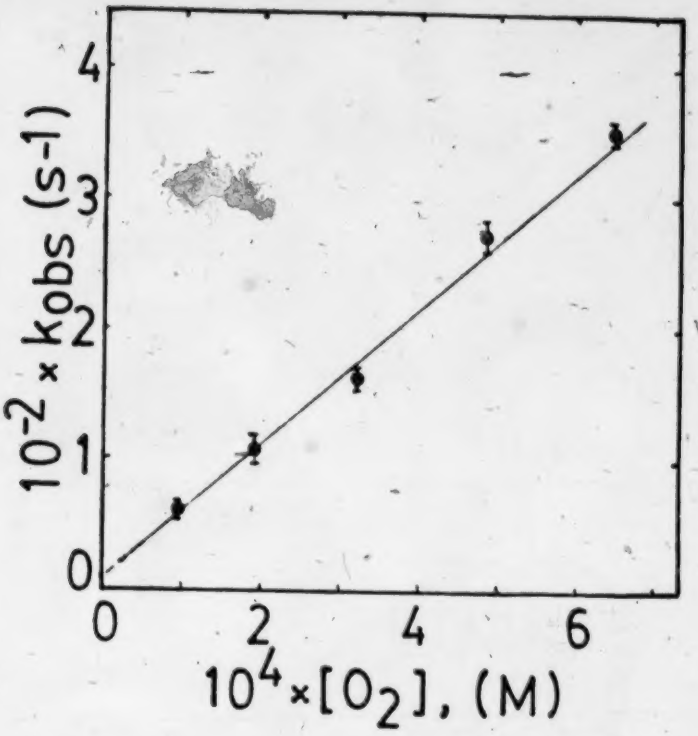

Figure IV.6 The observed pseudo-first order rate constants (k_{obs}) are plotted as a function of oxygen concentration at pH 7.30 and 4°C. The cytochrome P-450_{scc} concentration was 2.25 μM. The straight line is the weighted least squares best-fit line.

intercept, which indicates that the reaction is reversible. The results are in good agreement with the equation

$$[1] \quad k_{obs} = k_{on}[O_2] + k_{off}$$

The second-order "on" rate constants (obtained from the slopes) and first-order "off" rate constants (obtained from the intercepts) are given in Table IV.1. The pH profiles of oxygen binding rate constants k_{on} and k_{off} for cholesterol-bound cytochrome P-450$_{scc}$ are shown in Fig. IV.7. The second order "on" rate constant is independent of pH for the pH range over which the oxygen binding was studied. The mean value of k_{on} is $(5.1\pm0.8)\times10^5$ M^{-1} s^{-1}. The "off" rate constants varied between 2.8 s^{-1} and 12.5 s^{-1}, with relatively larger errors, in a random fashion and virtually independent of pH over the pH range of the experiments. It should be stressed that the k_{off} values were obtained by extrapolation and therefore are less reliable than the k_{on} values.

The spontaneous decay of the oxyferrous complex of cholesterol-bound cytochrome P-450$_{scc}$ was studied by increasing the delay time of the stopped-flow apparatus from 63 ms (which is the mechanical delay time of the apparatus for the generation of the stopped-flow signal) to 110 ms (Fig. IV.8). The decay also occurs in a single exponential

TABLE IV.1. Kinetic Parameters for the Formation and Decay of Oxyferrous Complex of Beef Adrenocortical Cytochrome P-450$_{scc}$ as a Function of pH at 4°C

pH	$10^{-5}xk_{on}$ $(M^{-1}\ s^{-1})^a$	k_{off} $(s^{-1})^a$	k_{decay} $(s^{-1})^a$
5.07	5.1±0.3	12.5±6.2	9.7±0.4
5.22	-	-	10.2±0.2
5.45	4.2±0.5	2.8±0.9	10.3±0.2
5.74	-	-	10.6±0.2
6.03	5.4±0.5	2.9±1.0	9.9±0.2
6.29	-	-	9.0±0.1
6.53	6.5±0.6	6.9±1.2	8.7±0.1
6.79	-	-	8.4±0.1
7.03	5.4±0.2	4.6±0.4	8.1±0.1
7.30	5.1±0.2	9.8±2.9	7.2±0.2
7.52	3.8±0.3	4.7±2.5	6.3±0.2
7.98	4.8±0.4	10.1±4.9	6.0±0.2
8.78	5.3±0.5	4.1±0.8	5.5±0.2

[a]Errors of rate constants represent the standard deviation calculated from data at a given pH.

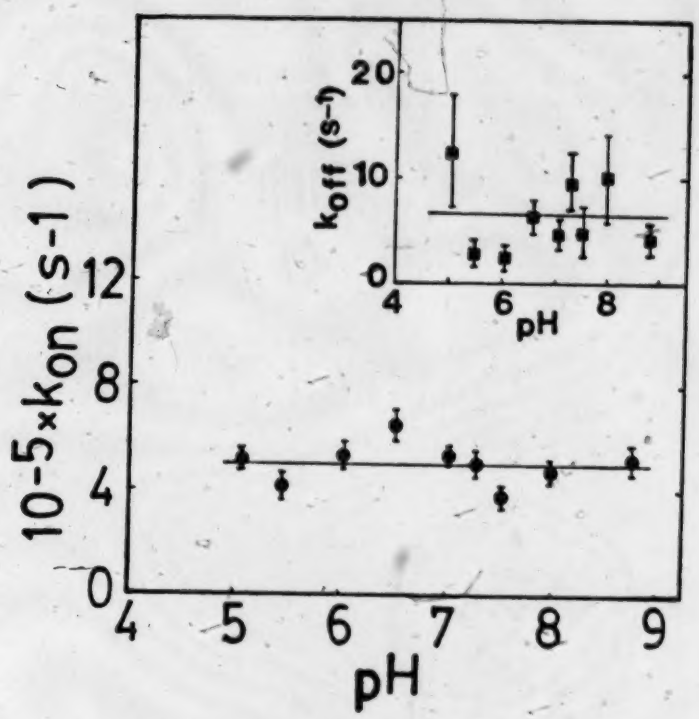

Figure IV.7 Plot of the second-order forward rate constant (k_{on}) for the formation of oxyferrous complex of cytochrome P-450_{scc} as a function of pH at 4°C. The inset shows the pH dependence of the reverse rate constant (k_{off}). The error limits drawn on the data points are based on the standard deviation calculated from the data.

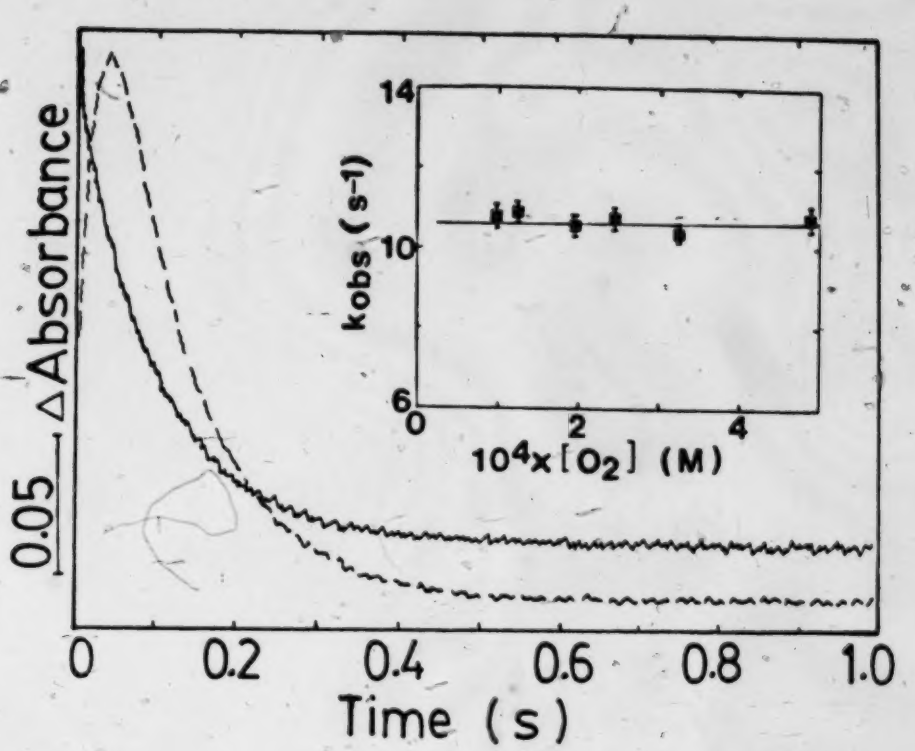

Figure IV.8 Decay of oxyferrous complex of cytochrome P-450$_{scc}$. Time dependence of the absorbance changes after mixing 3.5 μM ferrous cytochrome P-450$_{scc}$ with 487 μM oxygen at pH 5.74 and 4°C ($Na_2S_2O_4 \leq 100$ μM). Traces were recorded at 430 nm on the stopped-flow apparatus with delay times 63 ms (~ ~) and 110 ms (——). Traces are shifted vertically for clarity. The inset shows a first-order plot of the rate of decay of oxyferrous complex as a function of oxygen concentration at pH 5.74 and 4°C.

process, and the decay rate constants (k_{decay}) are independent of the oxygen concentration (Fig. IV.8). Thus, the overall process for oxygen binding to ferrous cholesterol-bound cytochrome P-450_{scc} (Fe^{2+}) is given by

$$[2] \quad Fe^{2+} + O_2 \underset{k_{off}}{\overset{k_{on}}{\rightleftharpoons}} Fe^{2+}{\cdot}O_2 \xrightarrow{k_{decay}} Fe^{3+} + O_2^{\cdot-}$$

The decay rate constants (k_{decay}) decrease with the increase of pH over the pH range of the study (Table IV.1). The logarithm of k_{decay} is plotted <u>versus</u> pH in Fig. IV.9. The results are in good agreement with the following simple mechanism:

$$[3] \quad \begin{array}{ccc} EH & \xrightarrow{k_1} & \text{products} \\ K_a \Vert \; \Vert H^+ & & \\ E & \xrightarrow{k_2} & \text{products} \end{array}$$

where EH and E represent the oxyferrous complex of cytochrome P-450_{scc} ($Fe^{2+}{\cdot}O_2$) with a catalytically important group protonated and deprotonated, K_a is the corresponding acid dissociation constant, and k_1 and k_2 are the first-order rate constants. The observed first-order rate constant (k_{decay}) is given by

$$[4] \quad k_{decay} = \frac{k_2 K_a + k_1 [H^+]}{K_a + [H^+]}$$

The best-fit parameters, given in Table IV.2, were used to

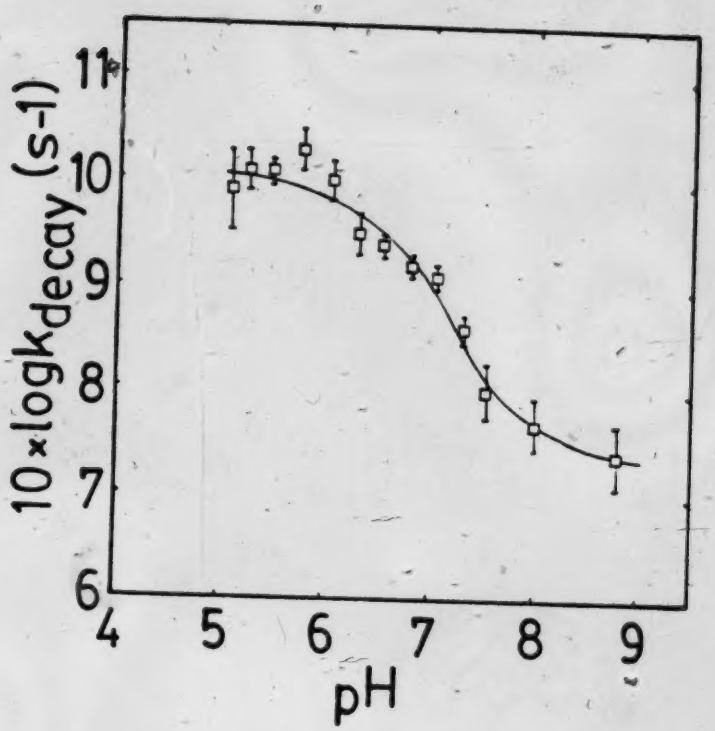

Figure IV.9 Plot of logarithm of first-order rate constant for the decay of oxyferrous complex of cytochrome P-450$_{scc}$ (k_{decay}) versus pH at 4°C. The error limits drawn on the data points are based on the standard deviation calculated from the data. The curve was computed on the basis of best-fit parameters obtained from a least-squares fit of the data to eq.4.

TABLE IV.2. Parameters Obtained from the pH Dependence of the First-Order Rate Constant for the Decay of Oxyferrous Complex of Beef Adrenocortical Cytochrome $P\text{-}450_{scc}$ at 4°C

Parameters	Value[a]
k_1 (s^{-1})	10.1±0.2
k_2 (s^{-1})	5.4±0.1
$\overline{pK_a}$	7.1±0.1

[a]The errors are plus or minus the relative standard deviation obtained from the nonlinear least-squares fit to the experimental data.

calculate the solid line in Fig. IV.9.

Discussion

Formation of the oxyferrous complex of cholesterol-bound cytochrome P-450$_{scc}$, as observed in the rapid-scan experiments, occurs within 40 ms of mixing at 4°C. This complex is unstable and spontaneously decays to the ferric cholesterol-bound cytochrome P-450$_{scc}$ and, presumably, superoxide. The spectrum of the oxyferrous complex of cytochrome P-450$_{scc}$ (Fig. IV.1) closely resembles those reported for the same enzyme at sub-zero temperatures (12,13), cytochrome P-450$_{cam}$ (6-8), cytochrome P-450$_{LM}$ (10,11,14) and Rhizobium cytochromes P-450 (15). The position of the Soret peak around 420 nm is characteristic of all the oxyferrous complexes of the cytochromes P-450 as well as those of other heme proteins. For example, horseradish peroxidase compound III and oxymyoglobin both have a peak at 418 nm (26,27).

The mean value of the second order "on" rate constants, $(5.8\pm0.8)\times10^5$ M^{-1} s^{-1} over the pH range which oxygen binding to cholesterol-bound ferrous cytochrome P-450$_{scc}$ was studied, corresponds well with the previously reported values for different cytochromes P-450 (5,7,28) and chloroperoxidase (29) measured under similar conditions, all ranging between 5×10^5 M^{-1} s^{-1} and 7×10^5 M^{-1} s^{-1}. The values

of k_{off} (Table IV.1) are comparable to those of 1.1 s^{-1} (at 4°C and pH 7.4) for cytochrome P-450$_{cam}$ (7), and 8 s^{-1} to 32 s^{-1} (over the pH range 3.5-6.0 at 4°C) for chloroperoxidase (29). Also, as expected from the temperature dependence, a higher k_{off} value of ~100 s^{-1} was observed for cytochrome P-450$_{scc}$ at pH 7.2 and 25°C (28). The results displayed in Fig. IV.8 suggest that both k_{on} and k_{off} for oxygen binding to cholesterol-bound ferrous cytochrome P-450$_{scc}$ are independent of pH over the pH range of the study. Similar observations of pH-independence of k_{on} and k_{off} for carbon monoxide binding to both cholesterol-free and cholesterol-bound ferrous cytochromes P-450$_{scc}$ have been made in our earlier studies (Kashem, M.A., Lambeir, A.-M. and Dunford, H.B., submitted for publication).

The cholesterol-bound oxyferrous complex of cytochrome P-450$_{scc}$ decayed to the ferric enzyme by a first order monophasic reaction (Fig. IV.7). This is in contrast to the oxyferrous complexes of Rhizobium cytochromes P-450 (15), liver microsomal cytochromes P-450$_{LM_4}$ and P-450$_{LM_{3b}}$ (14), and chloroperoxidase (29) which decay in a biphasic manner; but closely resembles the first order monophasic decay of the oxyferrous complex of cytochrome P-450$_{cam}$ (7,8). Although we have not detected superoxide as a product of the decay of the oxyferrous complex of cytochrome P-450$_{scc}$ superoxide formation is implied by the electron balance of

the reaction. The production of superoxide from the very similar decay process of the cytochrome P-450$_{cam}$ derivative is well documented (9,14).

Results of the present study suggest that the rate of decay of the oxyferrous complex is influenced by an acid group with a pK_a of 7.1 (Table IV.2) on the oxyferrous complex of cholesterol-bound cytochrome P-450$_{scc}$, and k_{decay} increases with the decrease of pH (Fig. IV.9). This is in complete accord with the previous observation that binding of cholesterol and 20α,22R-dihydroxy cholesterol to cholesterol-free cytochrome P-450$_{scc}$ is accompanied by an uptake of a proton by a group with a pK_a of 6.8, and that lowered pH produces an increase in the fraction of cytochrome P-450$_{scc}$ in the high-spin form (30). Other investigators have indicated that hydrogen ion concentration increases the first order decay rate dramatically of the oxyferrous complexes of cytochromes P-450$_{cam}$ (7,8) and P-450$_{scc}$ below pH 7 (16).

The observed first order decay rate constants (Table IV.1) are considerably higher than the reported value of 9.3×10^{-3} s^{-1} (at same temperature but at lower ionic strength, 0.06 M) for the oxyferrous complex of bovine adrenocortical cytochrome P-450$_{scc}$ (16). In fact, the decay rate constant increases with the increase of ionic strength of the reaction medium (7,16). This may partly be

attributable to the observed higher k_{decay} values in Table IV.1 (obtained at ionic strength greater than 0.06 M). Differences in the characteristics of the interaction of cholesterol with cytochrome $P\text{-}450_{scc}$ in beef adrenal mitochondria and in rat adrenal mitochondria have been reported (31). Consequently, caution must be exercised in extending conclusions made from studies using one tissue to another. Furthermore, the decay rate constants reported for the multiphasic decay processes of the oxyferrous complexes of Rhizobium cytochromes P-450 (15) are comparable to our results.

References

1. Burstein, S. and Gut, M (1976) Steroids **28**, 115-131.
2. White, R.E. and Coon, M.J. (1980) Annu. Rev. Biochem. **49**, 315-356.
3. Wagner, G.C. and Gunsalus, I.C. (1982) in "The Biological Chemistry of Iron" (Dunford, H.B., Dolphin, D., Raymond, K.N. and Sieker, L., eds.) pp.405-412, D. Riedel, Dordrecht.
4. Schleyer, M., Cooper, D.Y. and Rosenthal, O. (1971) in "Oxidases and Related Redox Systems" (King, T.E., Mason, H.S. and Morrison, M., eds.) pp.469-484, University Park press, Baltimore.
5. Tyson, C.A., Lipscomb, J.D. and Gunsalus, I.C. (1972) J. Biol. Chem. **247**, 5777-5784.
6. Ishimura, Y., Ulrich, V. and Peterson, J.A. (1971) Biochem. Biophys. Res. Commun. **42**, 140-146.
7. Peterson, J.A., Ishimura, Y. and Griffin, B.W. (1972) Arch. Biochem. Biophys. **149**, 197-208.
8. Eisenstein, L., Debey, P. and Douzou, P. (1977) Biochem. Biophys. Res. Commun. **77**, 1377-1383.
9. Sligar, S.G., Lipscomb, J.D., Debrunner, P.G. and Gunsalus, I.C. (1974) Biochem. Biophys. Res. Commun. **61**, 290-296.
10. Bonfils, C., Debey, P. and Maurel, P. (1979) Biochem. Biophys. Res. Commun. **88**, 1301-1307.

11. Maurel, P., Bonfils, C., Debey, P. and Balny, C. (1980) in "Microsomes, Drug Oxidations, and Chemical Carcinogenesis" (Coon, M.J., Conney, A.H., Estabrook, R.W., Gelboin, H.V., Gillette, J.R. and O'Brien, P.J., eds.) pp.359-362, Academic Press, New York.

12. Larroque, C. and Van Lier, J.E. (1980) FEBS Lett. **115**, 175-177.

13. Tuckey, R.C. and Kamin, H. (1982) J. Biol. Chem. **257**, 9309-9314.

14. Oprian, D.D., Gorsky, L.D. and Coon, M.J. (1983) J. Biol. Chem. **258**, 8684-8691.

15. Lambeir, A.-M., Appleby, C.A. and Dunford, H.B. (1985) Biochim. Biophys. Acta **828**, 144-150.

16. Hume, R., Kelly, R.W., Taylor, P.L. and Boyd, G.S. (1984) Eur. J. Biochem. **140**, 583-591.

17. Hanukoglu, I., Spitsberg, V., Bumpus, J.A., Dus, K.M. and Jefcoate, C.R. (1981) J. Biol. Chem. **256**, 4321-4328.

18. Lowry, O.H., Rosebrough, N.J., Farr, A.L. and Randall, R.J. (1951) J. Biol. Chem. **193**, 265-275.

19. Omura, T. and Sato, R. (1964) J. Biol. Chem. **239**, 2379-2385.

20. Orme-Johnson, W.H. and Beinert, H. (1969) J. Biol. Chem. **244**, 6143-6148.

21. March, S.C., Parikh, I. and Cuatrecasas, P. (1974) Anal. Biochem. **60**, 149-152.

22. Huang, J.J. and Kimura, T. (1973) Biochemistry **12**, 406-409.

23. Palcic, M.M., Rutter, R., Araiso, T., Hager, L.P. and Dunford, H.B. (1980) Biochem. Biophys. Res. Commun. **94**, 1123-1127.

24. Kido, T., Arakawa, M. and Kimura, T. (1979) J. Biol. Chem. **254**, 8377-8385.

25. Lange, N.A. and Forker, G.M. (eds.) (1967) Handbook of Chemistry, 10th ed., p.1101, McGraw-Hill, New York.

26. Wittenberg, J.B., Noble, R.W., Wittenberg, B.A., Antonini, E., Brunori, M. and Wyman, J. (1967) J. Biol. Chem. **242**, 626-634.

27. Hardman, K.D., Eylar, E.H., Ray, D.K., Banaszak, L.J. and Gurd, F.R.N. (1966) J. Biol. Chem. **241**, 432-442.

28. Tuckey, R.C. and Kamin, H. (1983) J. Biol. Chem. **258**, 4232-4237.

29. Lambeir, A.-M. and Dunford, H.B. (1985) Eur. J. Biochem. **147**, 93-96.

30. Lambeth, J.D., Kitchen, S.E., Farooqui, A.A., Tuckey, R.C. and Kamin, H. (1982) J. Biol. Chem. **257**, 1876-1884.

31. Jefcoate, C.R., Orme-Johnson, W.H. and Beinert, H. (1976) J. Biol. Chem. **251**, 3706-3715.

CHAPTER FIVE

KINETICS OF REDUCTION OF BEEF ADRENOCORTICAL CYTOCHROME P-450$_{scc}$ BY DITHIONITE

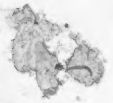

Introduction

The mechanism of the reduction of cytochrome P-450 by NADPH-P-450 reductase (enzymic reduction) and sodium dithionite has been a subject of considerable interest in recent years (1-8). It is now well established that during the steroidogenic electron transfer adrenodoxin, an iron sulfur protein, forms 1:1 complexes with both NADPH-adrenodoxin reductase (flavoprotein) (9,10) and cytochrome $P\text{-}450_{scc}$ (11-13). Adrenodoxin first forms its complex with and accepts an electron from the flavoprotein, then the complex dissociates. Finally it forms a 1:1 complex with and transfers an electron to cytochrome $P\text{-}450_{scc}$.

Dithionite ion is an important and widely used reducing agent in biochemistry. It is interesting kinetically in that it is able to react either as the $S_2O_4^{2-}$ ion or as the dissociated $SO_2^{\cdot-}$ radical anion (14,15). Previous reports have indicated that the reduction of cytochrome $P\text{-}450_{cam}$ by sodium dithionite is consistent with a monophasic process involving $SO_2^{\cdot-}$ as the reducing species (5), in contrast with the biphasic process found for cytochrome $P\text{-}450_{PB}$ (6) and $P\text{-}450_{scc}$ (2). A biphasic reduction process was also observed for the NADPH-dependent reduction of liver microsomal cytochrome $P\text{-}450_{PB}$, cytochrome $P\text{-}450_{LM_2}$ and cytochrome $P\text{-}450_{LM_4}$ (6-8); while a single phase one-electron reduction process was observed for cytochrome $P\text{-}450_{scc}$ (2).

Although the reduction reaction of cytochrome $P\text{-}450_{scc}$ has been studied by NADPH and dithionite titrations (2) the mechanism of the reaction is not fully understood. Moreover, there are no kinetic parameters available for this reaction. In the present study we have investigated the transient state kinetics as a function of pH for the dithionite reduction of purified beef adrenocortical cholesterol-bound cytochrome $P\text{-}450_{scc}$.

Materials and Methods

Cholesterol-bound cytochrome $P\text{-}450_{scc}$ was purified from beef adrenocortical mitochondria as described previously (16). The procedure involved cholate extraction, ammonium sulfate fractionation, aniline-Sepharose 4B and adrenodoxin-Sepharose 4B affinity chromatography. Purified $P\text{-}450_{scc}$ has an A_{280}/A_{393} ratio of 1.2, which corresponds to 13 nmol $P\text{-}450_{scc}$/mg protein as determined by the Lowry assay (17) and the reduced-CO difference spectrum (18). Adrenodoxin was purified from beef adrenal cortex using described methodology (16,19). Aniline-Sepharose 4B and adrenodoxin-Sepharose 4B were prepared according to the published procedures (16) using CNBr-activated Sepharose 4B rather than Sepharose 4B.

All experiments were performed in 10 mM potassium phosphate buffer at 25°C and ionic strength 0.11 M. The

ionic strength was adjusted with KCl, and all buffers contained 0.1 mM EDTA. The pH was measured after each experiment using a Fisher Microprobe electrode and Fisher digital pH meter. Rapid-scan and stopped-flow experiments were carried out in a Union Giken RA601 Rapid Reaction Analyzer. Solutions were made anaerobic by flushing with high-purity argon (zero gas, Canadian Liquid Air) purified by passage through an oxygen trap (Oxypurge N, Altech Associates). Argon was flushed over the surface of the enzyme solutions and bubbled through all other solutions. Solutions were handled and transferred by means of gas-tight Hamilton syringes. Sodium dithionite stock solutions were made by adding a weighed amount to 5 mL anaerobic buffer pH 6.8 (or 1 mM NaOH). The concentration of the dithionite was determined by the reaction with potassium ferricyanide (5). The final cytochrome P-450$_{scc}$ concentrations for the rapid-scan experiments were 5 μM and for the stopped-flow experiments were 2.0-2.5 μM. The kinetics of the reduction of cholesterol-bound cytochrome P-450$_{scc}$ were followed at 418 nm (the isosbestic wavelength between the ferrous and oxyferrous complexes of P-450$_{scc}$), and, as a check, at 393 nm (disappearance of oxidized P-450$_{scc}$). Consistent results were obtained. To avoid denaturation of cytochrome P-450$_{scc}$ below pH 6.0 (20) a pH jump method was used; buffer was placed only in the drive syringe containing dithionite. All

kinetic curves were found to be pseudo-first order with an initial lag (of variable length). Rate constants were determined from a non-linear least squares analysis. Between three to five determinations of the rate constants were performed for every dithionite concentration and the mean value for the observed rate constant was used in the calculations.

Results

The spectral changes observed during the reaction of cholesterol-bound cytochrome P-450$_{scc}$ with sodium dithionite are shown in Figs. V.1 and V.2. The reduction was very slow and no spectral changes were observed for the initial five seconds (spectra not shown). The spectra in Figs. V.1 and V.2 revealed no intermediates apart from the native ferric and ferrous cholesterol-bound cytochrome P-450$_{scc}$. The largest changes in absorbance occur in the vicinity of 393 nm and 420 nm (Fig. V.2) with an isosbestic point at 408 nm.

The kinetics of reduction of cholesterol-bound cytochrome P-450$_{scc}$ were studied between pH 5.2 and 7.9. At all pH values the reduction kinetics were found to be associated with an initial lag phase (of variable length) followed by a single exponential first order process (Fig. V.3). The linear dependence of the observed first order rate constant (k_{obs}) on the square root of the dithionite

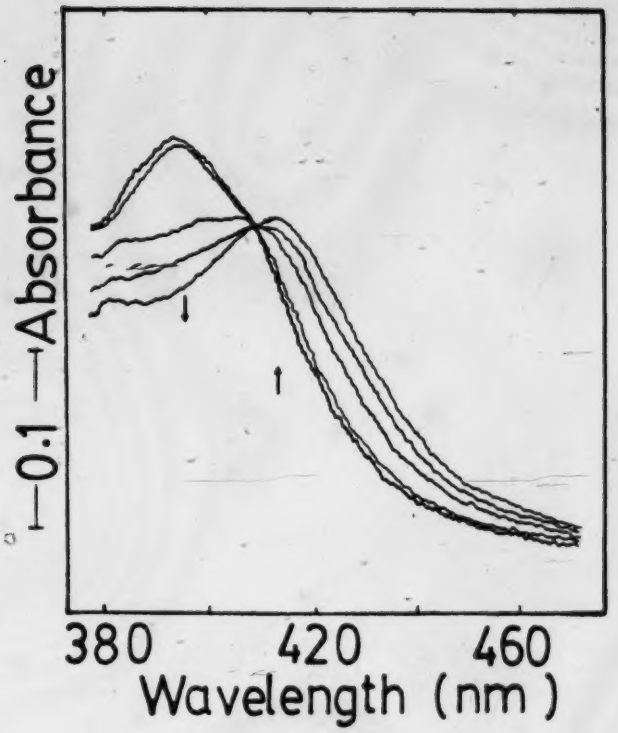

Figure V.1 Spectral changes associated with the reduction of cholesterol-bound cytochrome P-450$_{scc}$ by dithionite at pH 7.34 and 25°C. The arrows indicate the direction of the absorbance change with time. The final concentrations were 5.2 μM cytochrome P-450$_{scc}$ and 3.3 mM dithionite. The spectra presented here are ferric cholesterol-bound cytochrome P-450$_{scc}$, and traces recorded 8, 30, 60 and 120 s after mixing.

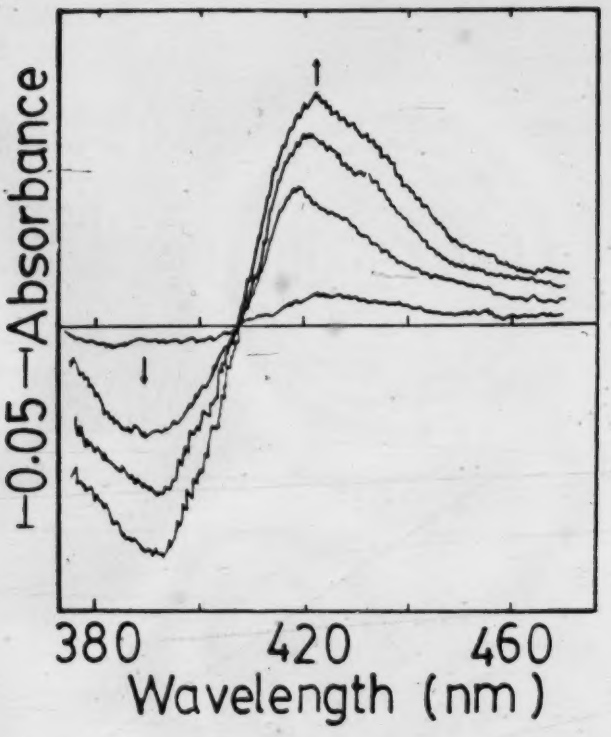

Figure V.2 Reduction of cholesterol-bound cytochrome P-450$_{scc}$. Conditions as described in Fig. V.1 caption. Difference spectra taken 8, 30, 60 and 120 s after mixing versus the ferric cholesterol-bound cytochrome P-450$_{scc}$.

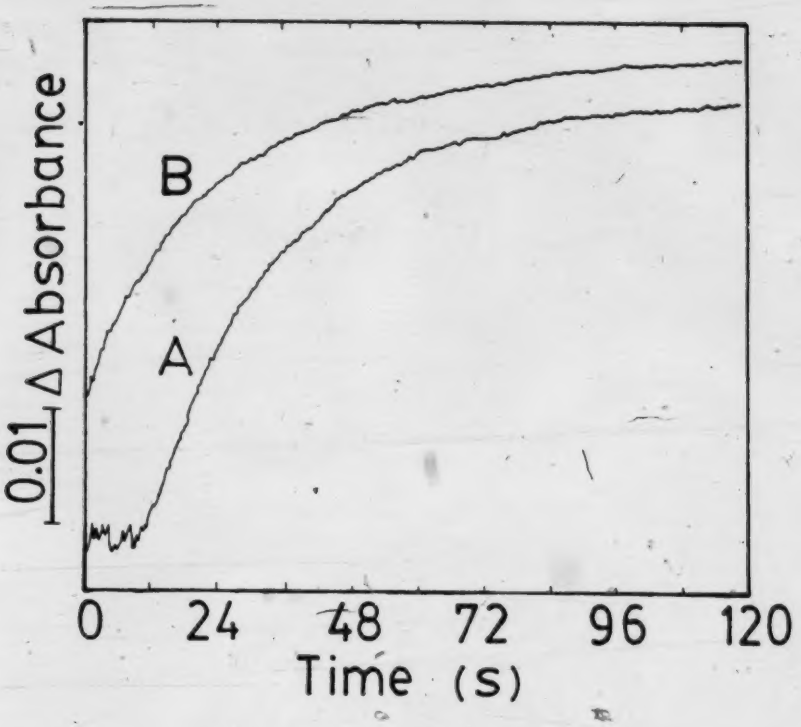

Figure V.3 Time dependence of the absorbance changes after mixing 3.3 mM dithionite with 5.2 μM cholesterol-bound cytochrome P-450$_{scc}$ at pH 6.87 and 25°C. Traces were recorded at 418 nm on the stopped-flow apparatus with delay times 63 ms (A) and 8.5 s (B). Traces are shifted vertically for clarity.

anion concentration extrapolates through zero in each case and implicates $SO_2^{\cdot-}$ as the reducing species (Fig. V.4).

Theoretically cytochrome P-450$_{scc}$ could react directly with $S_2O_4^{2-}$ or with the $SO_2^{\cdot-}$ radical. The corresponding pseudo-first order rate constant for reduction contains two terms (15):

$$[1] \quad k_{obs} = a[S_2O_4^{2-}] + b[S_2O_4^{2-}]^{1/2}.$$

The results in Fig. V.4 indicate that the first term is negligibly small and cytochrome P-450$_{scc}$ reacts preferentially with $SO_2^{\cdot-}$ according to the mechanism

$$[2] \quad S_2O_4^{2-} \rightleftharpoons 2SO_2^{\cdot-} \quad (K_1)$$

$$[3] \quad SO_2^{\cdot-} + \text{P-450}_{scc}(Fe^{3+}) \xrightarrow{k_2} SO_2 + \text{P-450}_{scc}(Fe^{2+})$$

where K_1 (M) is the dissociation constant of $S_2O_4^{2-}$. The observed pseudo-first order rate constants (k_{obs}) are related to the true second order rate constant (k_2) by

$$[4] \quad k_{obs} = k_2 K_1^{1/2} [S_2O_4^{2-}]^{1/2}.$$

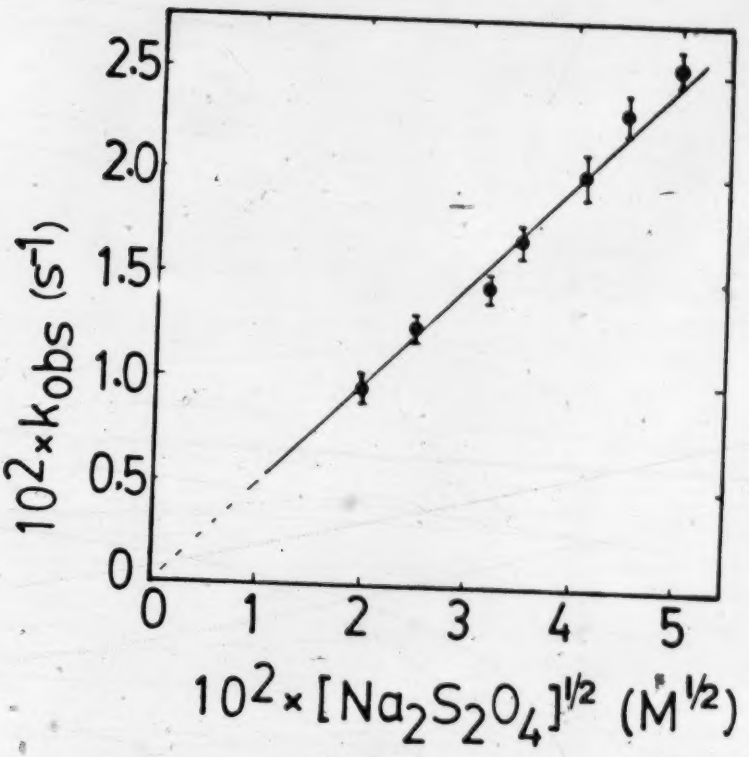

Figure V.4 The observed pseudo-first order rate constants (k_{obs}) are plotted as a function of the square root of the dithionite concentration at pH 7.34 and 25°C. The cytochrome P-450_{scc} concentration was 2.5 μM, and the straight line is the weighted least squares best-fit line.

With a K_1 value of 1.4×10^{-9} (M) (at 0.11 M ionic strength and 25°C) (14), the values of k_2 were calculated from the slopes of the plots (Fig. V.4). The results are summarized in Table V.1

Discussion

From the results reported in this work, it can be concluded that the reduction of cholesterol-bound cytochrome P-450_{scc} by sodium dithionite occurs by a mechanism consistent with $SO_2^{\cdot-}$ as the reducing species. The mechanism corresponds to a single electron-transfer reaction, according to eq.3. This is in good agreement with the observation made for the dithionite reduction of cytochrome P-450_{cam} (5), metmyoglobin (15), horseradish peroxidase (21) and chloroperoxidase (22). In contrast a stoichiometry of two electrons per P-450 molecule was found in a titration of cholesterol-bound cytochrome P-450_{scc} with sodium dithionite (2). The same workers obtained a stoichiometry of one, when cytochrome P-450_{scc} was titrated with NADPH in the presence of adrenodoxin reductase and adrenodoxin. Most recent studies using electrochemical titration methods revealed that all cytochromes P-450 have a redox stoichiometry of unity (4).

The presence of an initial lag was also observed during dithionite titration of cytochrome P-450_{scc} (2), and the

Table V.1 Rate constants for the reduction of cholesterol-bound cytochrome P-450$_{scc}$ by sodium dithionite as a function of pH at 25°C.

pH	$10^{-4} x k_2$ (M^{-1} s^{-1})[a]
5.23	1.7±0.1
5.94	1.9±0.3
6.87	2.2±0.2
7.34	1.4±0.2
7.93	2.0±0.1

[a]Errors of rate constants represent the standard deviation calculated from data at a given pH.

reduction of cytochrome P-450$_{scc}$ by NADPH in the presence of phenazine methosulfate (3). Two possibilities exist for this initial lag phase: the presence of a small amount of residual oxygen (2), and/or the formation of an intermediate complex between the reductant and cytochrome P-450$_{scc}$ (3). However, the latter possibility can be excluded since no intermediate was detected in the rapid-scan experiment (Fig. V.1 and V.2). Furthermore, there was no accompanying absorbance changes associated with the lag phase.

The values of the second order rate constant (k_2) for the reduction of cholesterol-bound cytochrome P-450$_{scc}$ by $SO_2^{\cdot-}$ (Table V.1) are considerably smaller than for metmyoglobin or horseradish peroxidase (15,21) (with rate constants of 2.7×10^6 M^{-1} s^{-1} and 5.0×10^5 M^{-1} s^{-1}, respectively). It was reported earlier that complete reduction of cytochrome P-450 by sodium dithionite required 2 to 5 min, and the rate of the reduction was slow compared to other heme proteins (23). However the values of k_2 listed in Table V.1 are comparable to those of 1.6×10^4 M^{-1} s^{-1} for camphor-bound cytochrome P-450$_{cam}$ (5), and 7.7×10^4 M^{-1} s^{-1} for chloroperoxidase (22).

The reduction kinetics of cholesterol-bound cytochrome P-450$_{scc}$ by $SO_2^{\cdot-}$ appear to be pH independent with a second order rate constant of $(1.8 \pm 0.3) \times 10^4$ M^{-1} s^{-1} (Table V.1) over the pH range of the study (5.2 to 7.9). This is in

complete accord with the previous finding that the midpoint potential of the cytochrome P-450$_{scc}$-substrate complex (-282 mV) is independent of pH from 6 to 8 (2). Similar pH independent kinetic behaviour was observed for the reduction of cytochrome P-450$_{cam}$ by dithionite (5).

References

1. Light, D.R. and Orme-Johnson, N.R. (1981) J. Biol. Chem. **256**, 343-350.
2. Lambeth, J.D. and Pember, S.O. (1983) J. Biol. Chem. **258**, 5596-5602.
3. Usanov, S.A., Chernogolov, A.A., Chashchin, V.L. and Akhrem, A.A. (1985) Biokhimiya **50**, 1702-1711.
4. Huang, Y.Y., Hara, T., Sligar, S., Coon, M.J. and Kimura, T. (1986) Biochemistry **25**, 1390-1394.
5. Hintz, M.J. and Peterson, J.A. (1980) J. Biol. Chem. **255**, 7317-7325.
6. Davydov, D.R. and Kurganov, B.I. (1982) Biokhimiya **47**, 1476-1482.
7. Peterson, J.A., Ebel, R.E., O'Keeffee, D.H., Matsubara, T. and Estabrook (1976) J. Biol. Chem. **251**, 4010-4016.
8. Oprian, D.D., Vatsis, K.P. and Coon, M.J. (1979) J. Biol. Chem. **254**, 8895-8902.
9. Chu, J.-W. and Kimura, T. (1973) J. Biol. Chem. **248**, 5183-5187.
10. Lambeth, J.D., McCaslin, D.R. and Kamin, H. (1976) J. Biol. Chem. **251**, 7545-7550.
11. Katagiri, M., Takikawa, O., Sato, H. and Suhara, K. (1977) Biochem. Biophys. Res. Commun. **77**, 804-809.
12. Seybert, D.W., Lambeth, J.D. and Kamin, H. (1978) J. Biol. Chem. **253**, 8355-8358.

13. Seybert, D.W., Lancaster, J.R., Jr., Lambeth, J.D. and Kamin, H. (1979) J. Biol. Chem. **254**, 12088-12098.

14. Chien, J.C.W. and Dickinson, L.C. (1974) J. Biol. Chem. **253**, 6965-6972.

15. Lambeth, D.O. and Palmer, G. (1973) J. Biol. Chem. **248**, 6095-6103.

16. Hanukoglu, I., Spitsberg, V., Bumpus, J.A., Dus, K.M. and Jefcoate, C.R. (1981) J. Biol. Chem. **256**, 4321-4328.

17. Lowry, O.H., Rosebrough, N.J., Farr, A.L. and Randall, R.J. (1951) J. Biol. Chem. **193**, 265-275.

18. Omura, T. and Sato, R. (1964) J. Biol. Chem. **239**, 2379-2385.

19. Orme-Johnson, W.H. and Beinert, H. (1969) J. Biol. Chem. **244**, 6143-6148.

20. Hume, R., Kelly, R.W., Taylor, P.L. and Boyd, G.S. (1984) Eur. J. Biochem. **140**, 583-591.

21. Balahura, R.J. and Wilkins, R.G. (1983) Biochim. Biophys. Acta **724**, 465-472.

22. Lambeir, A.-M. and Dunford, H.B. (1985) Eur. J. Biochem. **147**, 93-96.

23. Schenkman, J.B., Cha, Y.-N., Moldeus, P., and Cinti, D.L. (1973) Durg. Metab. Dispos. **1**, 516-522.

CHAPTER SIX

GENERAL DISCUSSION AND CONCLUSIONS

Transient state kinetics provides a powerful tool in the elucidation of the reaction mechanism of enzymes. This thesis describes the kinetics of reactions of two different heme enzymes, horseradish peroxidase (HRP) and cytochrome $P\text{-}450_{scc}$. These two enzymes have several points in common. The chemical and physiological properties of the two enzymes have been summarized in the introductory Chapter.

The mechanism of oxidation of NADH by HRP is of importance in peroxidase chemistry because it is the single known reaction of HRP which oscillates (1,2). When an aerobic solution of NADH is mixed with HRP in a closed system, an extremely complicated reaction cycle occurs, which passes through induction, initial burst, steady state and termination phases (1,2). The start of the reaction requires a small amount of H_2O_2, which, in fact, can be present in the NADH solution owing to a slow autoxidation process. In Chapter II, the observed pH dependent transient state kinetics of oxidation of NADH by HRP-I and HRP-II have been discussed.

At all pH values the HRP-I-NADH reaction obeys a second order kinetics; this is indicated by the linearity and zero intercept of the plots of pseudo-first order rate constant versus NADH concentration. On the other hand, a positive intercept in the plots for the HRP-II-NADH reaction suggests

that the reaction is reversible. As mentioned in Chapter II, the reduction potential of NAD•/NADH couple is estimated to be about +0.30 V at pH 7.0 (3,4). The reduction potential of HRP-II/HRP couple is pH dependent (5) and varies from 0.97 V (pH 6.0) to 0.50 V (pH 12.0). Thus, it appears that HRP-II/HRP couple has more positive reduction potential than NAD• NADH couple. This means that the transport of electron from HRP to NAD• is not a thermodynamically advantageous process. However, the observed reversibility of HRP-II-NADH reaction indicates that HRP is, in fact, oxidized by NAD•. Also the values of reverse rate constant (k_{-2}) (Table II.5) decreases with increasing pH, which is contrary to the pH dependence of the oxidation/reduction potential of the HRP-II/HRP couple (5). This behaviour is not clearly understood. However, it is believed to be related to the complexities of the oxidase reaction of HRP with NADH. It has also been reported that in enzyme reactions involving NADH several factors, such as local pH and polarity of the molecular environment of the NADH, affect the reduction potential and electron transfer process (3).

The second order rate constant for the HRP-I-NADH reaction varies from 2.6×10^5 to 5.6×10^2 M^{-1} s^{-1} and for the HRP-II-NADH reaction from 4.4×10^4 to 4.1 M^{-1} s^{-1} at 25°C over the pH range 4 to 10. An analysis of the pH dependence

of the second order rate constants revealed that an ionizable group on the enzyme with a pK_a of 4.7±0.5 for HRP-I and a pK_a of 4.2±1.4 for HRP-II is important in the oxidation process. The pK_a of 4.7±0.5 for HRP-I is in complete accord with the value of ~5 obtained previously with several reducing substrates (6). In contrast the pK_a value of 4.2±1.4 for HRP-II is not in agreement with either one of the two values ~0 and 8.6 reported for most other substrates (6). However the pH-rate profile of HRP-II-NADH reaction (Fig. II.6) closely resembles that obtained for the reaction of HRP-II with bisulfite, a substrate which attacks the heme after a few reaction cycles (7,8). An acid group on HRP-II with a pK_a of 3.9 appeared to be important for the latter reaction (7). The reaction of HRP-II with reducing substrate is usually rate limiting. The data in Table II.4 and II.5 show that the rate constants for both HRP-I-NADH and HRP-II-NADH reactions are almost similar below pH 6. However, at higher pH the rate constants for HRP-I-NADH reaction are significantly higher than for HRP-II-NADH reaction. Previous reports indicate that at low pH, p-aminobenzoic acid has almost similar rate constants for the reduction of both HRP-I and HRP-II (9). The protein residue of pK_a ~5, obtained in all pH-dependent reactions of HRP-I, has been suggested to be the distal His-42 (10). It is possible that the same group may be responsible for the

observed pH-dependent kinetics of HRP-II-NADH reaction (pK_a of 4.2±1.4). The acid group corresponding to pK_a of ~8.6, obtained previously for the reaction of several reducing substrates (p-cresol, p-aminobenzoic acid and ferrocyanide) is also a distal group (6). Arg-38, Leu-39, His-40, Phe-41, His-42 and Asp-43 are potential candidates (10,11).

Chapter III describes the first intensive studies of the kinetics of carbon monoxide binding to both cholesterol-free and cholesterol-bound forms of cytochrome $P\text{-}450_{scc}$. These two forms of $P\text{-}450_{scc}$ were purified from beef adrenocortical mitochondria using different procedures. Carbon monoxide binding was investigated by means of rapid-scan and stopped-flow spectrometry at 25°C. Rapid-scan spectra in the Soret region indicated the reversible formation of reduced-CO complex without any intermediates. Isosbestic points occurred at the following wavelengths: between reduced-CO and reduced cholesterol-free $P\text{-}450_{scc}$ at 434 and 471 nm; between reduced-CO and reduced cholesterol-bound $P\text{-}450_{scc}$ at 433 and 469 nm. Carbon monoxide binding for both forms of $P\text{-}450_{scc}$ is found to be a simple monophasic bimolecular process and is consistent with that observed for cytochromes $P\text{-}450_{cam}$ (12), $P\text{-}450_{scc}$ (13) and $P\text{-}450_{PB}$ (14). The previously reported biphasic CO binding process for cytochromes $P\text{-}450_{LM2}$, $P\text{-}450_{LM4}$ and $P\text{-}450_{PB}$ (15,16) was suggested to be due to heterogeneity of the protein

preparations (14).

Both "on" (k_1) and "off" (k_{-1}) rate constants for CO binding to cytochromes P-450$_{scc}$ are pH independent between pH 5 and 9. The mean values of k_1 for cholesterol-free ($(1.8\pm0.2)\times10^5$ M^{-1} s^{-1}) and cholesterol-bound ($(1.9\pm0.1)\times10^5$ M^{-1} s^{-1}) P-450$_{scc}$ are almost identical, and are in close agreement with the reported values at a single pH 7.2 (13). Contrary to the reported values at a single pH (13), the mean value of k_{-1} for cholesterol-free P-450$_{scc}$ ($(2.3\pm0.3)\times10$ s^{-1}) is almost double to that for cholesterol-bound P-450$_{scc}$ ($(1.2\pm0.1)\times10$ s^{-1}). The data fit to the general P-450 behaviour that the reduced-CO (oxygen) complex is kinetically stabilized by substrate binding (17-19).

Recently, the technique of resonance Raman spectroscopy has been applied to characterize the carbon monoxide complex of cytochromes P-450$_{cam}$ (20), and P-450$_{scc}$ (21,22). It has been reported that the Fe-CO stretching frequency in the cholesterol-free cytochrome P-450$_{scc}$-CO complex lies at 477 cm^{-1}. Upon addition of substrate, cholesterol, the Fe-CO stretching frequency shifted to 483 cm^{-1} (22). A similar Fe-CO stretching frequency shift was also observed for the resonance Raman spectra of cytochrome P-450$_{cam}$ (20). This finding indicates that the bound substrate interacts predominantly with the Fe-CO portion of the enzyme molecule (20,22). In addition, an enhanced stability of the native

form ("P-450") was observed in the presence of cholestrol (22). Without cholesterol the CO complex of cytochrome $P\text{-}450_{scc}$ became its denatured form (CO complex of P-420). To the contrary, in the presence of cholesterol, the CO complex of cytochrome $P\text{-}450_{scc}$ was found to be extremely stable for more than several hours when kept irradiated by laser light at room temperature. The latter observation is consistent with our kinetic results.

The formation of the oxyferrous complex of cytochrome P-450 is the initial step in the enzyme activation of molecular oxygen. The rapid-scan and stopped-flow results obtained for the formation and spontaneous decay of the oxyferrous complex of cholesterol-bound cytochrome $P\text{-}450_{scc}$ are presented in Chapter IV. A significant finding of this study is the detection of the oxyferrous complex of cholesterol-bound $P\text{-}450_{scc}$ for the first time above 0°C (at 4°C), the spectral characteristics of which are consistent with those observed previously at sub-zero temperatures for $P\text{-}450_{scc}$ (18,23), $P\text{-}450_{cam}$ (19) and $P\text{-}450_{LM2}$ (24,25). The oxyferrous complex, the formation of which occurs within 40 ms with a Soret peak at 422 nm, is unstable and autoxidizes to the ferric cholesterol-bound $P\text{-}450_{scc}$. Isosbestic points occurred at 418 nm between ferrous and oxyferrous complex and at 411 nm between oxyferrous and ferric $P\text{-}450_{scc}$.

The overall kinetics is found to be consistent with the

equation:

$$Fe^{2+} + O_2 \underset{k_{off}}{\overset{k_{on}}{\rightleftharpoons}} Fe^{2+}\cdot O_2 \xrightarrow{k_{decay}} Fe^{3+} + O_2^{-}\cdot \quad .$$

In agreement with the CO binding results, both k_{on} and k_{off} for oxygen binding are pH independent. The mean value of k_{on} at 4°C is $(5.1\pm0.8)\times10^5$ M^{-1} s^{-1} over the pH range 5 to 9, which corresponds well with the values reported for other cytochromes P-450 (13,26,27) and choloroperoxidase (28) measured under identical conditions. The rate constant for the second process, k_{decay}, appears to be influenced by an acid group with a pK_a of 7.1±0.1 at the active site of the oxyferrous complex. A dramatic increase in k_{decay} below pH 7 was observed earlier for cytochromes $P\text{-}450_{cam}$ (19,27) and $P\text{-}450_{scc}$ (29). In this connection it is of interest to note that cholesterol plays a critical role on the stability of the oxyferrous complex of cytochrome $P\text{-}450_{scc}$. It was not possible to detect a stable oxyferrous complex of cholesterol-free cytochrome $P\text{-}450_{scc}$ under the conditions of this study. This observation extends the evidence that the substrate kinetically stabilizes the reduced-CO (oxygen) complex.

Earlier studies also indicate that the binding of cholesterol to cytochrome $P\text{-}450_{scc}$ causes a 15-fold increase in the stability of the oxyferrous complex of $P\text{-}450_{scc}$ at

-17°C (18); and a 12-fold increase in the half-time for the autoxidation of the oxyferrous complex of P-450$_{cam}$ at -20°C in 50% ethylene glycol, when camphor is bound (19). Interestingly, the binding of the hydroxycholesterol intermediates to cytochrome P-450$_{scc}$ causes a further 3-17-fold increase in the stability of the oxyferrous complex in the order 20α,22R-dihydroxycholesterol>22R-hydroxycholesterol>20α-hydroxycholesterol>cholesterol (18). However, the analogous carbon monoxide complex of P-450$_{scc}$ is destabilized by 150- and 300-fold, indicating a unique interaction between the 22R-hydroxyl and oxygen, while the same substituent interferes with carbon monoxide complex formation. This stabilization of the oxyferrous complex derives from 150- to 1000-fold decrease in the dissociation rates of the respective complexes that more than offset slower association rates (13). The mechanism by which the hydroxycholesterols markedly change the kinetic constants for oxygen and carbon monoxide is unknown. A close proximity of the cholesterol side chain and heme-bound oxygen has been predicted based on the positions where hydroxylation occurs. There is some evidence that an amino group at the 22-position of the side chain of cholesterol can coordinate directly to the heme iron (30).

Finally, in Chapter V the kinetics of dithionite reduction of cholesterol-bound cytochrome P-450$_{scc}$, studied

by rapid-scan and stopped-flow spectrometry at 25°C, has been described. The reaction has an initial lag, which was also found during dithionite titration of cytochrome $P\text{-}450_{scc}$ (31). The processes responsible for this lag phase are not clearly understood. However the possibility of complex formation between the reductant and $P\text{-}450_{scc}$ is ruled out by the rapid-scan experiment, which indicates no intermediates apart from ferric and ferrous $P\text{-}450_{scc}$. One possible explanation: the lag is caused by the presence of residual oxygen.

Under the pseudo-first order conditions used throughout this investigation, k_{obs} is found to be linearly dependent on the square root of the concentration of sodium dithionite. This is consistent with a single electron transfer mechanism involving dithionite anion radical, $SO_2^{\cdot-}$, as the reducing species. A similar kinetic pattern was observed for the dithionite reduction of cytochrome $P\text{-}450_{cam}$ (32), metmyoglobin (33), horseradish peroxidase (34) and chloroperoxidase (28). The presence of $SO_2^{\cdot-}$ at low concentrations in solutions of dithionite has been well documented (33,35). The rate constant for monomerization of dithionite anion vary widely from 1.7 s^{-1} (33) to 42.5 s^{-1} (36) depending on experimental conditions. The lowest of these reported values for monomerization is 20 to 100 times greater than the rate of reduction of $P\text{-}450_{scc}$ by $SO_2^{\cdot-}$,

which suggests that the transfer of the single electron from $SO_2^{\cdot-}$ to P-450$_{scc}$ is the rate limiting step. The observed second order rate constant is pH independent and is in complete accord with the finding that the heme mid-point potential of P-450$_{scc}$-cholesterol complex is independent of pH (31). Also the mean value of the second order rate constants, $(1.8\pm0.3)\times10^4$ M^{-1} s^{-1} over the pH range 5 to 8, is comparable to the values reported for cytochrome P-450$_{cam}$ (32) and chloroperoxidase (28). The evidence presented provide an additional confirmation that cytochrome P-450$_{scc}$-cholesterol is an one-electron acceptor.

Although the kinetics of dithionite reduction of cholesterol-free cytochrome P-450$_{scc}$ has not been investigated by this study, it is interesting to note that Lambeth and Pember (31) have observed that enzymatic reduction occurs only in the case of the cholesterol-bound cytochrome P-450$_{scc}$. The spin state of the heme iron of different forms of cytochrome P-450 has a significant effect on the rate and degree of reduction (37). The reduction potential of low-spin cholesterol-free P-450$_{scc}$ would seem to preclude reduction because its potential is -412 mV (38). However, the potential of the high-spin, cholesterol-bound P-450$_{scc}$ is -305 mV (38). This dramatic shift in the reduction potential is believed to order the reaction cycle in the case of P-450$_{scc}$ (31,37). Similar shifts in the

reduction potential of bacterial cytochrome P-450$_{scc}$ have been demonstrated (39).

Problems for the Future

As described throughout this thesis, the key step in the catalytic cycle of cholesterol side-chain cleavage reaction is the formation of the oxyferrous complex of P-450$_{scc}$. Little is known about the chemical and biochemical properties of this species of P-450$_{scc}$. A thorough investigation of the effects of cholesterol and analogues on the kinetics of formation and decay of this species will help us to fully understand the chemical mechanism of the reaction cycle of P-450$_{scc}$. Another area related to this step of oxygen activation will be to study the kinetics of one-electron reduction of P-450$_{scc}$ by physiologic reductant (NADPH in the presence of adrenodoxin and adrenodoxin reductase). Electron transfer from NADPH to cytochrome P-450$_{scc}$ appears to occur via three sequential processes: (i) the interaction of adrenodoxin reductase with NADPH and reduction of flavo-protein; (ii) electron transfer from reduced adrenodoxin reductase to adrenodoxin; (iii) electron transfer from reduced adrenodoxin to cytochrome P-450$_{scc}$. Rapid-scan and transient state kinetic experiments will provide more exciting information about this complex electron transfer process and the intermediates involved.

References

1. Yokota, K. and Yamazaki, I. (1977) Biochemistry **16**, 1913-1920.
2. Olsen, L.F. (1984) in "Stochastic Phenomena and Chaotic Behaviour in Complex Systems" (Schuster, P., ed.), pp.116-123, Springer-Verlag, Berlin.
3. Farrington, J.A., Land, E.J. and Swallow, A.J. (1980) Biochim. Biophys. Acta **590**, 273-276.
4. Anderson, R.F. (1980) Biochim. Biophys. Acta **590**, 277-281.
5. Hayashi, Y. and Yamazaki, I. (1979) J. Biol. Chem. **254**, 9101-9106.
6. Dunford, H.B. and Stillman, J.S. (1976) Coord. Chem. Rev. **19**, 187-251.
7. Roman, R. and Dunford, H.B. (1973) Can. J. Chem. **51**, 588-596.
8. Araiso, T., Miyoshi, K. and Yamazaki, I. (1976) Biochemistry **15**, 3059-3063.
9. Dunford, H.B. and Cotton, M.L. (1975) J. Biol. Chem. **250**, 2920-2932.
10. Dunford, H.B. (1982) in "Adv. Inorg. Biochem." (Eichhorn, G.L. and Margilli, L.G., eds.) Vol. 4, Elsevier Biomedical, New Yok, pp.41-68.
11. Welinder, K.G. and Mazza, G. (1977) Eur. J. Biochem. **73**, 353-358.

12. Peterson, J.A. and Griffin, B.W. (1972) Arch. Biochem. Biophys. **151**, 427-433.

13. Tuckey, R.C. and Kamin, H. (1983) J. Biol. Chem. **258** 4232-4237.

14. Oertle, M., Richter, C., Winterhalter, K.H. and DiIorio, E.E. (1985) Proc. Natl. Acad. Sci. U.S.A. **82**, 4900-4904.

15. Gray, R.D. (1982) J. Biol. Chem. **257**, 1086-1094.

16. Gray, R.G. (1983) J. Biol. Chem. **258**, 3764-3768.

17. Kido, T., Yamakura, F. and Kimura, T. (1981) Biochim. Biophys. Acta **666**, 370-381.

18. Tuckey, R.C. and Kamin, H. (1982) J. Biol. Chem. **257**, 9309-9314.

19. Eisenstein, L., Debey, P. and Douzou, P. (1977) Biochem. Biophys. Res. Commun. **77**, 1377-1383.

20. Uno, T., Nishimura, Y., Makino, R., Iizuka, T., Ishimura, Y. and Tsuboi, M. (1985) J. Biol. Chem. **260**, 2023-2026.

21. Tsubaki, M. and Ichikawa, Y. (1985) Biochim. Biophys. Acta **827**, 268-274.

22. Tsubaki, M., Hiwatashi, A. and Ichikawa, Y. (1986) Biochemistry **25**, 3563-3569.

23. Larroque, C. and Van Lier, J.E. (1980) FEBS Lett. **115**, 175-177.

24. Bonfils, C., Debey, P. and Maurel, P. (1979) Biochem. Biophys. Res. Commun. **88**, 1301-1307.

25. Maurel, P., Bonfils, C., Debey, P. and Balny, C. (1980) in "Microsomes, Drug Oxidations, and Chemical Carcinogenesis" (Coon, M.J., Conney, A.H., Eastabrook, R.W., Gelboin, H.V., Gillette, J.R. and O'Brien, P.J., eds.) pp.359-362, Academic Press, New York.

26. Tyson, C.A., Lipscomb, J.D. and Gunsalus, I.C. (1972) J. Biol. Chem. **247**, 5777-5784.

27. Peterson, J.A., Ishimura, Y. and Griffin, B.W. (1972) Arch. Biochem. Biophys. **149**, 197-208.

28. Lambeir, A.-M. and Dunford, H.B. (1985) Eur. J. Biochem. **147**, 93-96.

29. Hume, R., Kelly, R.W., Taylor, P.L. and Boyd, G.S. (1984) Eur. J. Biochem. **140**, 583-591.

30. Sheets, J.J. and Vickery, L.E. (1983) J. Biol. Chem. **258**, 11446-11452.

31. Lambeth, J.D. and Pember, S.O. (1983) J. Biol. Chem. **258**, 5596-5602.

32. Hintz, M.J. and Peterson, J.A. (1980) J. Biol. Chem. **255**, 7317-7325.

33. Lambeth, D.O. and Palmer, G. (1973) J. Biol. Chem. **248**, 6095-6103.

34. Balahura, R.J. and Wilkins, R.G. (1983) Biochim. Biophys. Acta **724**, 465-472.

35. Mayhew, S.G. (1978) Eur. J. Biochem. **85**, 535-547.

36. Morello, J.A., Craw, M.R., Constantine, H.P. and Forster, R.E. (1964) J. Appl. Physiol. **19**, 522-525.

37. Usanov, S.A., Chernogolov, A.A., Chashchin, V.L. and Akhrem, A.A. (1985) Biokhimiya **50**, 1702-1711.

38. Light, D.R. and Orme-Johnson, N.R. (1981) J. Biol. Chem. **256**, 343-350.

39. Sligar, S. (1976) Biochemistry **15**, 5399-5406.

APPENDIX I

PURIFICATION OF CYTOCHROMES P-450$_{scc}$ AND ADRENODOXIN*

*These proteins were purified from beef adrenal glands for the first time in this laboratory by using established procedures reported elsewhere. In this section the author has described the details of the purification procedures which might be of tremendous benefit for any future investigation.

Purification of Cholesterol-free Cytochrome $P\text{-}450_{scc}$

Low-spin cholesterol-free cytochrome $P\text{-}450_{scc}$ was purified from beef adrenocortical mitochondria according to the previously described procedure (1). The purification was carried out at 0-4°C. Forty beef adrenal glands from freshly slaughtered animals were collected at a local slaughterhouse and brought to the laboratory on ice. Fat was carefully removed from the surface of each gland which was then bisected longitudinally, laid on aluminum foil, upside down on ice. The medulla (light yellow coloured) was scraped off with a scalpel. Following this, the cortex was scraped and put in ~1 L of 0.25 M sucrose, 10 mM Na phosphate, pH 7.4, containing 0.1 mM EDTA (kept on ice). The scrapings were stirred with a glass rod and allowed to stand for a while. The supernatant sucrose solution was drained and more sucrose solution added; this washing procedure was repeated for three or more times to remove the fat. About 2 L of the accumulated sucrose solution was added to the cortex scrapings and homogenized in a Waring Blendor for 90 s. The homogenate was centrifuged at 2,200 rpm for 10 min with a Sorvall GSA rotor to remove cellular debris and unbroken cells. The resulting supernatant was passed through three layers of cheesecloth and further centrifuged at 7,500 rpm for 30 min using the same rotor. The supernatant was then decanted with a pipette and lipids

attached on the centrifuge tube sides were wiped out by using Kimwipes. The precipitated mitochondrial fraction was suspended in 10 mM Na phosphate, pH 7.4, 0.1 mM ETDA with a Teflon homogenizer. This suspension was allowed to stand for 10 min and centrifuged again at 9,250 rpm for 20 min (using a Sorvall GSA rotor). Supernatant was decanted and discarded. The mitochondrial pellet was resuspended in 0.1 M Na pyrophosphate, pH 7.4, with a Teflon homogenizer. The resulting suspension was allowed to stand for 10 min and centrifuged at 9,250 rpm for 20 min. The supernatant was discarded. This procedure was repeated once. The pyrophosphate treatment was reported to remove almost all of the contaminating hemoglobin from liver microsomes (2). The resulting mitochondrial precipitates were suspended in 10 mM Na phosphate, pH 7.4, 0.1 mM EDTA and centrifuged once again as above (at 9,250 rpm for 20 min). The precipitates were finally resuspended in the same buffer to a final protein concentration of 25-30 mg/mL. Protein concentration was determined by the Lowry method (3). The purified mitochondria were then frozen in liquid nitrogen and stored at -20°C.

Frozen mitochondria (150 mL) containing 30 mg of protein/mL were thawed and homogenized by using a Teflon homogenizer. Protein concentration was adjusted to 20 mg/mL by 10 mM Na phosphate, pH 7.4, 0.1 mM EDTA. The suspension

was then sonicated with a Branson Sonifier 350, in 80 mL portions for 3 min. During sonication, the beaker was kept on ice but the temperature rose to 21°C at the end of sonication. A 10% neutralized Na cholate solution was added dropwise with stirring to the sonicate to a final cholate concentration of 1% (w/v) (0.5 mg of cholate/mg of protein). The turbid mixture was stirred for an additional 60 min in the cold room. This mixture was then centrifuged with a Beckman L5-75 Ultracentrifuge using a Type 42.1 rotor at 37,000 rpm for 60 min. Three layers were observed in the centrifuge tubes. Supernatants were carefully collected and saved, leaving the deeply coloured, fluffy, and tightly packed sediment layers at the bottom of the tubes. The combined supernatants are called cholate extract (160 mL, 2145 mg of protein).

The cholate extract was diluted with an equal volume of 10 mM Na phosphate, pH 7.4, 0.1 mM EDTA. It was then placed on a octylamine-Sepharose column (2.6x13 cm), previously equilibrated in 10 mM Na phosphate, pH 7.4, 0.1 mM EDTA. The column was washed with 10 mM Na phosphate, pH 7.4, containing 0.1 mM EDTA and 0.5% cholate until no material absorbing at the 280 nm region came out in the column wash. Cytochrome P-450$_{scc}$ was then eluted with 100 mM Na phosphate, pH 7.4, 1 mM EDTA, 0.5% cholate, and 0.1% Emulgen 913. Fig. A.1 shows the first octylamine-Sepharose column

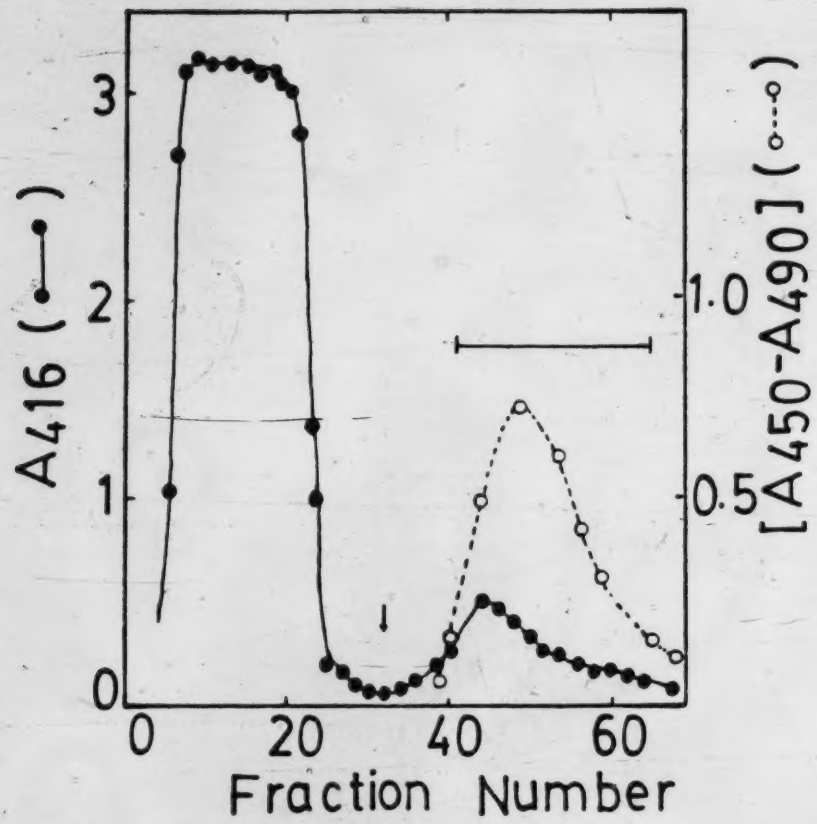

Figure A.1 First Octylamine-Sepharose column elution profile of adrenocortical cholesterol-free cytochrome P-450$_{scc}$. The solid line represents absorbance at 416 nm and the dotted line, the P-450$_{scc}$ assay. Cytochrome P-450$_{scc}$ was eluted (indicated by the arrow) with 100 mM Na phosphate buffer, pH 7.4, 1 mM EDTA, 0.1% Emulgen 913, and 0.5% cholate. Fractions of 14.3 mL were collected (0.95 mL/min) and the active fractions marked with the horizontal bar were pooled. For details see purification of cholesterol-free cytochrome P-450$_{scc}$.

elution profile of P-450$_{scc}$. The eluted enzyme was concentrated to a desired volume (10 mL) using an Amicon PM30 membrane at 25 psi nitrogen. The resulting concentrate was then centrifuged at 20,000 rpm for 30 min (Sorvall SS34 rotor) to remove the turbid material which was formed during concentration. The clear supernatant was collected and glycerol was added to give a final concentration of 20% (v/v). The solution was then dialyzed overnight against 1 L of 10 mM Na phosphate, pH 7.4, 0.1 mM EDTA, 1 mM dithiothreitol, and 20% glycerol. The resulting dialysate is called the first column eluate (12.5 mL, 157.7 mg of protein).

The first column eluate was placed on a second octylamine-Sepharose column (2.6x3.5 cm) which was equilibrated in 10 mM Na phosphate, pH 7.4, 0.1 mM EDTA and 20% glycerol. The column was washed extensively with the same buffer until no absorbance at 276 nm due to Emulgen 913 was detected in the washing. The column was washed again with the same buffer plus 0.5% cholate until no protein was detected in the washing. Finally, cytochrome P-450$_{scc}$ was eluted with 100 mM Na phosphate, pH 7.4, 1.0 mM EDTA, 0.5% cholate, 0.1% Emulgen 913, and 20% glycerol and the active fractions were pooled. The second octylamine-Sepharose column elution profile of cytochrome P-450$_{scc}$ is presented in Fig. A.2. The eluted P-450$_{scc}$ was then concentrated on

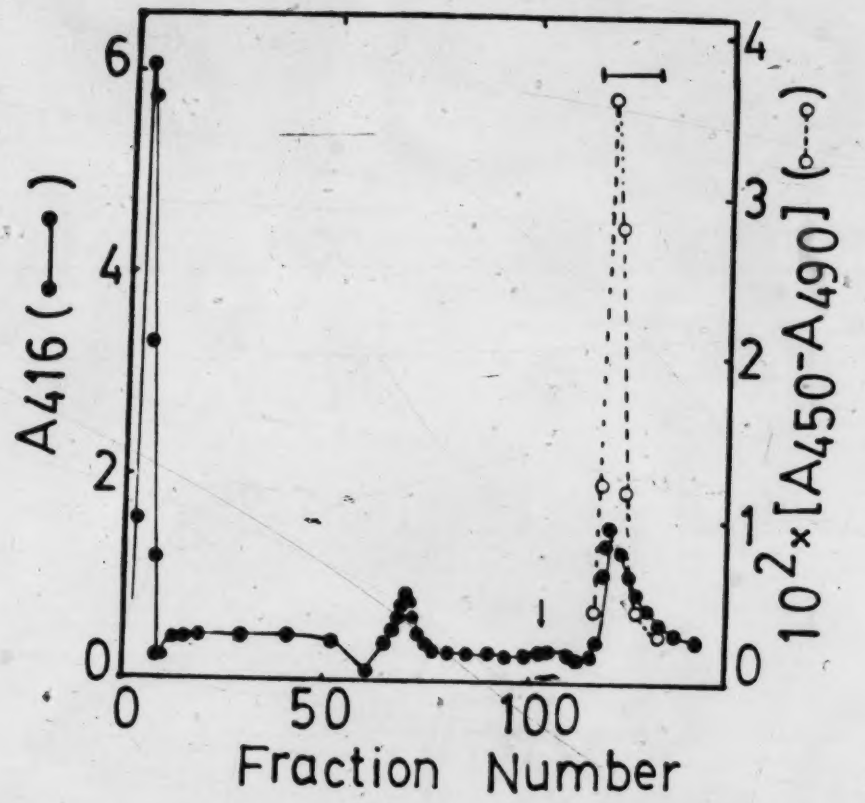

Figure A.2 Second Octylamine-Sepharose column elution profile of adrenocortical cholesterol-free cytochrome P-450$_{scc}$. The solid line represents the absorbance at 416 nm and the dotted line, the P-450$_{scc}$ assay. Cytochrome P-450$_{scc}$ was eluted (indicated by the arrow) with 100 mM Na phosphate buffer, pH 7.4, 1 mM EDTA, 0.5% cholate, 20% glycerol, and 0.1% Emulgen 913. Fractions of 7.6 mL were collected (0.76 mL/min) and the active fractions marked with the horizontal bar were pooled. See purification of cholesterol-free cytochrome P-450$_{scc}$ for details.

an Amicon PM30 membrane. The resulting concentrate was dialyzed overnight against 1 L of 10 mM Na phosphate, pH 7.4, 0.1 mM EDTA, 1 mM dithiothreitol, and 20% glycerol. The dialysate (6 mL), termed second column eluate (optically clear), was assayed for P-450 and protein contents. Second column eluate was in a very few cases contaminated with P-420. P-420 was removed by passing the eluate through a short DEAE-cellulose (DE 52) column (1x8 cm) which was previously equilibrated with 10 mM Na phosphate, pH 7.4, containing 0.1 mM EDTA and 20% glycerol. Purified cytochrome $P\text{-}450_{scc}$ (5 nmol/mg of protein) was stored under liquid nitrogen and retained essentially all its activity after thawing.

Purification of Cholesterol-bound Cytochrome $P\text{-}450_{scc}$

High-spin cholesterol-bound cytochrome $P\text{-}450_{scc}$ was purified from beef adrenocortical mitochondria using described methodology (4-5). All manipulations were carried out at 0-4°C. Beef adrenocortical scrapings (~1 kg from 80 adrenal glands) were washed with several litres of 0.25 M sucrose and homogenized with Waring blendor for 90 s. The homogenate was centrifuged at 2,200 rpm for 10 min with Sorvall GSA rotor to remove cellular debris and unbroken cells. The resulting supernatant was passed through three layers of cheesecloth and centrifuged again at 9,900 rpm for

10 min (same rotor). This supernatant, called 'SN_{ADX}' afterwards, was decanted and stored under liquid nitrogen for adrenodoxin purification. The mitochondrial pellet was suspended to a final protein concentration of 30-40 mg/mL in 100 mM K phosphate, pH 7.3, 200 μM EDTA, left overnight in the cold room. The suspension was then sonicated (Branson sonifier 350) in 50 mL portions in a 100 mL beaker kept on ice for 5 min. The sonicated suspension was centrifuged at 11,000 rpm (Sorvall GSA rotor) for 60 min. The supernatant was discarded. The pellet was suspended in 100 mM K phosphate, pH 7.3, 200 μM EDTA by using a Teflon homogenizer to a final protein concentration of 20-30 mg/mL and stored in 30-50 mL portions under liquid nitrogen.

The mitochondrial pellet (2,450 mg of protein) was thawed and solubilized in 50 mM K phosphate, pH 7.3, 100 μM EDTA, 100 μM dithiothreitol (buffer A) at 15 mg protein/mL by dropwise addition of 10% neutralized Na cholate to a final cholate concentration of 1% (w/v) (0.5 mg of cholate/mg of protein). The turbid mixture was stirred for an additional 1.5 h in the cold room. This suspension was centrifuged with Beckman L5-75 Ultracentrifuge using a Type 42.1 rotor at 37,000 rpm for 60 min. Three layers were observed in the centrifuge tubes. Supernatants were carefully collected and saved, leaving the deeply coloured, fluffy, and tightly packed sediment layers at the bottom of

the tubes. The combined supernatants, were called cholate extract (170 mL, 1125 mg of protein).

This cholate extract was diluted with an equal volume of ice-cold water and placed on an aniline-Sepharose column (2.6x16 cm), previously equilibrated with buffer A. The column was washed with 100 mL of buffer A and then with 100 mL of buffer A + 0.3% cholate + 50 mM KCl. The red band in the top quarter of the column was not shifted while the eluate contain hemoprotein with λ_{max} at 414 nm. Cytochrome P-450$_{scc}$ was then eluted from the column with buffer A + 0.3% cholate + 1 M KCl. The first aniline-Sepharose column elution profile of P-450$_{scc}$ is shown in Fig. A.3. Fractions with A_{280}/A_{393} = 3.0 or less were pooled (71 mL, 590 nmol) and fractionated with ammonium sulfate (25-45%). pH was maintained at 7.3 by dropwise addtion of 2 M NH_4OH. For 25% saturation 9.514 g of ammonium sulfate (134 g/L) was added to the P-450$_{scc}$ solution with stirring over a period of 20 min. The suspension was centrifuged at 10,000 rpm (Sorvall SS 34 rotor) for 10 min. Supernatant was decanted (72 mL) and then made to 45% saturation by adding 8.280 g of ammonium sulfate (115 g/L). The resulting suspension was centrifuged again as above, the supernatant was discarded and the pellet was suspended in 10 mL buffer A + 10% glycerol. The solution (15 mL) was then dialyzed overnight against 1 L of the same buffer.

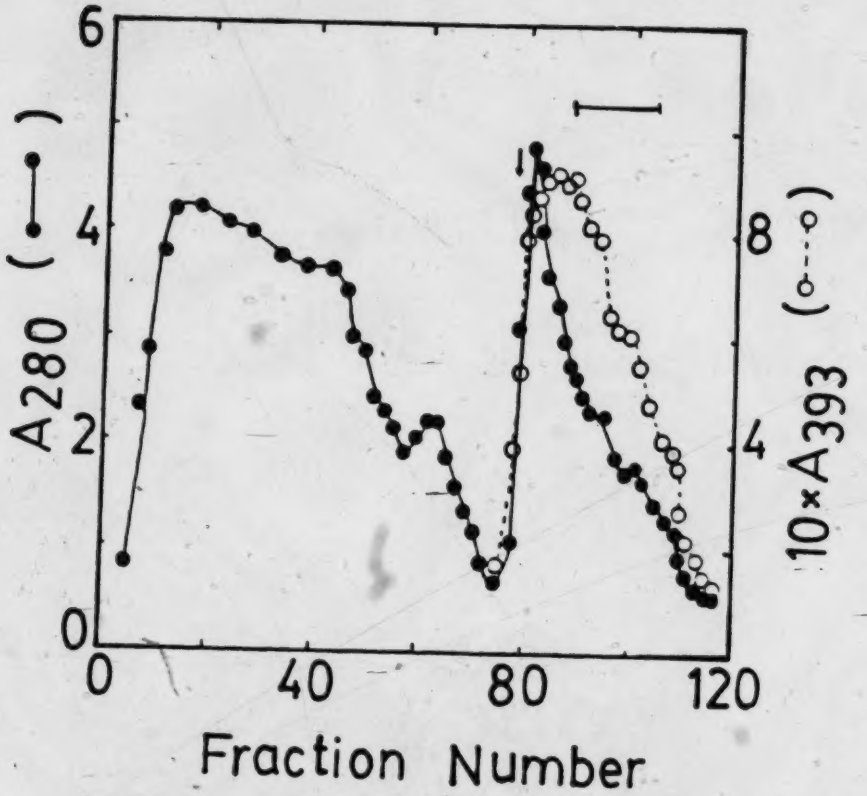

Figure A.3 First aniline-Sepharose column elution profile of adrenocortical cholesterol-bound cytochrome P-450$_{scc}$. The solid line represents absorbance at 280 nm and the dotted line, at 393 nm. Cytochrome P-450$_{scc}$ was eluted (indicated by the arrow) with buffer A + 0.3% cholate + 1 M KCl. Fractions of 6.5 mL were collected (1.0 mL/min) and the fractions with A_{280}/A_{393} = 3.0 or less (marked with the horizontal bar) were pooled. For details see purification of cholesterol-bound cytochrome P-450$_{scc}$.

The resulting dialysate (324 nmol of P-450$_{scc}$) was applied on to second aniline-Sepharose column (1.6x10 cm) which had been equilibrated with buffer A + 10% glycerol. Cytochrome P-450$_{scc}$ bound as a tight red band was eluted with buffer A + 0.2% cholate + 0.2 M KCl. Fig. A.4 shows the second aniline-Sepharose column elution profile of cytochrome P-450$_{scc}$. Fractions with A_{280}/A_{393} = 1.7 or less were pooled (36 mL, 150 nmol), dialyzed overnight against 2 L of buffer A + 10% glycerol and stored at -20°C.

When P-450$_{scc}$ was needed 10-15 mL of the above solution was thawed and applied on to an adrenodoxin-Sepharose column (0.9x10 cm), previously equilibrated with buffer A + 10% glycerol. The column was washed with 50 mL of the same buffer and then P-450$_{scc}$ was eluted with buffer A + 10% glycerol + 0.4 M KCl collecting 1.5 mL fractions. The elution profile of this column is presented in Fig. A.5. Fractions with A_{280}/A_{393} = 1.2 or less were combined and concentrated to a desired volume using an Amicon PM 30 membrane (25 psi nitrogen). The resulting concentrate was dialyzed for 3-4 h against 100 volumes of buffer A + 10% glycerol. Finally, P-450$_{scc}$ concentration was determined and the enzyme was stored at -20°C.

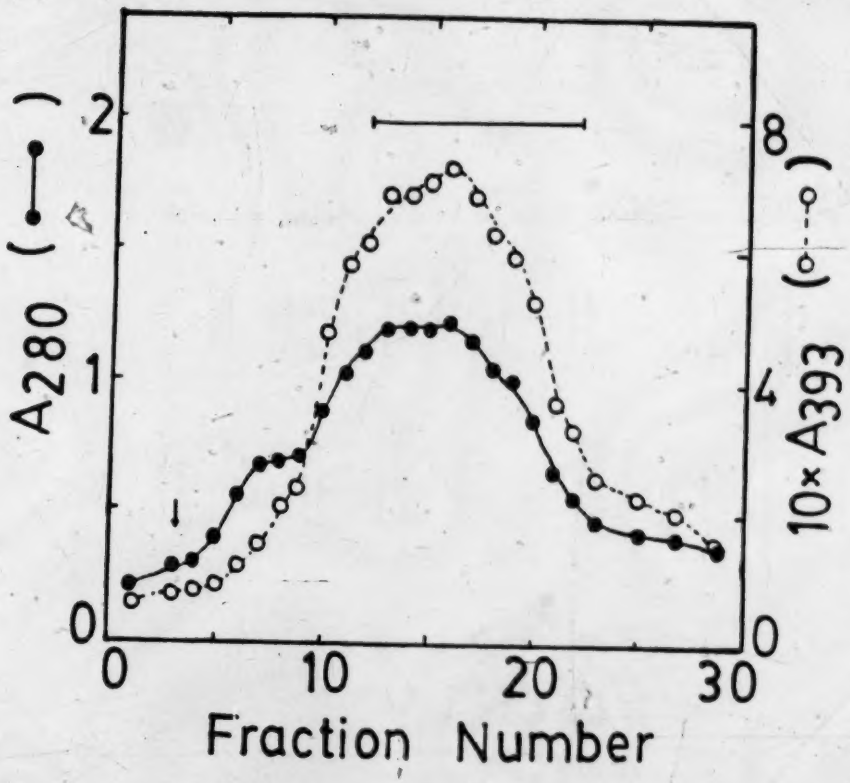

Figure A.4 Second aniline-Sepharose column elution profile of adrenocortical cholesterol-bound cytochrome P-450$_{scc}$. The solid line represents absorbance at 280 nm and the dotted line, at 393 nm. Cytochrome P-450$_{scc}$ was eluted (indicated by the arrow) with buffer A + 0.2% cholate + 0.2 M KCl. Fractions of 3.0 mL were collected (0.5 mL/min) and the fractions with A_{280}/A_{393} = 1.7 or less (marked with the horizontal bar) were pooled. See purification of cholesterol-bound cytochrome P-450$_{scc}$ for details.

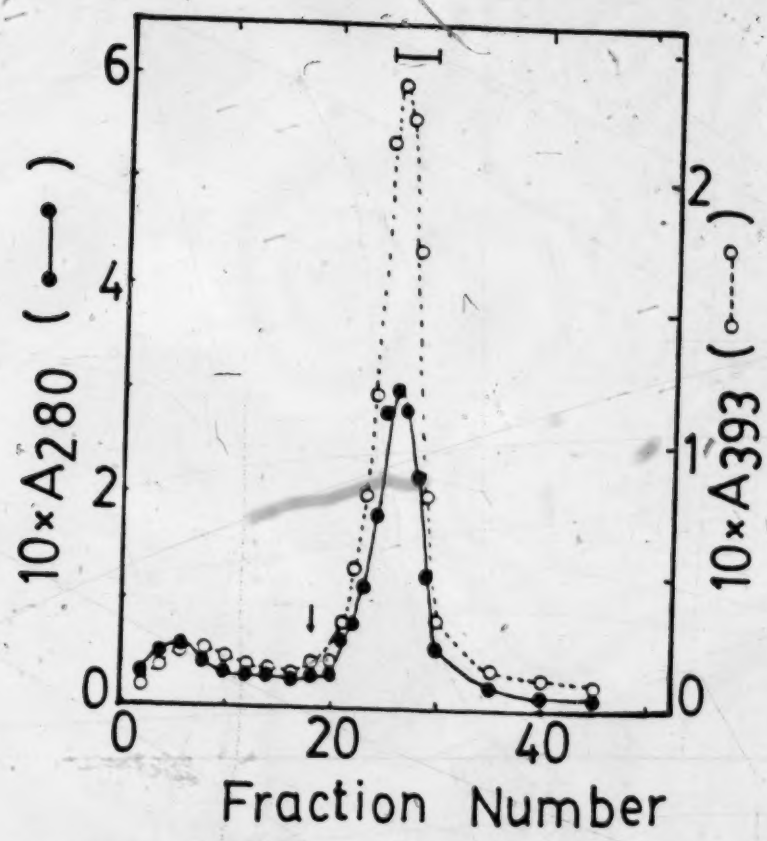

Figure A.5 Adrenodoxin-Sepharose column elution profile of adrenocortical cholesterol-bound cytochrome P-450$_{scc}$. The solid line represents absorbance at 280 nm and the dotted line, at 393 nm. Cytochrome P-450$_{scc}$ was eluted (indicated by the arrow) with buffer A + 10% glycerol + 0.4 M KCl. Fractions of 1.5 mL were collected (0.5 mL/min) and the fractions with A_{280}/A_{393} = 1.2 or less (marked with the horizontal bar) were pooled. For details see purification of cholesterol-bound cytochrome P-450$_{scc}$.

Purification of Adrenodoxin

Adrenodoxin (ADX) was purified from beef adrenal glands as described previously (5-6). The purification was carried out at 0-4°C. The frozen supernatant 'SN_{ADX}' (2,300 mL), obtained from the mitochondria preparation for cholesterol-bound cytochrome P-450_{scc}, was thawed in the cold room and suspended in 0.05 M K phosphate, pH 7.4. The suspension was filtered through double layers of cheesecloth to remove fat and then sonicated (Branson Sonifier 350) in 150 mL portions in a 200 mL beaker kept on ice for 1 min. The sonicated suspension was filtered through double layers of cheese-cloth. To the filtrate 300 mL packed volume of prepared DEAE-cellulose (DE 52) were added and stirred overnight in the cold room. The cellulose with ADX was recovered by centrifugation at 2,200 rpm (Sorvall GSA rotor). The precipitated cellulose mass was then suspended in 1 L of 10 mM Tris, pH 7.5, 100 mM KCl and centrifuged again as above. The resultant precipitate was resuspended in 1 L of the same buffer and filtered through Buchner funnel (using 10 cm Whatman #541 filter paper) under vacuum. Absorbed ADX was washed with 2 L of 10 mM Tris, pH 7.5, 100 mM KCl, until the wash was colourless and, finally, ADX was eluted with 10 mM Tris, pH 7.5, 0.5 M KCl. The dark brown coloured effluant was collected (1,300 mL), stored overnight in the cold room, and then diluted four-fold with ice-cold

distilled water and loaded on to a DE 52 column (2.6x17 cm) which was previously equilibrated with 10 mM Tris, pH 7.5, 100 mM KCl. The column was washed with 400 mL of 10 mM Tris, pH 7.5, 125 mM KCl, and the brown protein was then eluted with 10 mM Tris, pH 7.5, 350 mM KCl.

The eluate (370 mL) was stored overnight in the cold room and fractionated with ammonium sulfate (50-95% saturation) (pH was maintained at 7.5 by dropwise addition of 2 M NH_4OH). For 50% saturation 107.67 g ammonium sulfate (291 g/L) was added over a period of 20 min and the suspension was centrifuged at 11,000 rpm for 10 min (Sorvall GSA rotor). The supernatant (415 mL) was then made 95% saturation by adding 127.82 g ammonium sulfate (308 g/L) and centrifuged again as above. The pellet was suspended in 20 mL of 20 mM Tris, pH 7.5, 125 mM KCl and the suspension (28.0 mL) was loaded on to a Sephadex G-100 column (2.6x60 cm), previously equilibrated with 200 mL of 20 mM Tris, pH 7.5, 125 mM KCl and was eluted with the same buffer collecting 4.5 mL fractions. The darkest fractions were pooled (55 mL) and diluted with equal volume of ice-cold distilled water. ADX solution was loaded on to second DE 52 column (0.9x10 cm), previously equilibrated with 10 mM Tris, pH 7.5, 62.5 mM KCl. ADX was eluted with 10 mM Tris, pH 7.5, 0.5 M KCl directly on to a Sephadex G-50 column (1.6x85 cm) which had been equilibrated with the same

buffer. The brown protein was eluted with 10 mM Tris, pH 7.5, 0.5 M KCl and 1.4 mL fractions were collected at 20 cm head pressure. Coloured fractions were numbered (1-25) and fractions with A_{280}/A_{415} = 1.5-2.5 were pooled (20 mL), diluted five-fold with 10 mM Tris, pH 7.5, and then loaded on to third DE 52 column (0.9x7 cm) equilibrated with the same buffer. ADX was eluted from this column with 10 mM Tris, pH 7.5, 0.5 M KCl directly on to second Sephadex G-50 column (the same column used before), previously equilibrated with the above buffer. ADX was eluted using the same buffer and 1.4 mL fractions were collected. This procedure was repeated once more with third Sephadex G-50 column. Finally, ADX fractions (eluting from the third G-50 column) with A_{280}/A_{415} = 1.3 or less were pooled (6.2 mL). Fig. A.6 shows the chromatography of adrenodoxin on Sephadex G-50. The purified ADX was dialyzed against 1.2 L of 10 mM Tris, pH 7.5, for 6 h and stored under liquid nitrogen. The concentration of ADX was established using an extinction coefficient of 11 mM^{-1} cm^{-1} at 414 nm (7).

Other Procedures

Synthesis of Octylamine-Sepharose 4B

Octylamine-Sepharose gel was prepared by a modification of the described procedure (1). CNBr-activated Sepharose 4B was used as a starting gel instead of Sepharose 4B. 25 g of

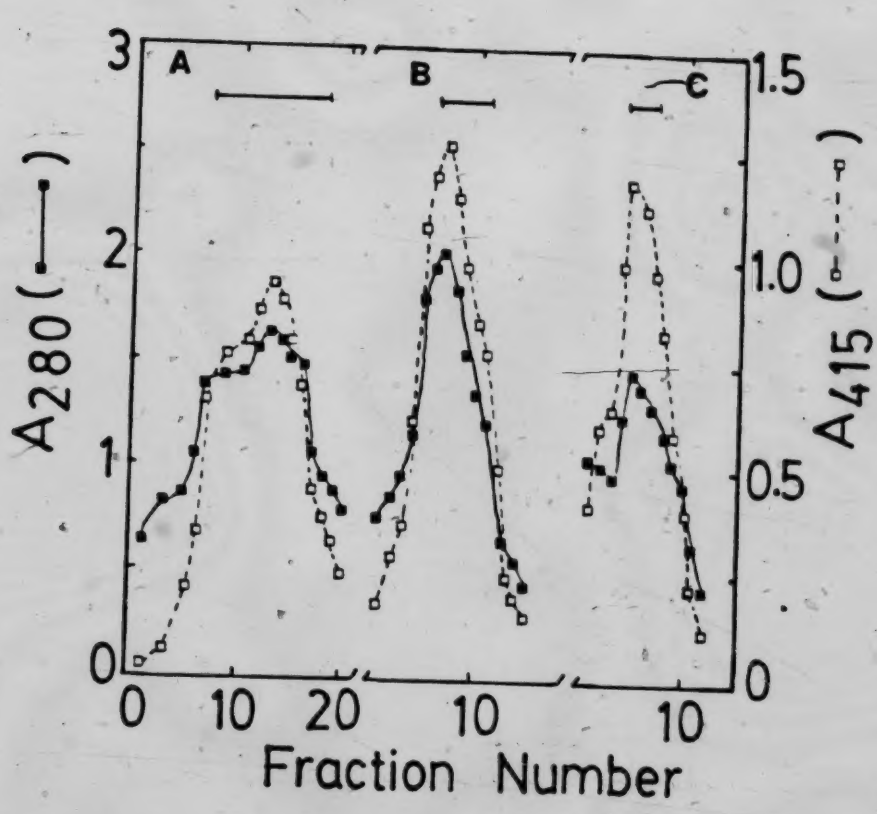

Figure A.6 Chromatography of adrenodoxin on Sephadex G-50. The solid lines represent absorbance at 280 nm and the dotted lines, at 415 nm. Procedures are described under purification of adrenodoxin. A, B and C are the first, second and third Sephadex G-50 columns elution profiles, respectively, of adrenodoxin. Active fractions marked with the horizontal bars were pooled.

freeze dried CNBr-activated Sepharose 4B powder was weighed out and swelled for 15 min in 150 mL of 1 mM HCl at room temperature. The suspension was washed with 4 L of 1 mM HCl in several additons on a Buchner funnel (sintered glass, porosity D) followed by 150 mL of coupling buffer (40% dioxane, 60% 0.1 M $NaHCO_3$, pH 9.0) and transferred immediately to a beaker containing 200 mL of ligand solution (1 M octylamine, 40% dioxane, 60% 0.1 M $NaHCO_3$, pH 9.0). The gel was gently stirred for 2 h at room temperature. Octylamine-Sepharose gel was then washed successively with 500 mL each of 40% dioxane solution; water; 0.1 M $NaHCO_3$, pH 9.0; 50 mM NaOH and water. To this washed gel, an equal volume of blocking solution (1 M glycine in 0.1 M $NaHCO_3$ buffer, pH 9.0) was added and the suspension was stirred at room temperature for 1 h to react with the residual activated Sepharose. The gel was washed alternately with three cycles of 0.1 acetate (pH 4.0) and 0.1 M $NaHCO_3$ (pH 9.0) buffers containing 0.5 M NaCl. Finally, the octylamine-Sepharose gel was extensively washed with water and stored in 10 mM Na phosphate, pH 7.4, 0.1 mM EDTA, 0.02% sodium azide in the cold room.

Synthesis of Aniline-Sepharose 4B

Aniline-Sepharose was prepared according to the described methodology (5) by a slight modification for CNBr-activated Sepharose 4B. 30 g of freeze-dried CNBr-activated Sepharose 4B powder was weighed out and swelled for 15 min in 200 mL of 1 mM HCl at room temperature. The suspension was washed with 6 L of 0.1 mM HCl in several additions on a Buchner funnel (sintered glass, porosity D) followed by 200 mL of coupling buffer (0.1 M $NaHCO_3$, pH 8.3, 0.5 M NaCl) and then transferred to a beaker containing 200 mL of ligand solution (10 mL freshly distilled aniline in 190 mL of coupling buffer). After stirring overnight in the cold room, the aniline-Sepharose gel was washed successively with 500 mL each of coupling buffer, water and coupling buffer. This washed gel was transferred to a beaker containing 500 mL of blocking solution (1 M glycine, 0.1 M $NaHCO_3$, pH 8.3) and gently stirred at room temperature for 1 h to react with the residual activated Sepharose. The product was then washed alternately with three cycles of 0.1 M acetate (pH 4.0) and 0.1 M $NaHCO_3$ (pH 8.3) buffers containing 0.5 M NaCl. Finally, the aniline-Sepharose was washed extensively with water and stored in the cold room in 50 mM K phosphate, pH 7.3, 0.02% sodium azide.

Synthesis of Adrenodoxin-Sepharose 4B

Adrenodoxin(ADX)-Sepharose was prepared by using CNBr-activated Sepharose 4B according to the previously described procedure (5,8). 2 g of freeze-dried CNBr-activated Sepharose powder was swelled for 15 min in 20 mL of 0.1 mM HCl at room temperature. The suspension was washed with 400 mL of 1 mM HCl in several additions on a Buchner funnel (sintered glass, porosity D) followed by 30 mL of coupling buffer (0.1 M $NaHCO_3$, pH 7.8, 0.4 M NaCl). The gel was then transferred to a beaker containing 25 mL of coupling buffer. Meanwhile a solution of ADX (6 mL, 1.9 µmol with A_{280}/A_{414} = 1.2) was dialyzed against 500 mL of 0.1 M $NaHCO_3$, pH 7.8, 0.4 M NaCl for 16 h in the cold room. This dialyzed ADX-solution was added to the beaker containing the gel and the coupling was performed in the cold room with gentle stirring for 40 h. The slurry was then filtered under vacuum and washed with 50 mL of coupling buffer. After filtration, the gel was stirred with 30 mL of blocking solution (0.5 M glycine, 0.1 M $NaHCO_3$, pH 7.8) for 4 h in the cold room. ADX-Sepharose was washed alternately with three cycles of 0.1 M acetate (pH 4.0) and 0.1 M $NaHCO_3$ (pH 7.8) buffers and then with water. Finally, the gel was stored in the cold room in 10 mM Tris, pH 7.5, 0.5 M KCl, 0.02% sodium azide.

Immediately after using a column, 10 mM Tris, pH 7.5, 0.5 M KCl, 0.02% sodium azide, was run through the column to prevent bacterial growth.

Assay of Cytochrome P-450$_{scc}$

A few grains of sodium dithionite were added to a sample of P-450$_{scc}$ in a buffered solution containing 10 mM Na(K) phosphate, pH 7.4, and 0.1 mM EDTA. The resulting reduced P-450$_{scc}$ was divided into two cuvettes and one of the cuvettes was then bubbled with carbon monoxide for about 30 s. The difference spectrum was recorded on a Cary 219 spectrophotometer, and the concentration of P-450$_{scc}$ was then calculated with the use of an extinction coefficient of 91 mM^{-1} cm^{-1} for A_{450}-A_{490} (9).

Determination of Protein Concentration by the Lowry Method (3)

Reagent A, 2 percent Na carbonate in 0.1 M Na hydroxide. Reagent B, 0.5% copper sulfate ($CuSO_4 \cdot 5H_2O$) in 1.0% K tartrate. Reagent C, Folin-Ciocalteu's phenol reagent. Standard protein solution (8.36 mg bovine serum albumin/mL).

Ten different working standard solutions were prepared from the standard protein solution diluted to 1- to 10-fold. 2.5 mL of reagent A and 100 μL protein solution

were added to 2.5 mL of reagent B in a test tube. After 10 min 0.25 mL of Folin reagent (reagent C) was added to the test tube and allowed to stand for 30 min. The absorbance of this solution at 500 nm was then determined on a Cary 219 spectrophotometer. The procedure was repeated with each of the above standard protein solutions and then a standard curve (Fig. A.7) was constructed by plotting the absorbance as a function of the concentration of the protein (mg/mL).

By using the same procedure the absorbance due to the unknown protein solution was determined under identical conditions. The concentration of the protein was then calculated from the standard curve.

Removal of Emulgen 913 from the Purified Cholesterol-free Cytochrome P-450$_{scc}$

Before the removal of Emulgen 913, the cholesterol-free cytochrome P-450$_{scc}$ sample was in pure low-spin form as judged by a visible absorption spectrum. In this stage, the enzyme could not be converted to high-spin form even if a saturated amount of cholesterol was added. This is due to the inhibitory effect of Emulgen 913 against substrate binding (10). Thus, it was necessary to remove Emulgen 913 from the purified cholesterol-free cytochrome P-450$_{scc}$ to study the effect of cholesterol binding.

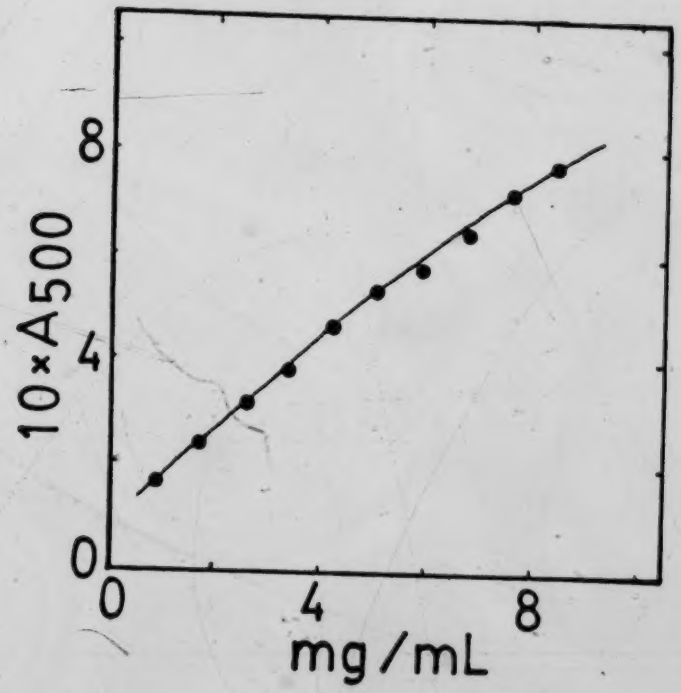

Figure A.7 Standard curve: standard solutions of bovine serum albumin (0.836 mg/mL - 8.36 mg/mL) were used to construct the curve by plotting the absorbance at 500 nm as a function of protein content (mg/mL).

Emulgen 913 in the purified cholesterol-free sample was removed by treatment with Bio-Beads SM2, a natural porous styrene-divinylbenzene copolymer (11-12). Prior to use, the beads were washed with 2-3 bed volumes of 100 mM Na phosphate, 1 mM EDTA, 20% glycerol (pH 7.4) followed by 2-3 bed volumes of water. 10 g of these moist beads were packed in a column (1x20 cm) avoiding formation of air pockets. Concentrated P-450$_{scc}$ solution was then placed on the top of the column. Cytochrome P-450$_{scc}$ was eluted with 100 mM Na phosphate, pH 7.4, containing 1 mM EDTA, 20% glycerol. The resulting P-450$_{scc}$ fractions were concentrated in the Amicon cell with a PM30 membrane to desired volume and stored under liquid nitrogen. This sample was in a pure low-spin cholesterol-free form and practically free from Emulgen 913 as judged by the absorption spectra in the ultraviolet region (i.e., absorbance at 276 nm due to Emulgen 913).

Preparation of DEAE-Cellulose, Sephadex G-100 and G-50

DEAE-cellulose (DE 52) was prepared by suspending 60 g of DE 52 (preswollen, microgranular, Whatman) in 1 L of 1 M Tris, pH 7.5, for 15 min. The pH of the slurry was adjusted to 7.5 using Tris-base. The suspension was then washed with several litres of 10 mM Tris, pH 7.5, using Buchner funnel. Finally, the slurry was equilibrated with 10 mM Tris, pH 7.5, 100 mM KCl.

Sephadex G-100 was prepared in 20 mM Tris, pH 7.5, 125 mM KCl, by heating ~20 g of the gel (superfine Sephadex G-100, Pharmacia Fine Chemicals) in a boiling water bath for 5 h.

Sephadex G-50 was prepared in 10 mM Tris, pH 7.5, by heating ~20 g of the gel (superfine) in a boiling water bath for 1 h.

Materials

CNBr-activated Sepharose 4B, Sephadex G-50 and Sephadex G-100 were purchased from Pharmacia Fine Chemicals. Bio-Beads SM2 and DEAE-cellulose were from Bio-Rad Laboratories (California) and Whatman, respectively. Sodium cholate, sodium pyrophosphate, dithiothreitol, n-octylamine, aniline, and Folin-Ciocalteu's phenol reagent were from Sigma. Emulgen 913 was from Kao-Atlas (Tokyo, Japan) and bovine serum albumin from Pentex (Kankakee, Illinois). All other reagents were of the best grade available from commercial sources.

Absorption Spectra of Purified Cytochromes P-450$_{scc}$ and Adrenodoxin

The absolute spectra of various forms of the purified cholesterol-free cytochrome P-450$_{scc}$ are shown in Fig. A.8. In the spectrum of the oxidized form, a maximum was

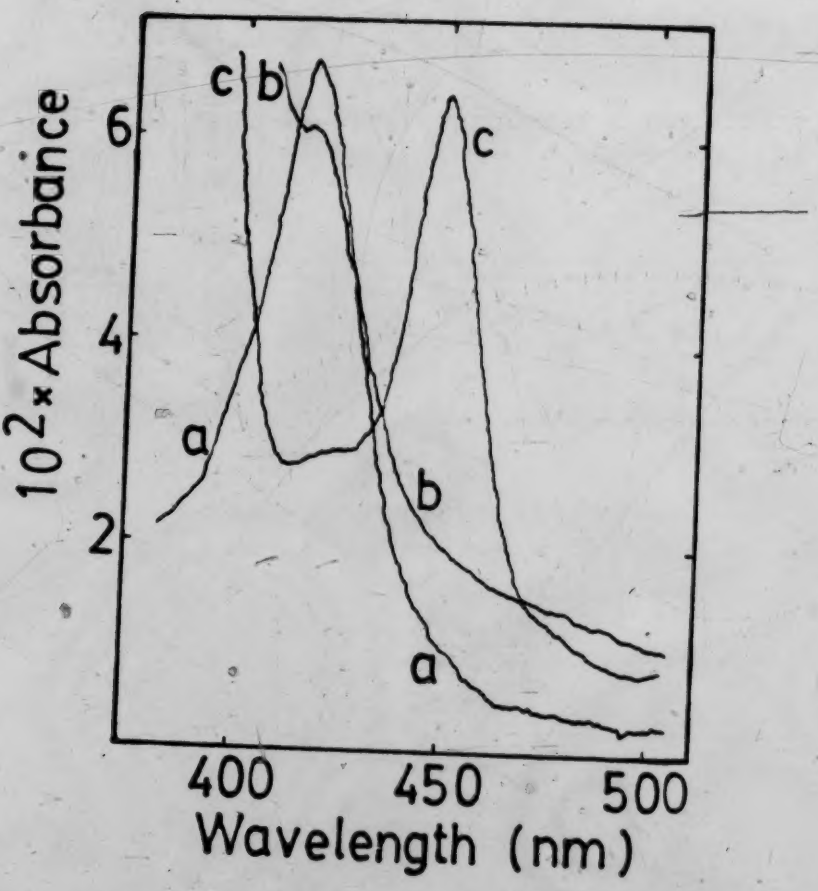

Figure A.8 Absorption spectra of various forms of purified cholesterol-free cytochrome P-450_{scc} (0.51 μM) at 25°C in 10 mM Na phosphate buffer, pH 7.4, and 0.1 mM EDTA; (a) ferric cholesterol-free form, (b) dithionite reduced form, and (c) ferrous carbon monoxide-complexed form.

seen at 416 nm in the Soret region. Upon reduction of the protein by solid sodium dithionite, the absorbance of the Soret band was decreased without shifting the maximum wavelength. The spectrum of the CO complex of the reduced P-450$_{scc}$ showed a peak at 450 nm with a slight shoulder at 420 nm. This shoulder was not detected in the reduced-CO difference spectrum (Fig. A.9). Addition of cholesterol to cholesterol-free cytochrome P-450$_{scc}$ (Emulgen 913 depleted) resulted in a decrease in absorbance at 416 nm and an increase in absorbance at 393 nm with isosbestic points at 406 nm and 457 nm (Fig. A.10), producing cytochrome P-450$_{scc}$ in the high-spin state. These data are in fair agreement with those reported earlier (1,13).

Fig. A.11 shows the absolute spectrum of purified cholesterol-bound cytochrome P-450$_{scc}$ with absorption maximum at 393 nm in the Soret region and an A_{280}/A_{393} ratio of 1.2. The absorbance ratio of 1.2 corresponds to 13 nmol P-450$_{scc}$/mg protein as determined by the Lowry assay (3) and the reduced-CO difference spectrum (9). This data is in good agreement with those reported elsewhere (5,14).

The absorption spectrum of purified adrenodoxin is presented in Fig. A.12. There are absorption maxima at 455 nm and 415 nm, with a broad maximum at 320 nm.

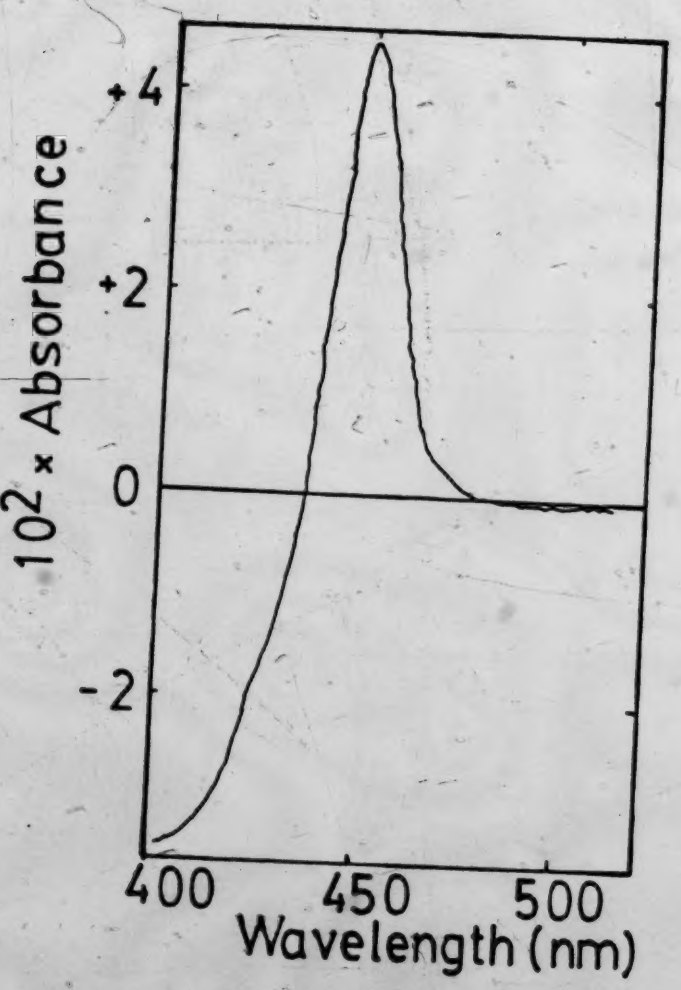

Figure A.9 Difference spectrum of carbon monoxide-complexed versus reduced cholesterol-free cytochrome P-450$_{scc}$ (0.51 μM) at 25°C in 10 mM Na phosphate buffer, pH 7.4, and 0.1 mM EDTA.

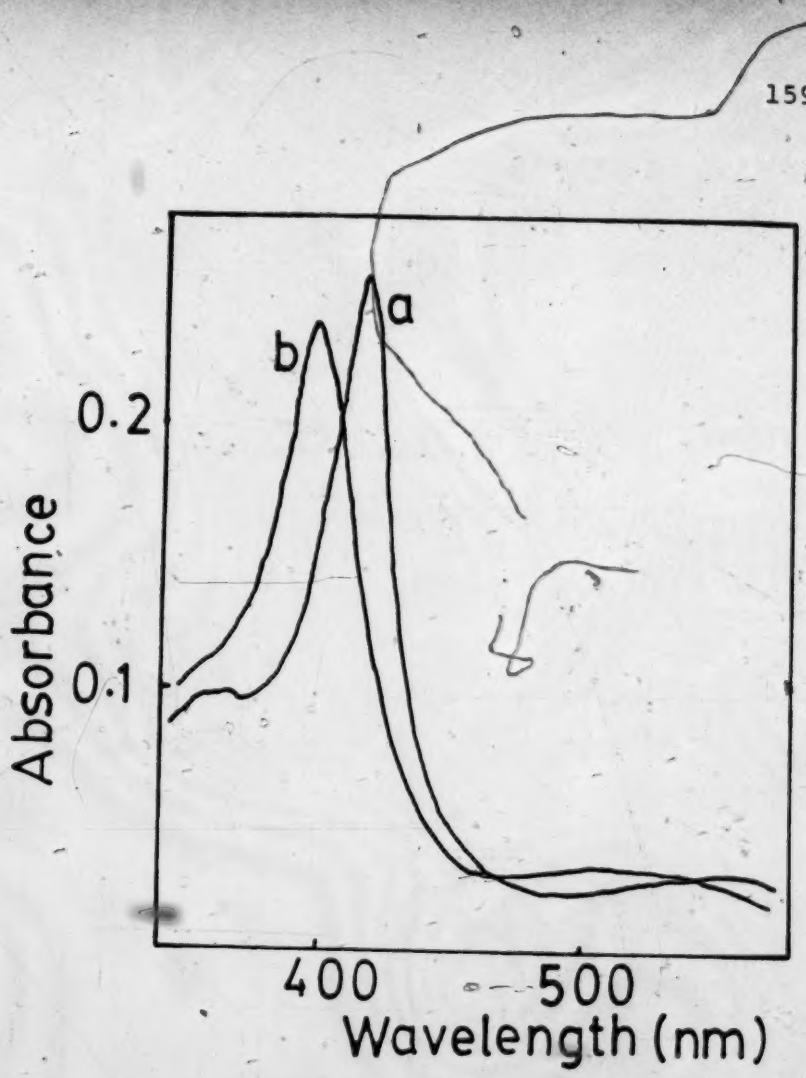

Figure A.10 Spectral changes on addition of cholesterol to low-spin cytochrome P-450$_{scc}$ at 25°C. Final concentrations were 1.76 μM cytochrome P-450$_{scc}$, 20 μM cholesterol. Spectrum (a) low-spin cholesterol-free cytochrome P-450$_{scc}$ and (b) high-spin cholesterol-bound cytochrome P-450$_{scc}$ were recorded after incubation for 17 hours at 25°C in 10 mM Na phosphate buffer, pH 7.4 and 0.1 mM EDTA.

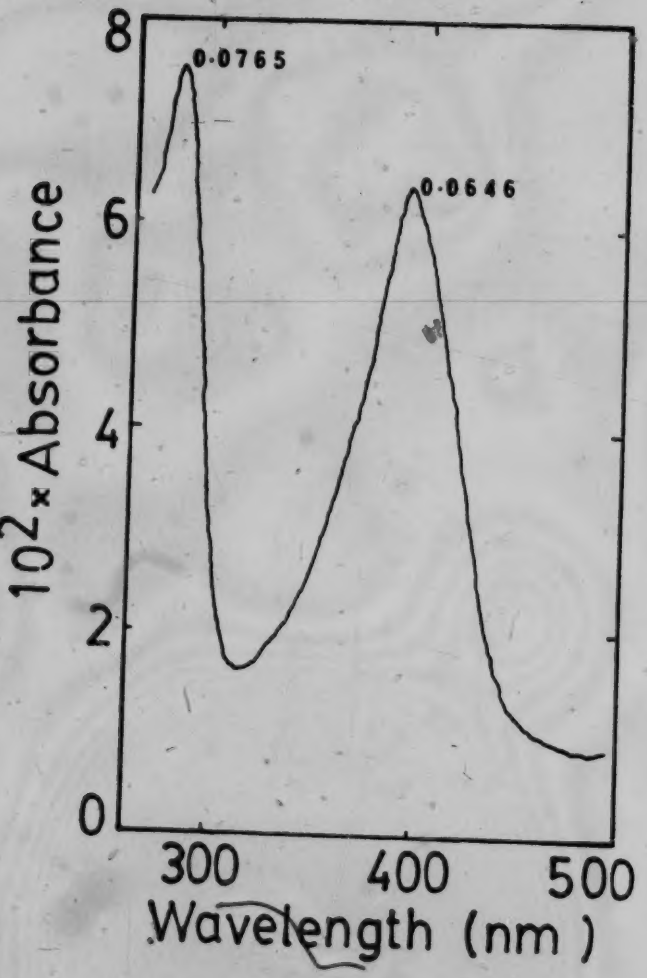

Figure A.11 Absorption spectrum of ferric cholesterol-bound cytochrome P-450_{scc} (0.69 μM) at 25°C in 10 mM K phosphate, pH 7.32, 0.1 mM EDTA.

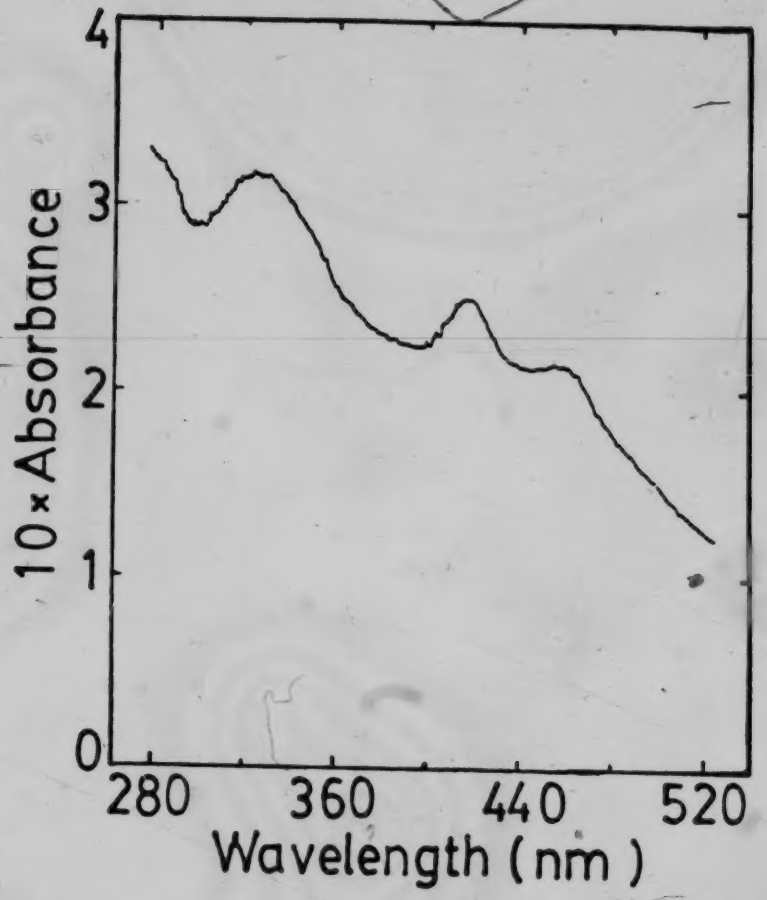

Figure A.12 Absorption spectrum of purified adrenodoxin (21.8 μM) in 10 mM Tris, pH 7.5.

References

1. Wang, H.-P. and Kimura, T. (1976) J. Biol. Chem. **251**, 6068-6074.
2. Welton, A. and Aust, S. (1972) Biochem. Biophys. Res. Commun. **49**, 661-666.
3. Lowry, O.H., Rosebrough, N.J., Farr, A.L. and Randall, R.J. (1951) J. Biol. Chem. **193**, 265-275.
4. Takemori, S., Suhara, K., Hashimoto, S., Sato, H., Gomi, T. and Katagiri, M. (1975) Biochem. Biophys. Res. Commun. **63**, 588-593.
5. Hanukoglu, I., Spitsberg, V., Bumpus, J.A., Dus, K.M. and Jefcoate, C.R. (1981) J. Biol. Chem. **256**, 4321-4328.
6. Orme-Johnson, W.H. and Beinert, H. (1969) J. Biol. Chem. **244**, 6143-6148.
7. Huang, J.J. and Kimura, T. (1973) Biochemistry **12**, 496-501.
8. March, S.C., Parikh, I. and Cuatrecasas, P. (1974) Anal. Biochem. **60**, 149-152.
9. Omura, T. and Sato, R. (1964) J. Biol. Chem. **239**, 2379-2385.
10. Kido, T., Arakawa, M. and Kimura, T. (1979) J. Biol. Chem. **254**, 8377-8385.
11. Gibson, G.G. and Schenkman, J.B. (1978) J. Biol. Chem. **253**, 5957-5963.

12. Holloway, P.W. (1973) Anal. Biochem. **53**. 304-308.

13. Hume, R., Kelly, R.W., Taylor, P.L. and Boyd, G.S. (1984) Eur. J. Biochem. **140**, 583-591.

14. Kowluru, R.A., George, R. and Jefcoate, C.R. (1983) J. Biol. Chem. **258**, 8053-8059.

APPENDIX II

BASIC EQUATION FOR PSEUDO-FIRST ORDER KINETIC MEASUREMENTS

All kinetic experiments, described in this thesis, were performed on the stopped-flow spectrophotometer under pseudo-first order conditions. The basic kinetics can be explained by considering the reversible formation of a complex, ES, between an enzyme, E, and a substrate, S:

$$[1] \qquad E + S \underset{k_{-1}}{\overset{k_1}{\rightleftharpoons}} ES$$

The rate equation governing this reaction is

$$[2] \qquad -\frac{d[E]}{dt} = k_1[E][S] - k_{-1}[ES]$$

If the total substrate concentration, $[S]_o$, is much greater than the total enzyme concentration, $[E]_o$, it can be assumed to remain constant during the course of the reaction. The reaction now becomes pseudo-first order, and the pseudo-first order rate constant, $k_1' = k_1[S]$. Then equation [2] becomes

$$[3] \qquad -\frac{d[E]}{dt} = k_1'[E] - k_{-1}[ES]$$

At equilibrium, $-\frac{d[E]}{dt} = 0$ and

$$[4] \qquad k_1'[E]_\infty = k_{-1}[ES]_\infty$$

$$[5] \qquad K = \frac{k_1'}{k_{-1}} = \frac{[ES]_\infty}{[E]_\infty}$$

also from stoichiometry,

$$[6] \qquad [E]_o + [ES]_o = [E]_\infty + [ES]_\infty = [E] + [ES]$$

Substitution of equations [5] and [6] into [3], and rearrangement affords the relation:

$$[7] \qquad -\frac{d[E]}{dt} = (k_1' + k_{-1})([E] - [E]_\alpha)$$

Integration between the limits (from t = o to t = t) gives

$$[8] \qquad \ln \frac{[E] - [E]_\infty}{[E]_o - [E]_\infty} = -(k_1' + k_{-1})t$$

In the stopped-flow experiment, the formation or decay of a single reactant species is observed by measuring the absorbance as a function of time. The absorbance, A, is directly proportional to concentration, "c", according to Beer's law: A = abc, since "a", the molar absorptivity, is a constant, and "b", the path length through the solution, is also constant. Then equation [8] becomes

$$\ln \frac{A - A_\infty}{A_o - A_\infty} = -(k_1' + k_{-1})t$$

or

[9] $$\ln \frac{\Delta A_t}{\Delta A_o} = -(k_1[S] + k_{-1})t$$

(since $k_1' = k_1[S]$)

Equation [9] can also be written as

$$\Delta A_t = \Delta A_o \, e^{-(k_1[S] + k_{-1})t}$$

or

[10] $$\Delta A_t' = \Delta A_o \, e^{-k_{obs} \cdot t}$$, where

[11] $$k_{obs} = k_1[S] + k_{-1}$$

The observed rate constant, k_{obs}, is calculated from the time dependence of the absorbance changes by non-linear least squares analysis of equation [10]. The values of second order forward rate constant, k_1, and first order reverse rate constant, k_{-1}, are then calculated from the slope and intercept, respectively, of the plot of k_{obs} versus [S] (equation [11]).